AD A051605

DDC FILE COPY

SDAC-TR-76-10

12

STUDY OF SELECTED KAMCHATKA EARTHQUAKES IN A SEISMIC DISCRIMINATION CONTEXT

D. H. von Seggern & P. A. Sobel

Seismic Data Analysis Center

Teledyne Geotech, 314 Montgomery Street, Alexandria, Virginia 22314

August 16, 1977

APPROVED FOR PUBLIC RELEASE; DISTRIBUTION UNLIMITED.

Sponsored by

The Defense Advanced Research Projects Agency (DARPA)

ARPA Order No. 2551

DDC
RECEIVED
MAR 22 1978
B

Monitored By

AFTAC/VSC

312 Montgomery Street, Alexandria, Virginia 22314

Disclaimer: Neither the Defense Advanced Research Projects Agency nor the Air Force Technical Applications Center will be responsible for information contained herein which has been supplied by other organizations or contractors, and this document is subject to later revision as may be necessary. The views and conclusions presented are those of the authors and should not be interpreted as necessarily representing the official policies, either expressed or implied, of the Defense Advanced Research Projects Agency, the Air Force Technical Applications Center, or the US Government.

Unclassified

SECURITY CLASSIFICATION OF THIS PAGE (When Data Entered)

REPORT DOCUMENTATION PAGE

READ INSTRUCTIONS BEFORE COMPLETING FORM

1. REPORT NUMBER: (14) SDAC-TR-76-10
2. GOVT ACCESSION NO.:
3. RECIPIENT'S CATALOG NUMBER:

4. TITLE (and Subtitle): (6) STUDY OF SELECTED KAMCHATKA EARTHQUAKES IN A SEISMIC DISCRIMINATION CONTEXT.

5. TYPE OF REPORT & PERIOD COVERED: (9) Technical rept.,

6. PERFORMING ORG. REPORT NUMBER:

7. AUTHOR(s): (10) D. H. von Seggern, P. A. Sobel

8. CONTRACT OR GRANT NUMBER(s): (15) F08606-77-C-0014, ARPA Order 2551

9. PERFORMING ORGANIZATION NAME AND ADDRESS:
Teledyne Geotech
314 Montgomery Street
Alexandria, Virginia 22314

10. PROGRAM ELEMENT, PROJECT, TASK AREA & WORK UNIT NUMBERS:
VT/7709

11. CONTROLLING OFFICE NAME AND ADDRESS:
Defense Advanced Research Projects Agency
Nuclear Monitoring Research Office
1400 Wilson Blvd. Arlington, Virginia 22209

12. REPORT DATE: (11) 16 Aug[illegible]77

13. NUMBER OF PAGES: 112

14. MONITORING AGENCY NAME & ADDRESS (if different from Controlling Office):
VELA Seismological Center
312 Montgomery Street
Alexandria, Virginia 22314

15. SECURITY CLASS. (of this report): Unclassified

15a. DECLASSIFICATION DOWNGRADING SCHEDULE:

16. DISTRIBUTION STATEMENT (of this Report):

(12) 115 p.

APPROVED FOR PUBLIC RELEASE; DISTRIBUTION UNLIMITED

17. DISTRIBUTION STATEMENT (of the abstract entered in Block 20, if different from Report):

18. SUPPLEMENTARY NOTES:
Author's Report Date: July 26, 1976

RE: Classified references-
Rept. SDAC-TR-76-10
Document should remain for unlimited distribution per Capt. G. B. Young, AFTAC/VELA-SC

19. KEY WORDS (Continue on reverse side if necessary and identify by block number):
Seismic Discrimination
M_s versus m_b
Kamchatka Earthquakes
Seismic Source Spectrum

20. ABSTRACT (Continue on reverse side if necessary and identify by block number):
Seismic discrimination in the Kamchatka source region is studied using data from earthquakes, inferences from measurements of teleseismic explosions, and results from the Amchitka tests. A small suite of 9 earthquakes, most having low M_s for their m_b, was selected in the range $5 < m_b < 6$ and with depth of focus < 50 km. These earthquakes lay near the top of the downgoing Pacific plate and had predominantly a thrust mechanism. Major source and transmission path effects on signals recorded at LASA, NORSAR, HGLP, and WWSSN stations are identified and related to discrimination parameters. On the basis of several →

DD FORM 1 JAN 73 1473 EDITION OF 1 NOV 65 IS OBSOLETE

Unclassified

SECURITY CLASSIFICATION OF THIS PAGE (When Data Entered)

408258

20. ABSTRACT (Continued)

parameters taken together, such as M_s-m_b, spectral ratio, corner frequency, ~~pP~~, complexity, long-period body-wave excitation, and shear-wave excitation, discrimination of events of this type in the Kamchatka region poses no special problems so long as discrimination against shot arrays is not at issue. If shot arrays are considered, then the problem is more difficult, but still tractable.

STUDY OF SELECTED KAMCHATKA EARTHQUAKES IN A SEISMIC DISCRIMINATION CONTEXT

SEISMIC DATA ANALYSIS CENTER REPORT NO.: SDAC-TR-76-10

AFTAC Project Authorization No.:	VELA T/7709/B/ETR
Project Title:	Seismic Data Analysis Center
ARPA Order No.:	2551
ARPA Program Code No.:	7F10
Name of Contractor:	TELEDYNE GEOTECH
Contract No.:	F08606-77-C-0014
Date of Contract:	01 October 1976
Amount of Contract:	$2,697,947
Contract Expiration Date:	30 September 1977
Project Manager:	Robert R. Blandford (703) 836-3882

P. O. Box 334, Alexandria, Virginia 22314

APPROVED FOR PUBLIC RELEASE; DISTRIBUTION UNLIMITED

ACCESSION for
NTIS White Section ☑
DDC Buff Section ☐
UNANNOUNCED ☐
JUSTIFICATION
BY
DISTRIBUTION/AVAILABILITY CODES
Dist. AVAIL. and/or SPECIAL
A

ABSTRACT

Seismic discrimination in the Kamchatka source region is studied using data from earthquakes, inferences from measurements of teleseismic explosions, and results from the Amchitka tests. A small suite of 9 earthquakes, most having low M_s for their m_b, was selected in the range $5 < m_b < 6$ and with depth of focus < 50 km. These earthquakes lay near the top of the downgoing Pacific plate and had predominantly a thrust mechanism. Major source and transmission path effects on signals recorded at LASA, NORSAR, HGLP, and WWSSN stations are identified and related to discrimination parameters. On the basis of several parameters taken together, such as M_s-m_b, spectral ratio, corner frequency, pP, complexity, long-period body-wave excitation, and shear-wave excitation, discrimination of events of this type in the Kamchatka region poses no special problems so long as discrimination against shot arrays is not at issue. If shot arrays are considered, then the problem is more difficult, but still tractable.

PRECEDING PAGE NOT FILMED
BLANK

TABLE OF CONTENTS

	Page
ABSTRACT	3
INTRODUCTION	9
TECTONIC SETTING	11
General Features	11
Source Mechanisms of Earthquakes	18
Velocity Model	23
DATA	26
Earthquakes	26
Seismic Stations	29
Revision of Locations	29
SIGNAL ANALYSIS	32
Source Effects	32
Propagation Effects	63
DISCRIMINATION ASPECTS	88
M_S-m_b	88
Corner Frequency	91
Long-Period Body-Wave Excitation	91
Depth of Focus	97
Complexities	99
Spectral Ratios	99
Radiation Patterns	101
Short-Period S/P Excitation	101
SUMMARY	106
ACKNOWLEDGEMENTS	109
REFERENCES	110

LIST OF FIGURES

Figure No.	Title	Page
1	Physiographic features of the Kamchatka Arc.	12
2	Schematic cross-section of Kamchatka Arc through 1-1 in Figure 1 (from Veith, 1974).	13
3	Schematic cross-section of Kamchatka Arc through 2-2 in Figure 1 (from Veith, 1974).	14
4	Schematic cross-section of Kamchatka Arc through 3-3 in Figure 1 (from Veith, 1974).	15
5	Schematic cross-section of Kamchatka Arc through 4-4 in Figure 1 (from Veith, 1974).	16
6	Plan view of seismicity in the Kamchatka Arc (NEIS epicenter file from 01/07/66 to 07/08/74).	17
7	Cross-section view of all Kamchatka seismicity shown in Figure 6, as projected on a plane normal to the NNE tectonic trend.	19
8	Cross-section of Kamchatka seismicity in region A of Figure 6.	20
9	Cross-section of Kamchatka seismicity in region B of Figure 6.	21
10	Cross-section of Kamchatka seismicity in region C of Figure 6.	22
11	P-wave nodal planes projected on the lower half of the focal sphere and LR amplitude radiation pattern (T = 20 sec) for a typical thrust earthquake (Event 22) at shallow depth in the Kamchatka source region.	24
12	First motions for Kamchatka earthquakes in the lower half of the focal sphere (Wulff net).	33 thru 40
13	Theoretical LR excitation (T = 20 sec) for events of constant seismic moment at various depths in a Kamchatka earth model.	42
14	Teleseismic P-wave amplitude on WWSSN short-period recording for dilatational source at various depths in Kamchatka.	44
15	Teleseismic P-wave amplitude on WWSSN long-period recordings for dilatational sources at various depths in Kamchatka.	45
16	Teleseismic P-wave amplitude on HGLP long-period recordings for dilatational sources at various depths in Kamchatka.	46

LIST OF FIGURES (Continued)

Figure No.	Title	Page
17	LASA A0 subarray spectra of P-waves from Kamchatka earthquakes with instrument response and attenuation removed (t* = .25).	48 thru 56
18	Seismic moment versus corner frequency for Kamchatka earthquakes from LASA P recordings.	57
19	Synthetic and observed long-period vertical-component seismograms for P-waves from the 03/04/73 Kamchatka earthquake.	59
20	Observed vs. predicted long-period P-wave amplitudes for 03/04/73 Kamchatka earthquake.	60
21	Synthetic and observed long-period vertical-component seismograms for S-waves from the 03/04/73 Kamchatka earthquake.	61
22	Short-period P-wave recorded at NORSAR (C3 subarray beam) and LASA (A0 subarray beam) for Kamchatka earthquakes.	62
23	Theoretical and observed LR amplitude (T = 20 sec) for Kamchatka earthquakes of this study.	72 thru 79
24	Ratio of average Kazakh explosion spectra to average Kamchatka earthquake spectra recorded at NORSAR.	81
25	Ratio of average LASA spectra to average NORSAR spectra for four Eastern Kazakh explosions.	82
26	Ratio of average Kamchatka earthquake spectra to average Kazakh explosion spectra recorded at LASA.	83
27	Predicted LR raypaths (T = 20 sec) from event 12.	85
28	Predicted LR raypaths (T = 20 sec) from event 16.	86
29	Predicted LR raypaths (T = 20 sec) from event 20.	87
30	M_S vs. m_b for selected Kamchatka earthquakes of thrust-type mechanism.	90
31	LASA A0 subarray spectra of P-wave from MILROW with instrument response and attenuation removed (t* = .25).	92
32	Long-period spectral level vs. corner frequency for Kamchatka earthquakes from LASA P recordings.	93
33	Distribution of log (SH/LR) for ratios of ground displacements from Kamchatka earthquakes.	94
34	Distribution of log (SV/LR) for ratios of ground displacements from Kamchatka earthquakes.	95

LIST OF FIGURES (Continued)

Figure No.	Title	Page
35	Distribution of log (P/LR) for ratio of ground displacements from Kamchatka earthquakes.	96
36	Short-period P spectral ratio vs. m_b for Kamchatka earthquakes recorded at NORSAR and LASA.	102
37	Distribution of ratio (SV/P) for ground displacement from short-period recordings of Kamchatka earthquakes.	103
38	Distribution of ratio (SH/P) for ground displacement from short-period recordings of Kamchatka earthquakes.	104

LIST OF TABLES

Table No.	Title	Page
I	Velocity Structure off the East Coast of Kamchatka.	25
II	NEIS Parameters for Kamchatka Earthquakes.	27
III	Usable Long-Period Digital Data for Selected Kamchatka Earthquakes.	28
IV	Magnitude Data for Selected Kamchatka Earthquakes.	64
V	Long-Period Body-Wave Minus Rayleigh-Wave Magnitudes for Selected Kamchatka Earthquakes.	98
VI	Complexities for Kamchatka P-Waves.	100

INTRODUCTION

Seismological techniques for the verification of an underground nuclear test ban treaty have advanced considerably in recent years, and several authors have presented large bodies of data (Evernden, 1969; Evernden et al., 1971; Weichert and Basham, 1973; Ericsson, 1970; and Evernden, 1975) which imply a high degree of confidence in identification of underground explosions. Perhaps the overriding concern is that, in fact, for only one area of the globe, namely the southwestern United States, has an adequate number of explosions occurred amongst shallow-focus earthquakes to permit one to draw firm conclusions about our capability to identify. That region is studied in a companion report, where it is shown that in a number of ways several earthquakes and explosions there are only marginally distinguishable. Suggestions that explosions can be identified in all regions of the globe rest on extrapolations of data from a very small number of test sites; however, we feel that these extrapolations in most cases are well-founded and geophysically reasonable.

The way to solidify our confidence in discrimination capability is to intensely study the characteristics of further earthquake source regions and attempt to identify those aspects of the source mechanisms or of the propagation paths which will influence the values commonly used in discrimination. Parameters such as M_S, m_b, spectral ratios, radiation patterns, error ellipses on focal depth, and shear-wave generation should be included. To that end, we will examine the Kamchatka source region in this report. This is a very

---

Evernden, J., 1969. Identification of earthquakes and explosions by use of teleseismic data, J. Geophys. Res., v. 74, 3828-3856.

Evernden, J., W. J. Best, P. W. Pomeroy, T. V. McEvilly, J. M. Savino, and L. R. Sykes, 1971. Discrimination between small magnitude earthquakes and explosions, J. Geophys. Res., v. 76, 8042-8055.

Wiechert, D. H., and P. W. Basham, 1973. Deterrence and false alarms in seismic discrimination, Bull. Seism. Soc. Am., v. 63, p. 1119-1132.

Ericsson, U. A., 1970. Event identification for test ban control, Bull. Seism. Soc. Am., v. 60, p. 1521-1546.

Evernden, J., 1975. Further studies on seismic discrimination, Bull. Seism. Soc. Am., v. 65, p. 359-392.

seismically active region in the U.S.S.R. which received attention as a possible test site where the frequency of nearby earthquakes might permit evasion by hiding test signals in earthquake signals. This evasion technique has been extensively dealt with by Blandford et al. (1971), Blandford and Husted (1973), and Evernden (1976); and we do not consider it in this report. Evasion may also by practiced by means of shot array techniques. The impact of such techniques on discrimination is briefly discussed in the report as appropriate. Our emphasis is on the identification capabilities presented by signals from real earthquakes in Kamchatka, on the possibility of identifying a hypothetical explosion there, and on elucidating the effects of source and path on waveforms seen by a teleseismic network.

Blandford, R. R., T. J. Cohen, and H. L. Husted, 1971. Opportunities for foreign nations to hide an underground nuclear test in an earthquake (U), SDL Report Number 283, Teledyne Geotech, Alexandria, Virginia. Classified

Blandford, R. R., and H. L. Husted, 1973. Extension of Hide-In-Earthquakes (HIE) technique to include probability of detection (U), SDL Report Number 303, Teledyne Geotech, Alexandria, Virginia. Classified

Evernden, J. F., 1976. Study of seismological evasion, Part III: Evaluation of evasion possibilities using codas of large earthquakes, Bull. Seism. Soc. Am., v. 66, 549-592.

TECTONIC SETTING

General Features

The general features of the Kuril-Kamchatka Arc have been discussed by Goryatchev (1962), Tokarev (1970), and Veith (1974), among others. Here we will merely summarize the important features and illustrate the major known properties.

Shallow eastern Kamchatka earthquakes coincide with a zone between the deep sea trench and the Holocene, but extinct, volcanic arc (Figure 1). Present volcanic activity occurs along a parallel arc to the west of the older Holocene Arc. Large faults dissect the continental shelf east of Kamchatka, and a trench lies parallel to and east of the events discussed in this report. The Pacific plate is dipping under Kamchatka in a west-northwest direction and with a dip of about 50° at depth (Tokarev, 1970). The top of the dipping plate lies about 100 km below the active volcanic arc in eastern Kamchatka and reaches the surface near the trench as its dip angle lessens. The earthquakes used in this study occur in the seismic zone at the top of the dipping plate and somewhat east of the Kamchatka coast as shown in Figure 1. (These are revised locations, as explained in a later section.) Figures 2 through 5 (from Veith, 1974) show cross-sections through Kamchatka along several parallel planes normal to the general tectonic trend of NNE.

A plot of nearly a decade of seismicity projected to the surface in Kamchatka, as listed in the NEIS bulletin, is shown in Figure 6. The abrupt termination of seismicity near the Kamchatka Cape corresponds to the inter-

---

Goryatchev, A. V., 1962. On the relationship between geotectonic and geophysical phenomena of the Kuril-Kamchatka folding zone at the junction zone of the Asiatic continent with the Pacific Ocean, in The Earth Beneath the Continents, AGU Monograph 10, American Geophysical Union, Washington D.C.

Tokarov, P., 1970. On the focal layer, seismicity, and volcanicity of the Kurile-Kamchatka Zone, Izvestia, Physics of the Solid Earth, Number 3, page. 152-160.

Veith, K., 1974. The relationship of island arc seismicity to plate tectonics, Ph.D. Thesis, Southern Methodist University, Dallas, Texas.

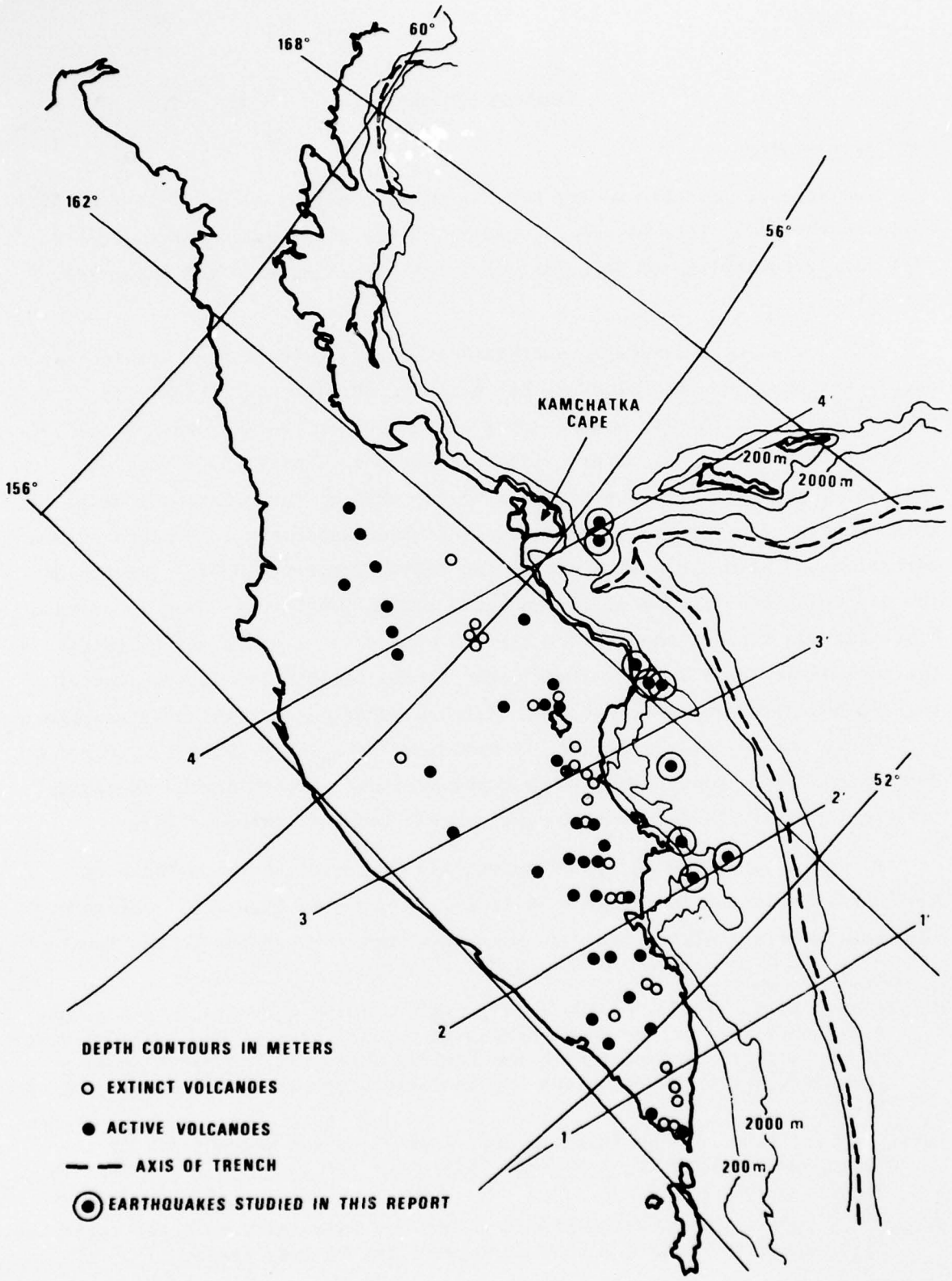

Figure 1 Physiographic features of the Kamchatka Arc.

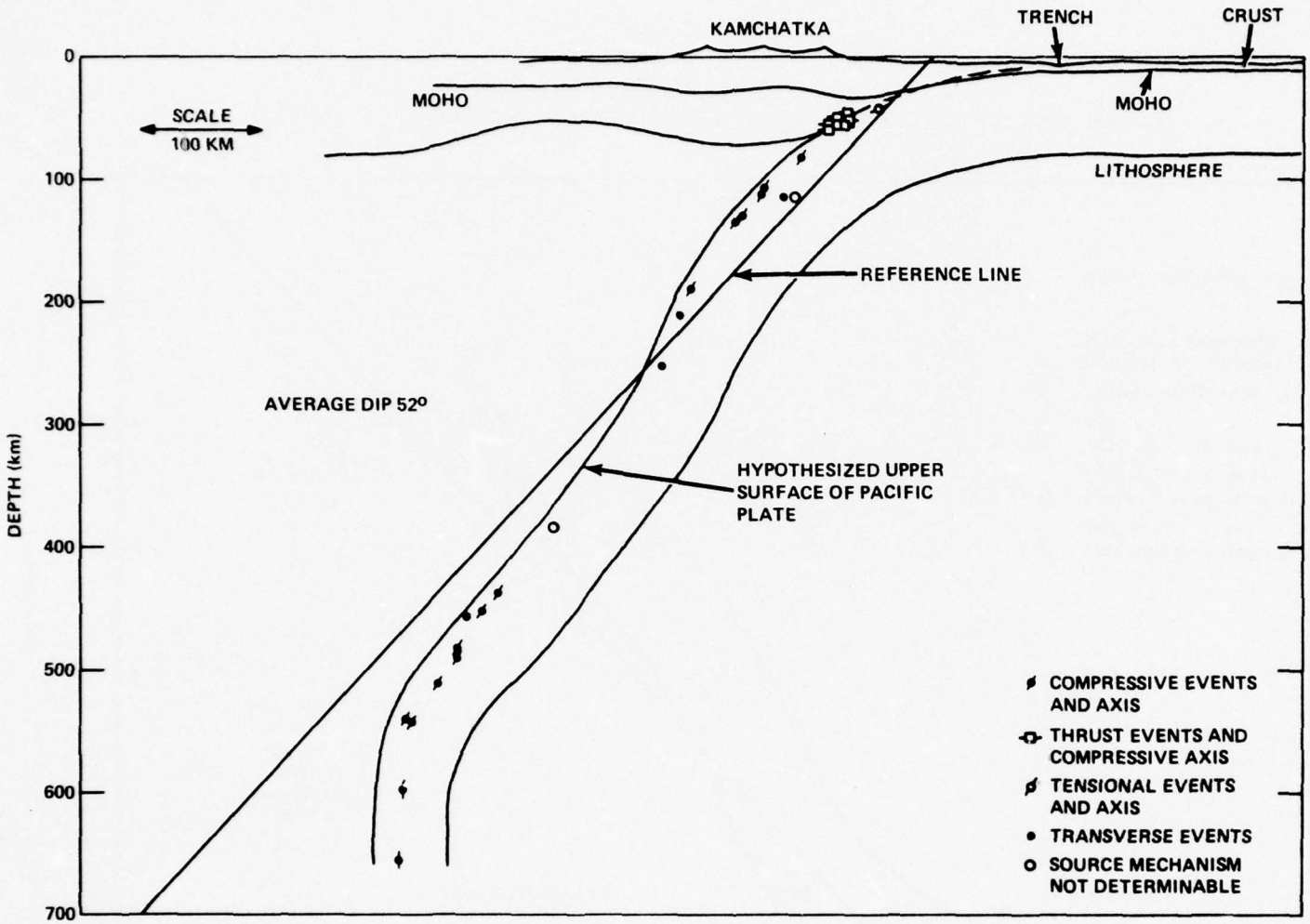

Figure 2 Schematic cross-section of Kamchatka Arc through 1-1 in Figure 1 (from Veith, 1974).

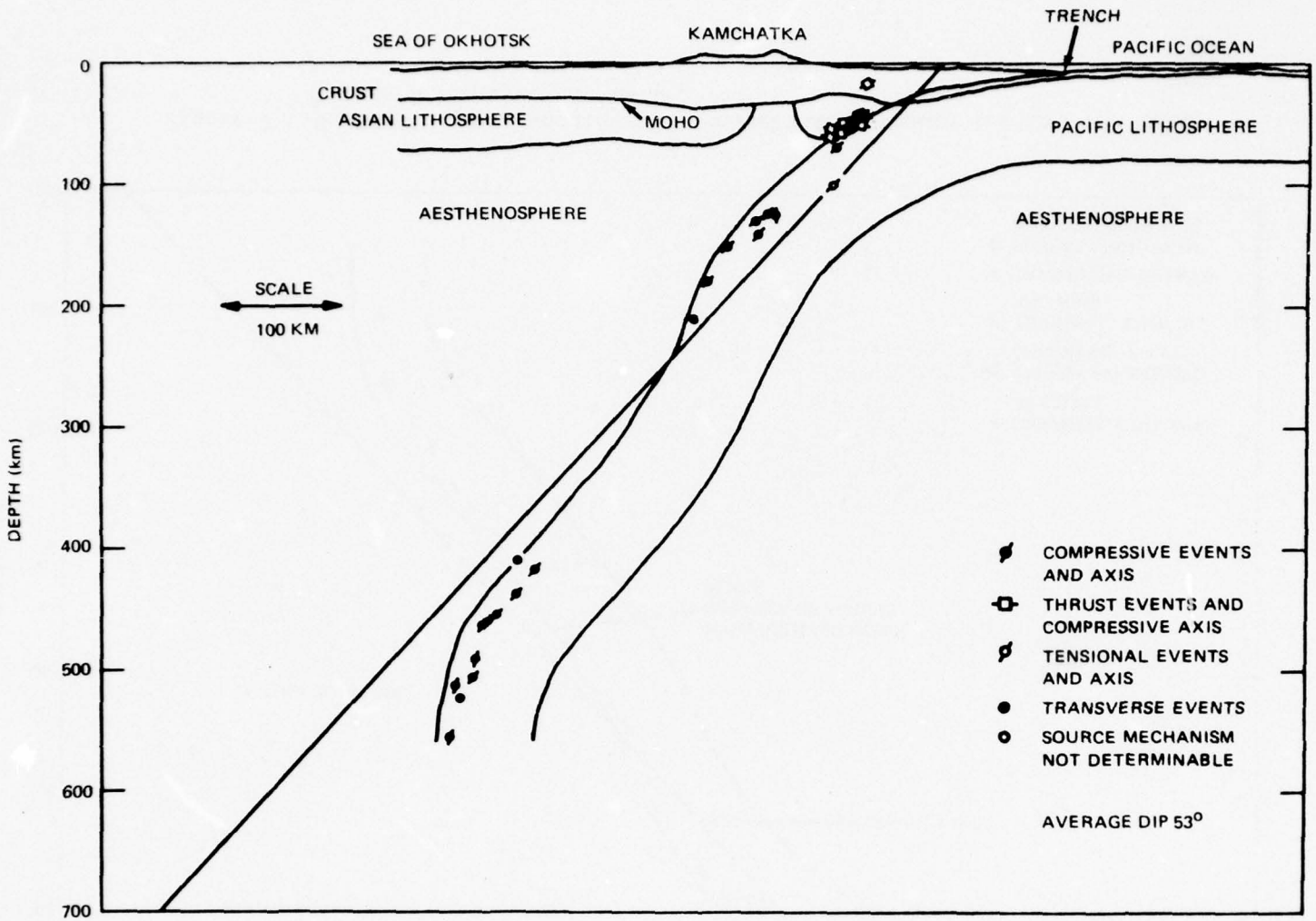

Figure 3 Schematic cross-section of Kamchatka Arc through 2-2 in Figure 1 (from Veith, 1974).

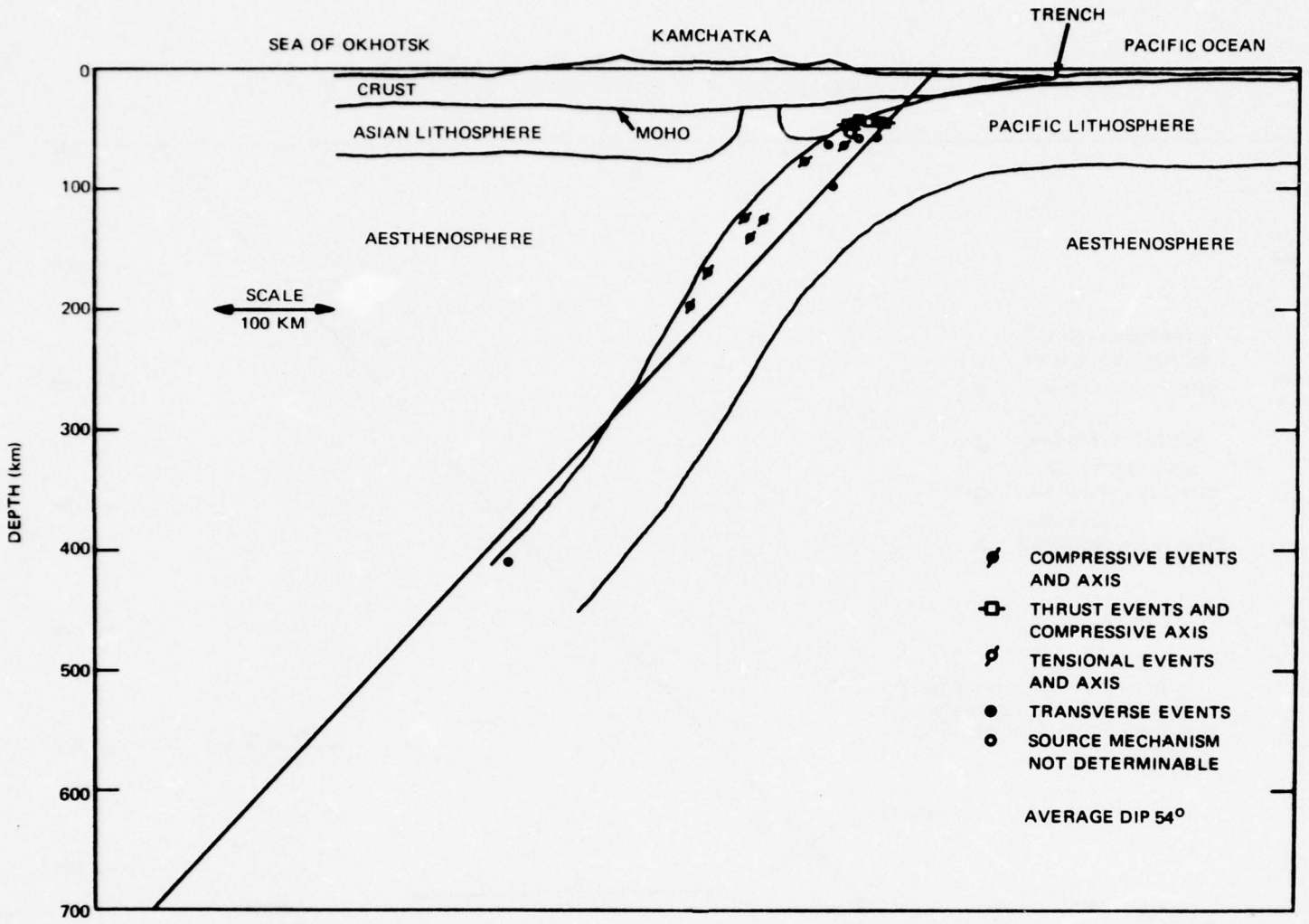

Figure 4 Schematic cross-section of Kamchatka Arc through 3-3 in Figure 1 (from Veith, 1974).

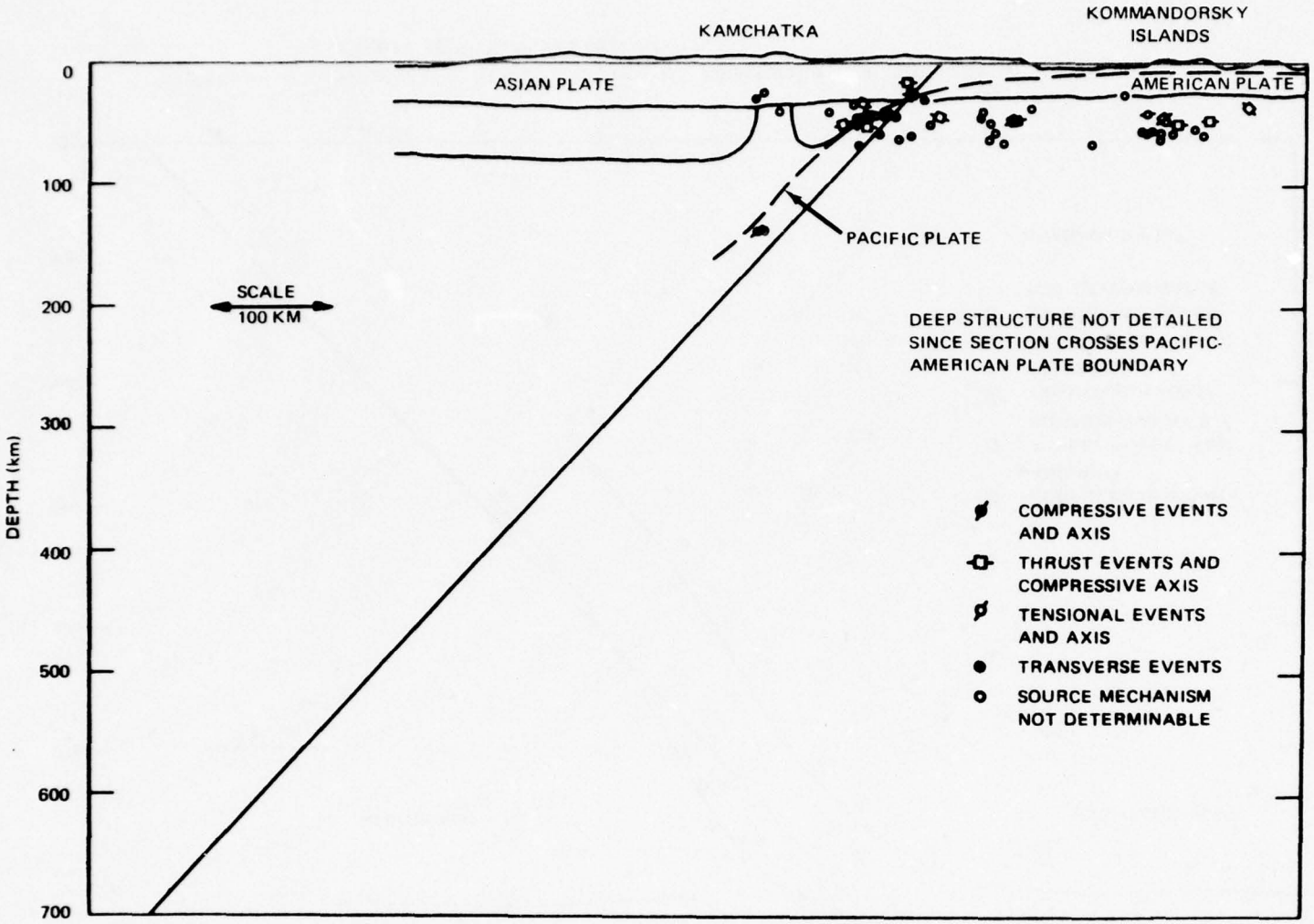

Figure 5 Schematic cross-section of Kamchatka Arc through 4-4 in Figure 1 (from Veith, 1974).

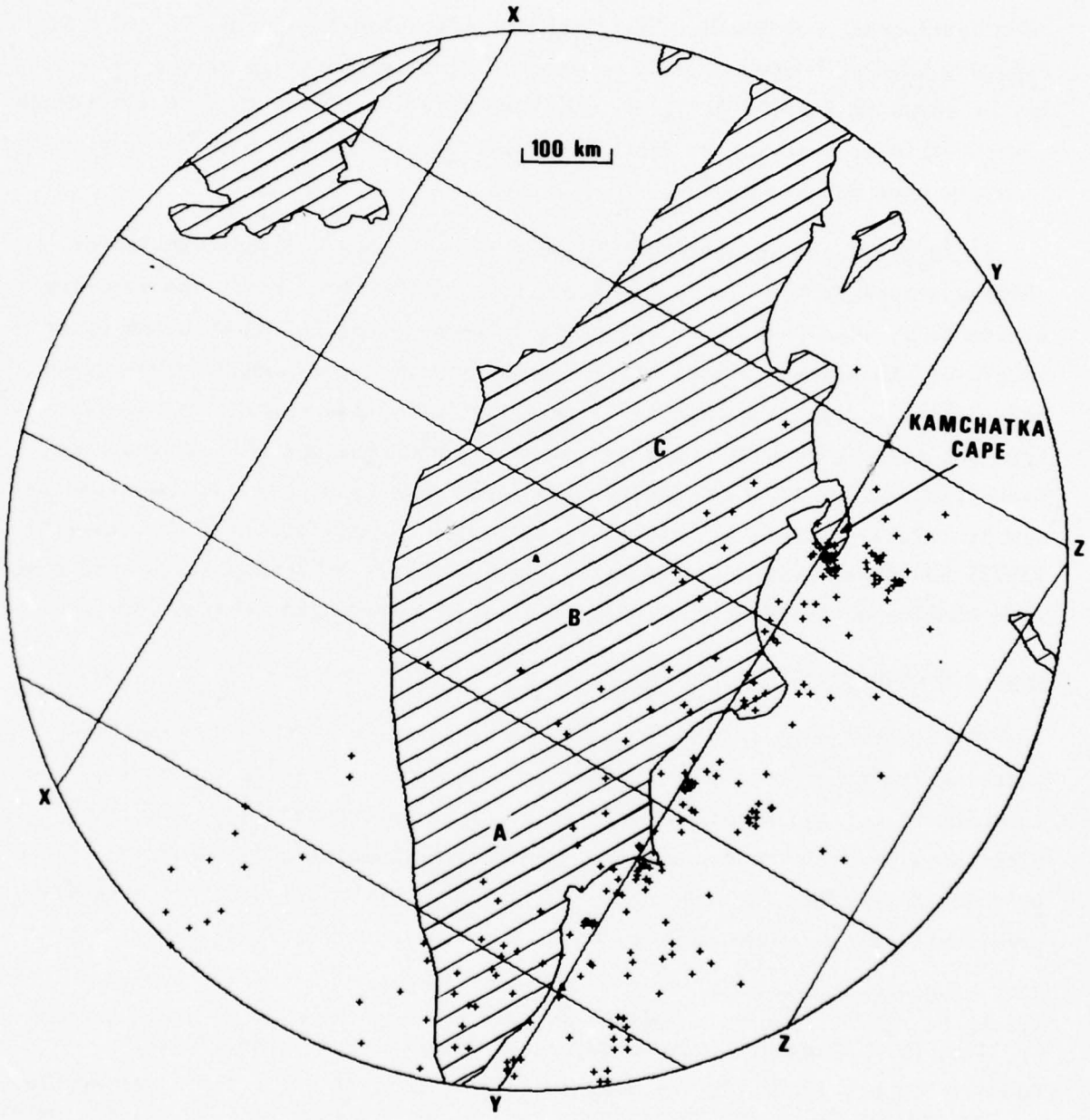

Figure 6 Plan view of seismicity in the Kamchatka Arc (NEIS epicenter file from 01/07/66 to 07/08/74).

section of the Aleutian Island structure with the Asian continent and is commonly regarded as a plate boundary. Figure 7 shows a vertical plot of all the seismicity in Figure 6. The line Y-Y of Figure 6 here translates to the zero horizontal coordinate. The roughly rectangular regions A, B, and C in Figure 6 have been used to define narrower vertical sections of the seismicity as shown in Figures 8, 9, and 10, respectively. These figures illustrate how the seismic activity at depth progressively abates NNE toward the plate boundary near Kamchatka Cape.

It is pertinent to note that Figures 7 to 10 give a distorted view of shallow seismicity due to hypocenter errors in the NEIS list. The majority of events at less than 30 km are probably deeper, coinciding with the upper margin of the dipping plate. Application of well-determined station-region travel-time corrections results in very little shallow seismicity inwards from the trench, most of which is associated with the volcanic activity on Kamchatka (Veith, 1974). Fedotov (1968) also suggests that shallow seismicity is relatively slight. In the tectonically similar Aleutian Arc, Engdahl (1972) has shown that there is very little activity at depths < 20 km and that this shallow activity is generally of lower magnitude than that of deeper events.

Source Mechanisms of Earthquakes

The relationship of source mechanism to position in the lithospheric plate is important to understanding the nature of earthquake activity in the Kamchatka Arc. The direction of motion of the earthquake foci associated with the dipping lithospheric plate confirm the idea of underthrusting of the oceanic plate under the continent. These earthquakes are mostly compressive events with the maximum compression axis almost horizontal and parallel to

---

Veith, K., 1974. The relationship of island arc seismicity to plate tectonics, Ph.D. Thesis, Southern Methodist University, Dallas, Texas.

Fedotov, S. A., 1968. On the deep structure, properties of the upper mantle, and volcanism of the Kuril-Kamchatka Island Arc according to seismic data, in The Crust and Upper Mantle of the Pacific Area, AGU Mono. 12, American Geophysical Union, Washington, D.C.

Engdahl, E. R., 1972. Seismic effect of the Milrow and Cannikin nuclear explosions, Bull. Seism. Soc. Am., v. 62, p. 1411-1424.

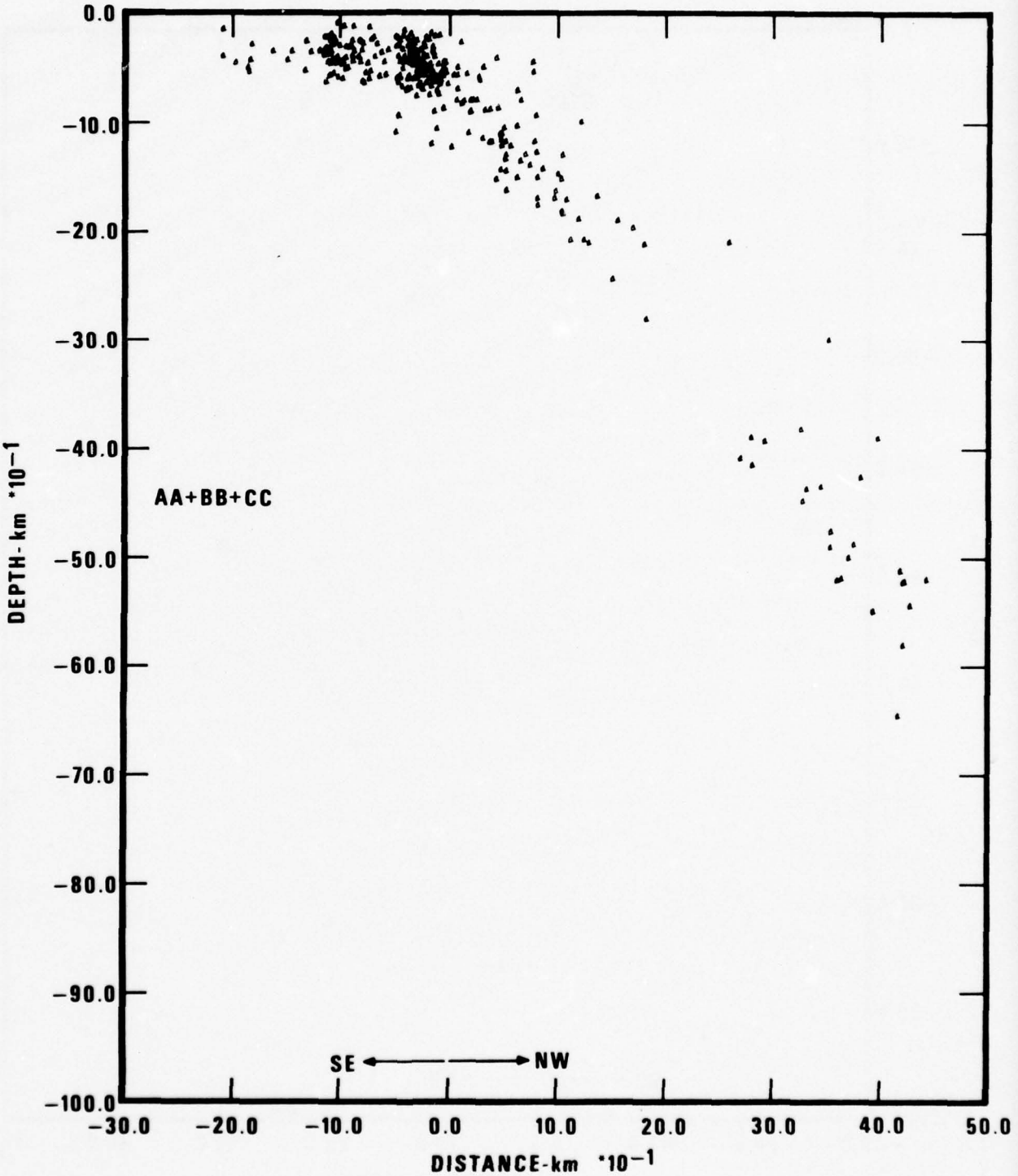

Figure 7 Cross-section view of all Kamchatka seismicity shown in Figure 6, as projected on a plane normal to the NNE tectonic trend.

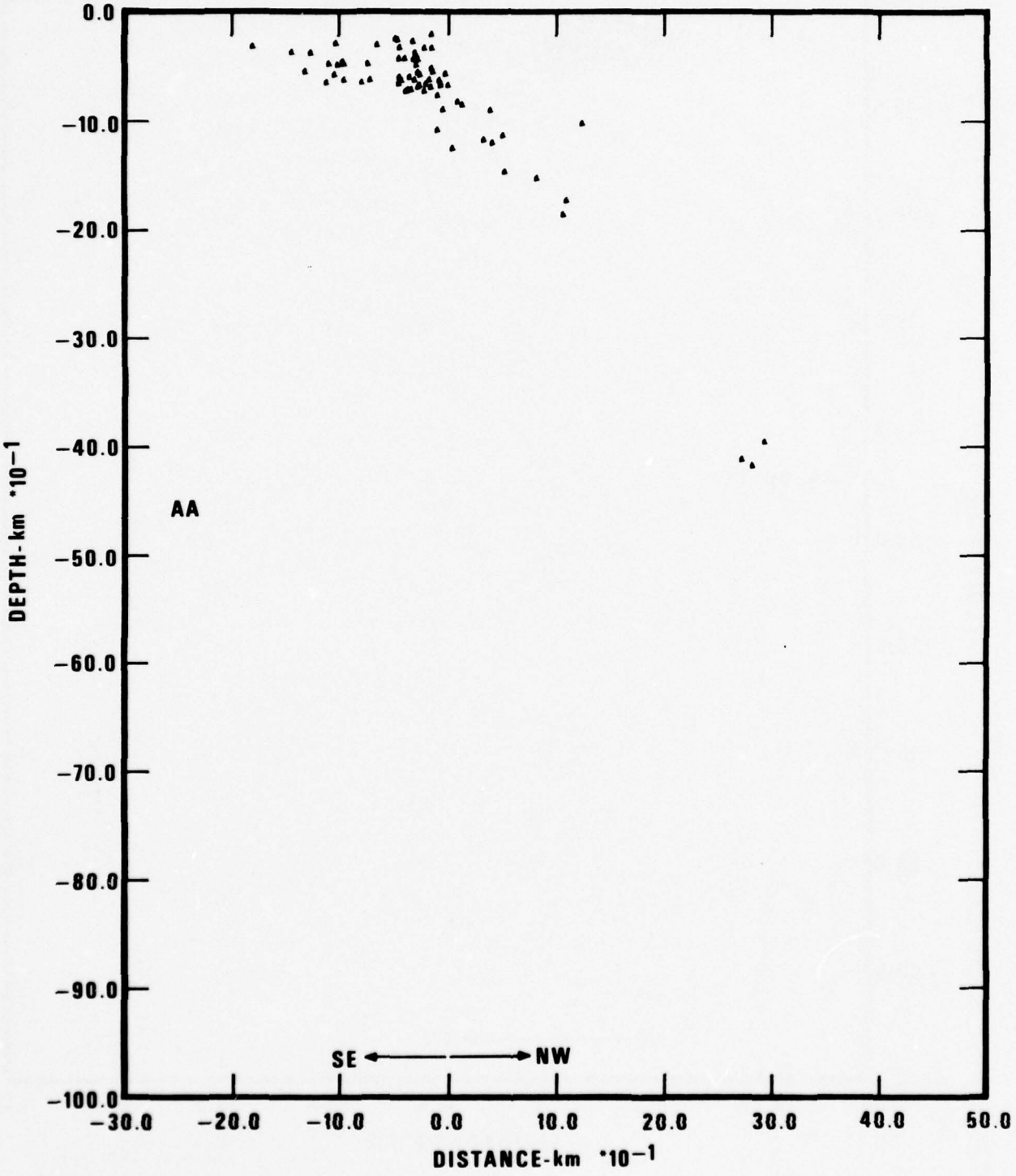

Figure 8 Cross-section of Kamchatka seismicity in region A of Figure 6.

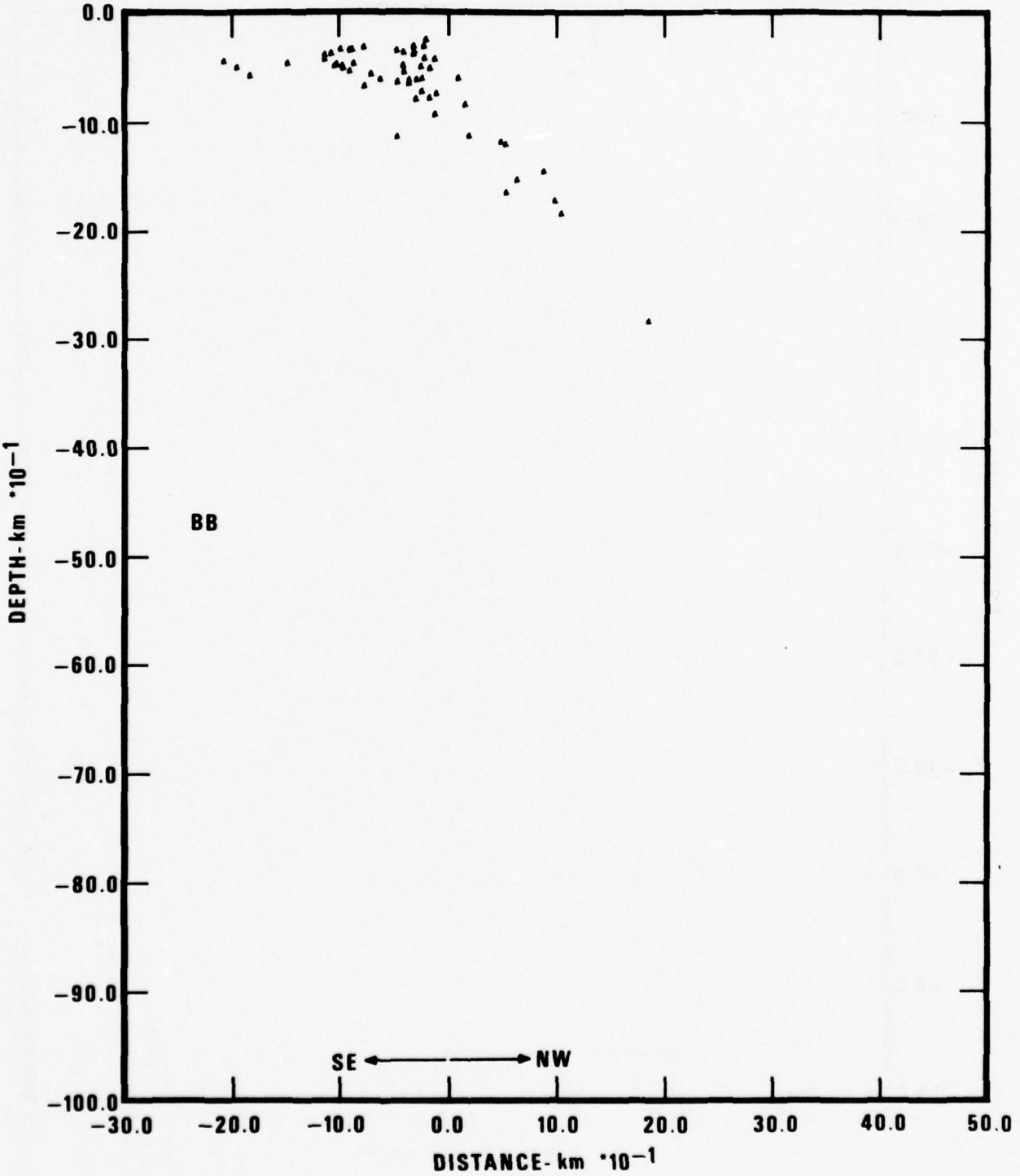

Figure 9 Cross-section of Kamchatka seismicity in region B of Figure 6.

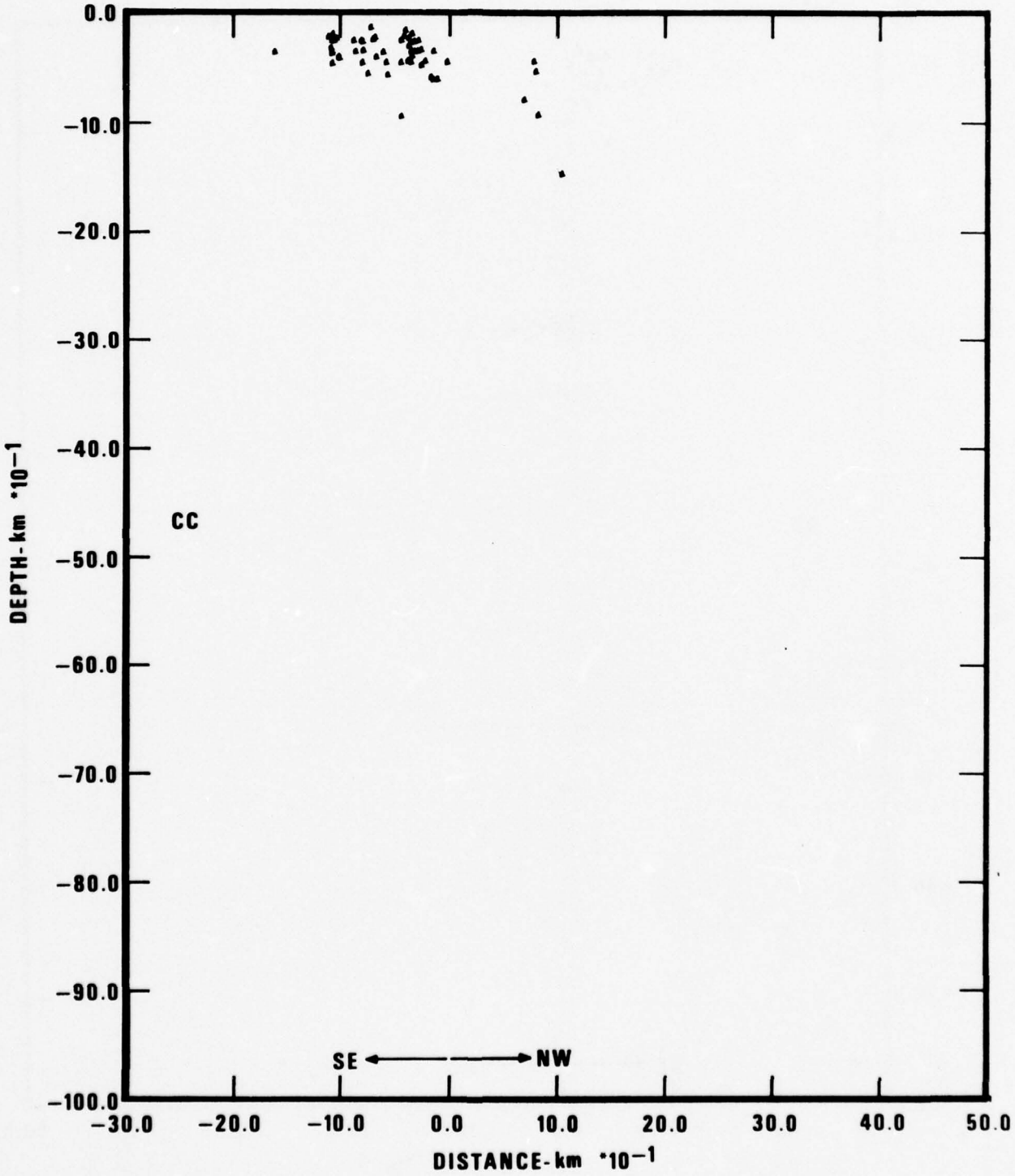

Figure 10 Cross-section of Kamchatka seismicity in region C of Figure 6.

the presumed dip direction of the plate. The focal mechanisms of earthquakes lying between the dipping plate and the surface are varied. Thrust faulting, the dominant type of faulting in this region, occurs along the zone of interaction between the two plates down to a depth of about 50 km. Transverse faulting occurs among independent plate segments of the arc (Veith, 1974). Figures 2 through 5 illustrate the relationship of source mechanism to position in the underthrusting plate.

Figure 11 illustrates a typical source mechanism for the events selected for this study. The earthquake fault plane strikes SSW parallel to the tectonic trend and dips approximately 25° in the WNW direction. These characteristic events are thrust faults with a slip angle of roughly 90 degrees. Note that the maximum of the P radiation pattern is downward, giving positive first motion to teleseismic signals.

Velocity Model

The velocity model for eastern Kamchatka was taken from Weizman (1966) for depth to 100 km, and from Veith (1974) for depths greater than 100 km. The velocity profile is shown in Table I; the crustal part is based on deep seismic sounding studies off the east coast of Kamchatka. As stated before, the earthquakes used in this study, when epicenter bias is accounted for, occurred just off the east coast of Kamchatka underneath the continental shelf. The depth of the water layer varies considerably over the presumed location of our events. It may be as little as 1 km or as much as 3 km, and thus, we have not included it in the model. For body-waves, the effect of this water layer should be to complicate pP waveforms, and for Rayleigh-waves, the effect should be negligible for periods greater than approximately 20 seconds.

Weizman, P., 1966. On the deep structure in the Kurile-Kamchatka region, in Continental Margins and Island Arcs, ed. W. Poole, Special Paper 66-15 Geological Survey of Canada, p. 244-251.

Veith, K., 1974. The relationship of island arc seismicity to plate tectonics, Ph.D. Thesis, Southern Methodist University, Dallas, Texas.

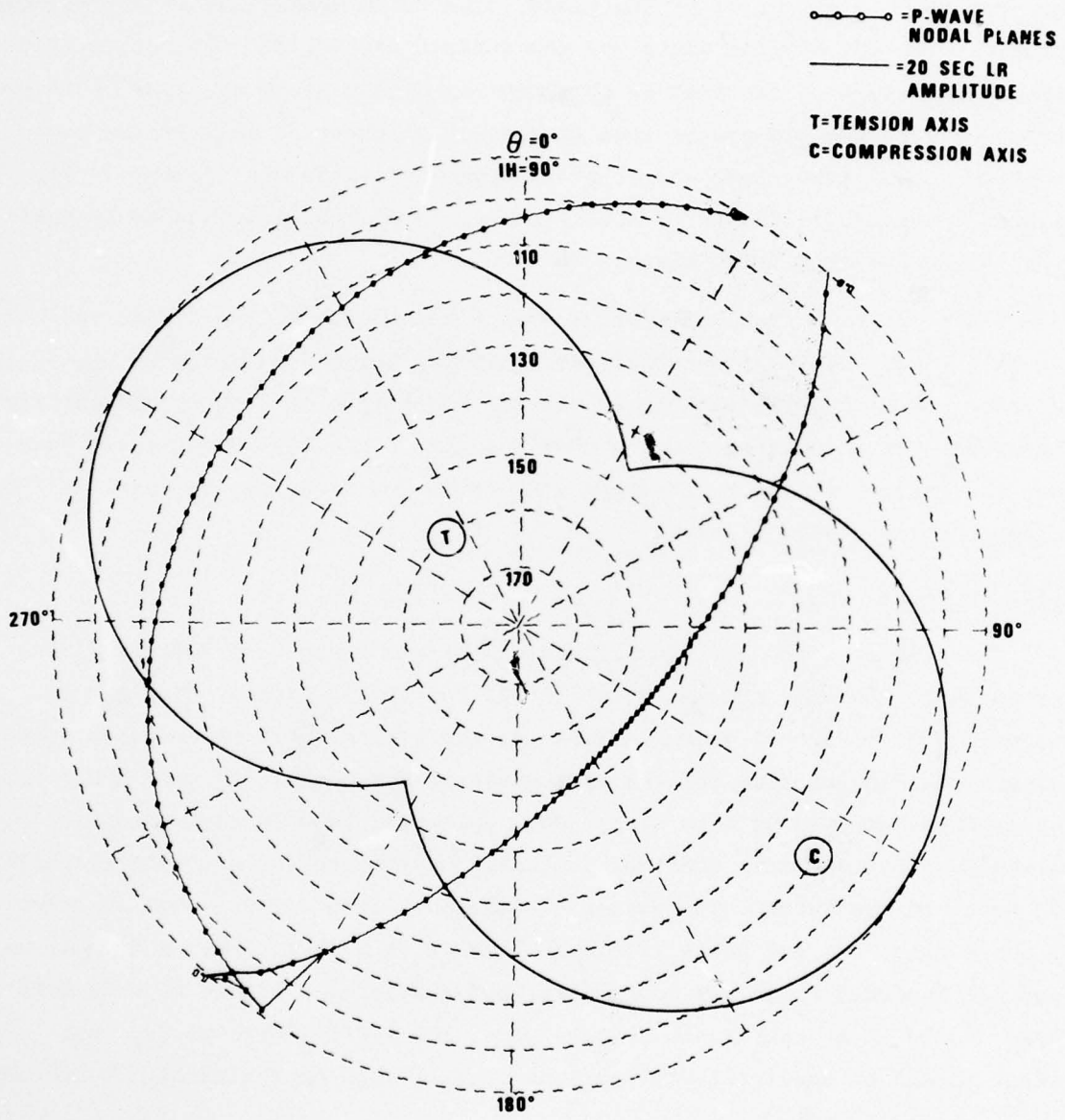

Figure 11 P-wave nodal planes projected on the lower half of the focal sphere and LR amplitude radiation pattern (T = 20 sec) for a typical thrust earthquake (Event 22) at shallow depth in the Kamchatka source region.

TABLE I

Velocity Structure off the East Coast of Kamchatka

Thickness (km)	V_p (km/sec)	V_s (km/sec)	Density (g/cm^3)
3	2.8	1.6	2.2
4	6.4	3.7	2.9
21	6.7	3.9	2.9
62	8.1	4.6	3.4
20	7.7	4.4	3.3
40	7.5	4.3	3.3
45	7.7	4.4	3.3
15	7.8	4.5	3.3
25	8.0	4.6	3.4
45	8.2	4.7	3.4
50	8.4	4.9	3.5
20	8.5	4.9	3.5
30	9.1	5.2	3.6
70	9.3	5.4	3.7
75	9.6	5.5	3.7
25	9.8	5.7	3.9
50	9.9	5.7	3.9
100	10.3	5.9	4.2

DATA

Earthquakes

Data for this report were selected through several criteria as follows. The paramount consideration was for earthquakes which had low reported M_s for their m_b since this relation is of high importance in discriminating earthquakes from explosions. Any events which would fall close to the explosion category on the basis of M_s-m_b must be necessarily resolved. In this regard, Blandford and Clark (1975) list a large group of earthquakes in Kamchatka, some of which apparently have low M_s relative to a global earthquake population; but their values are based on one station (LASA). A second criterion was shallow (<50 km) depth for the event; depths were confirmed by published ISC data or by LASA signals which contained a well-defined pP. A third criterion was that the earthquakes be large enough to yield multisite recordings with good signal/noise ratios. Only with the larger events could the objectives of this study be accomplished, and extrapolation of results to smaller events may not be justified. A fourth criterion was that the earthquakes be in the years 1971-1975 so that we could utilize data from the large seismic arrays and the HGLP network, both of which were present on digital tapes at the SDAC. The third criterion eliminated all but a few of the events in Blandford and Clark's list, and we supplemented them with two additional low M_s-m_b events from the NEIS list. One more event in our time period was selected from those with focal mechanisms determined by Stauder and Mualchin (1976). This event did not have a anomalous M_s-m_b relation, but was merely taken as a reference event. We selected then a total of 9 earthquakes as listed in Table II. Clearly, so few events cannot be claimed to represent the entire Kamchatka source region. However, we do claim that these events are representative of the type of earthquake there which will be most troublesome in any discrimination context. As will be demonstrated, these events

---

Blandford, R. R., and D. M. Clark, 1975. Variability of seismic waveforms at LASA from small subregions of Kamchatka, SDAC Report No. TR-75-10, Teledyne Geotech, Alexandria, Virginia.

Stauder, W., and L. Mualchin, 1975. Fault motion in the larger earthquakes of the Kurile-Kamchatka Arc and of the Kurile-Hokkaido Corner, J. Geophys. Res., v. 81, p. 297-308.

TABLE II

NEIS Parameters for Kamchatka Earthquakes

Event	Date	O.T.	Lat.	Lon.	Depth	m_b
8	1/25/73	18:32:27.4	54.570N	161.603E	31	5.3
12	6/9/73	22:45:58.9	52.911	160.080	33	5.4
16	11/3/73	00:19:51.5	54.618	161.447	40*	5.3
18	2/26/74	06:23:45.3	53.321	159.697	49	5.6
20	4/27/74	10:01:02,2	55.906	162.862	26	5.0
22	3/4/73	17:57:43.5	54.828	161.599	32	6.1
23	8/2/72	21:38:50.4	56.052	163.235	33	5.7
24	12/25/72	18:55:58.1	53.011	159.377	52	5.7
25	10/21/74	12:48:13.6	53.929	160.482	33	5.7

*Depth determined by this study. All other depths are from the NEIS list.

TABLE III

Usable Long-Period Digital Data for Selected Kamchatka Earthquakes

Event	ALPA	LASA	NORS	ALQ	CHG	CTA	EIL*	KIP	KON	MAT	OGD*	TLO	ZLP**
8	X	X			X			X	X				
12	X	X						X					
16		X	X	X				X		X			
18	X	X	X	X					X			X	
20		X	X						X	X			
22	X	X								X			
23						X		X				X	
24	X	X	X		X	X			X	X			
25	X	X	X					X		X		X	

*Unusable vertical components in all cases where recoverable

**S/N ratio too low in all cases where recoverable

have dominantly thrust motion on a shallow-dipping plane, precisely the sort of mechanism whose M_s-m_b relation Douglas et al. (1971) theoretically showed to be most likely confused with an explosion via M_s-m_b. Also the fact that teleseismic stations will all lie in a compressional quadrant of first motion (see Figure 11) means that rarefactions distinctive of earthquake sources may not be observed from most Kamchatka sources, as stressed by Evernden (1969).

Seismic Stations

Digital data from the three large arrays--LASA, ALPA, and NORSAR--and from the available HGLP stations were gathered for these events, and Table III shows the usable data from these sources. Usable data here implies recordings with measurable signals; however, most of the data omissions are due to an inability to recover a time series from the tapes and not due to undetected signals. The inability to consistently recover data from the HGLP network was unfortunate since lack of this data impeded certain portions of our study. We also ordered long-period and short-period film chips from several reliable sites in the WWSSN to supplement our magnitude calculations and focal mechanisms investigations.

Revision of Locations

An essential feature of the data base is reasonably accurate hypocenters for the events we have chosen. Although no large explosions have been detonated in Kamchatka with which to determine travel-time residuals, we know that due to the plate configuration and composition described above a uniform NW bias of locations should occur for our events. Such a bias toward the dipping side of the plate has been documented for the explosion LONG SHOT in the Aleutian Arc (Herrin and Taggart, 1968), which has a similar structure. Another part of the location problem is the fact that the NEIS locations are

---

Douglas, A., J. A. Hudson, and V. K. Kembhavi, 1971. The relative excitation of seismic surface and body-waves by point sources, Geophys. J., v. 23, p. 451, 460.

Evernden, J., 1969. Identification of earthquakes and explosions by use of teleseismic data. J. Geophys. Res., v. 74, p. 3828-3856.

Herrin, E., and J. N. Taggart, 1968. Source bias in epicenter determination Bull. Seism. Soc. Am., v. 58, p. 1791-1796.

not based on a station set identical for all the events, thus introducing a random error to the locations. The final problem with the NEIS epicenters is the lack of depth control.

With these problems in mind, we first attempted to establish the depths of the events. Using readings from the WWSSN and the exceptionally good pP phases at LASA, we calculated depths which, except for one case, did not differ appreciably (>5 km) from the NEIS depths listed in Table II. The one event for which we changed the depth, 11/03/73, was originally 61 km on the NEIS list. A check of the available ISC bulletins showed good consistency between their depths estimates and those of the NEIS, with no more than 8 km discrepancy. The three 33 km depths in Table II were found to be reasonable even though they were undoubtedly "normal" depths routinely assigned to events whose depth becomes negative in the hypocenter calculation by NEIS. Thus, overall we accept the NEIS depths as sufficiently accurate for our purposes; they indicate that these earthquakes occur near the top of the actively descending Pacific plate and are consistent with the depth range of those earthquakes identified as thrust events by Veith (1974) which are illustrated in Figures 2 to 5.

With these depths held restrained, we proceeded to relocate the events with a common network of 13 stations which generally allowed accurate measurements of P arrival times. There were some missing data, and so travel-time residuals were obtained from a master event, in this case the 03/04/73 earthquake since it was the largest of the group, and applied to the remainder of the available arrival times at each station. Events were then relocated relative to this master event. This procedure clearly does not remove any systematic epicenter bias from the events. According to Veith's (1974) work we estimate that systematic bias for our group is roughly 50 km WNW perpendicular to the trend of the dipping plate. The NEIS epicenters as listed in Table II were corrected for this estimated bias before being plotted in Figure 1. Epicenter bias was not removed in Figures 2 through 10 where all the

---

Veith, K., 1974. The relationship of island arc seismicity to plate tectonics, Ph.D. Thesis, Southern Methodist University, Dallas, Texas.

other events were plotted strictly according to the NEIS locations which are biased by an amount depending on their location within the seismic zone (Veith, 1974).

Veith, K., 1974. The relationship of island arc seismicity to plate tectonics, Ph.D. Thesis, Southern Methodist University, Dallas, Texas.

SIGNAL ANALYSIS

In this section we identify the effects of source mechanism and propagation path on the observed body-wave and surface-wave phases from the eastern Kamchatka events. All these events are assumed to be thrust faults, although we have a well-defined source mechanism for only one--the 03/04/73 event (Stauder and Mualchin, 1976). Assuming a source mechanism, one can predict the radiation pattern for body-wave and surface-wave phases. Assuming a near field displacement waveform for the source model, a crustal model at the source, and the attenuation along the propagation path, we will create theoretical body-wave seismograms and compare them to the observed signals. Surface-wave ray tracing for 20-second Rayleigh waves will be compared to observed amplitudes, and average short-period attenuation along paths from Kamchatka to LASA and NORSAR will also be determined.

Source Effects

Determination of the fault planes for earthquakes whose magnitude is below 6.0 is generally not reliable with teleseismic data; and, except for our 03/04/73 reference event with mechanism already determined, all of our earthquakes have $m_b < 6$. The mechanism of the 03/04/73 event is shown in Figure 11. Veith (1974) has determined focal mechanisms for many earthquakes of $m_b < 6$ in Kamchatka using a combination of local and regional data from USSR stations and teleseismic data. By personal communication, Veith has confirmed in a preliminary sense that the other eight events used here are largely of the same thrust mechanism as the 03/04/73 event. We have plotted first motions read from selected WWSSN, HGLP, and array recordings in Figure 12 for the other eight events selected for study. Here the usual problems of inconsistency among short-period first motions is evident. It is impossible on the basis of these plots alone to determine any fault planes; but we can state that, in general, the data do not contradict a thrust mechanism such as shown in Figure 11 for the 03/04/73 event.

Stauder, W., and L. Mualchin, 1976. Fault motion in the larger earthquakes of the Kurile-Kamchatka Arc and of the Kurile-Hokkaido Corner, J. Geophys. Res., v. 81, p. 297-308.

Veith, K., 1974. The relationship of island arc seismicity to plate tectonics, Ph.D. Thesis, Southern Methodist University, Dallas, Texas.

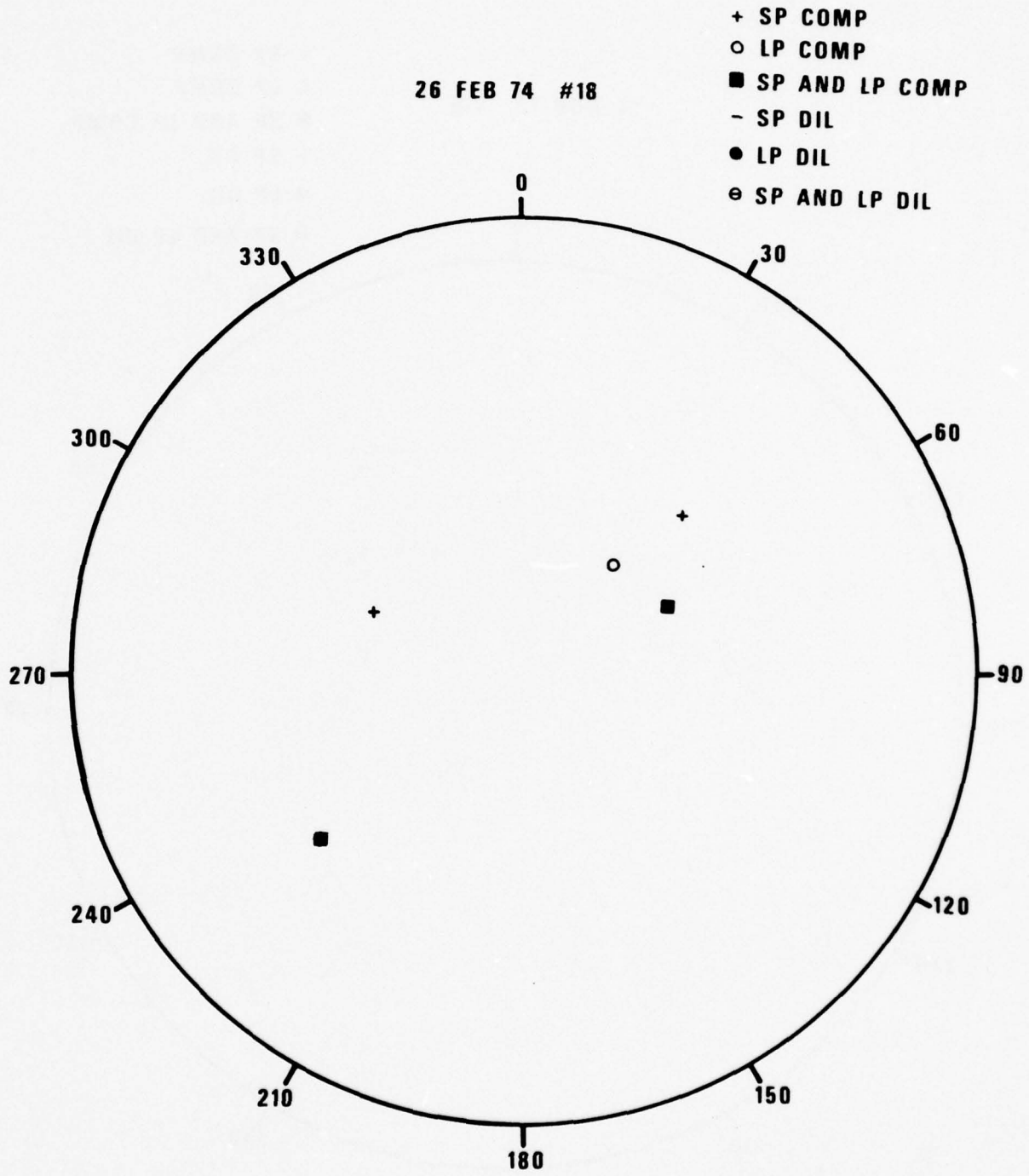

Figure 12 First motions for Kamchatka earthquakes in the lower half of the focal sphere (Wulff net).

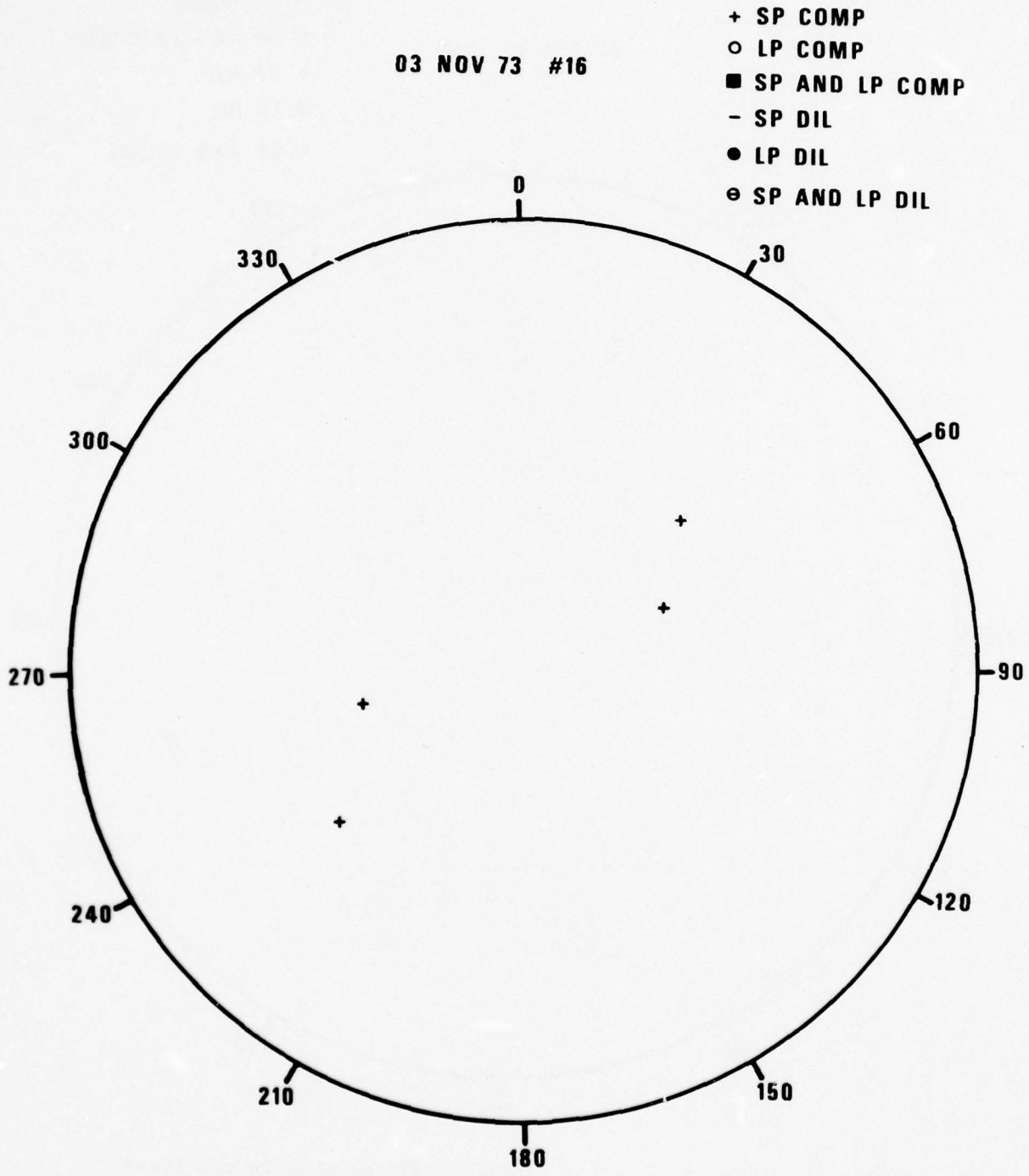

Figure 12 (Cont.) First motions for Kamchatka earthquakes in the lower half of the focal sphere (Wulff net).

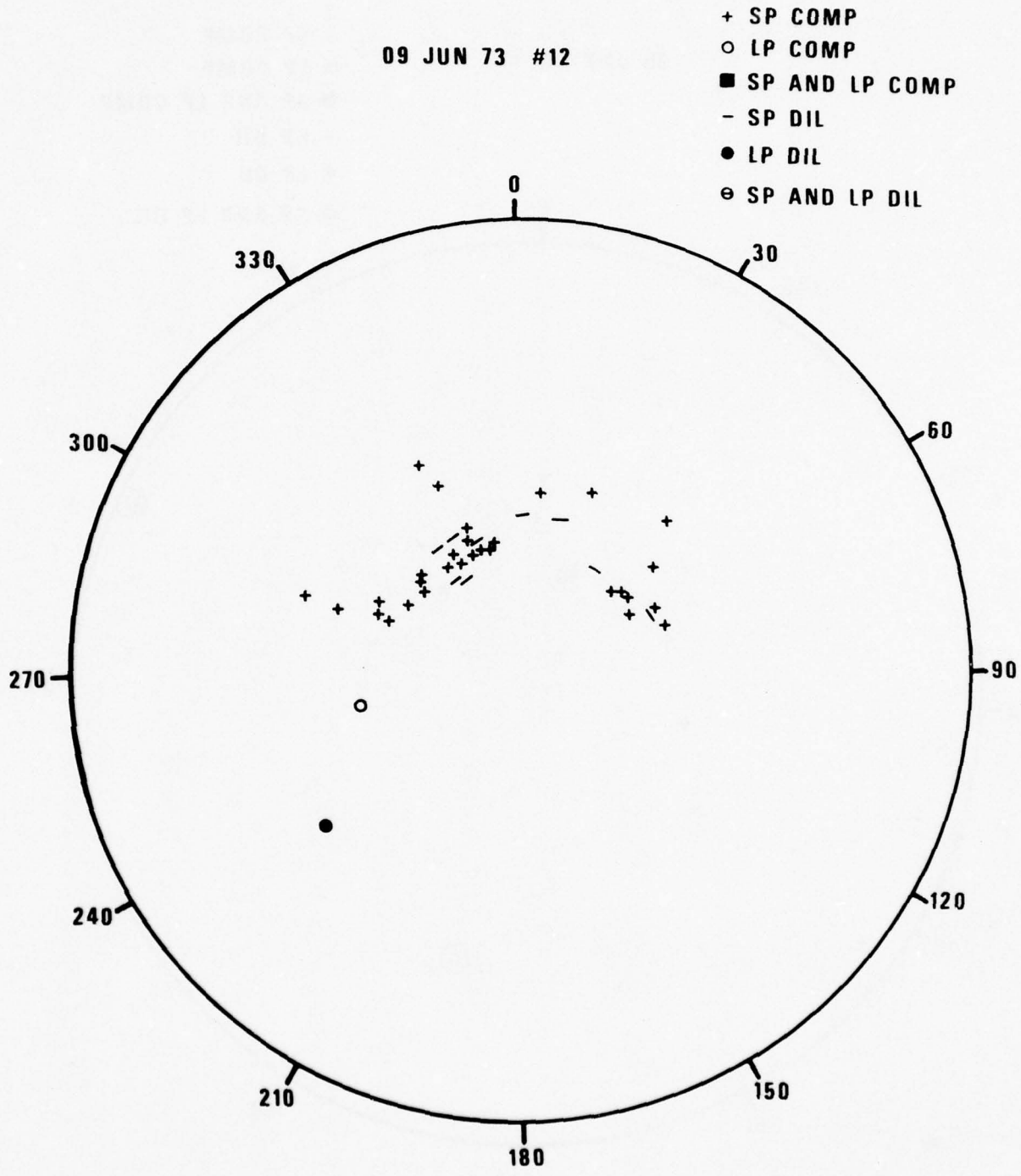

Figure 12 (Cont.) First motions for Kamchatka earthquakes in the lower hemisphere of the focal sphere (Wulff net).

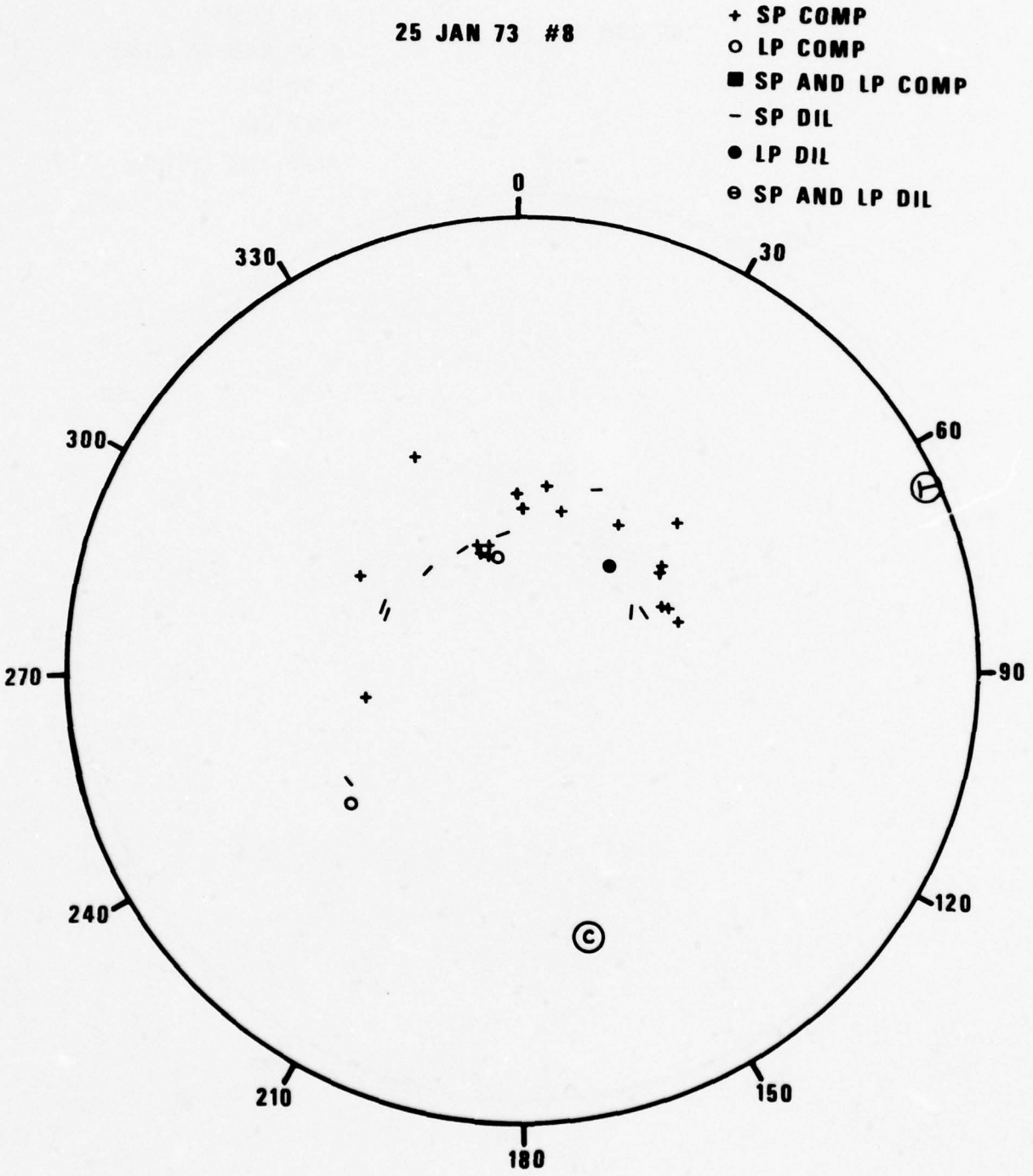

Figure 12 (Cont.) First motions for Kamchatka earthquakes in the lower half of the focal sphere (Wulff net).

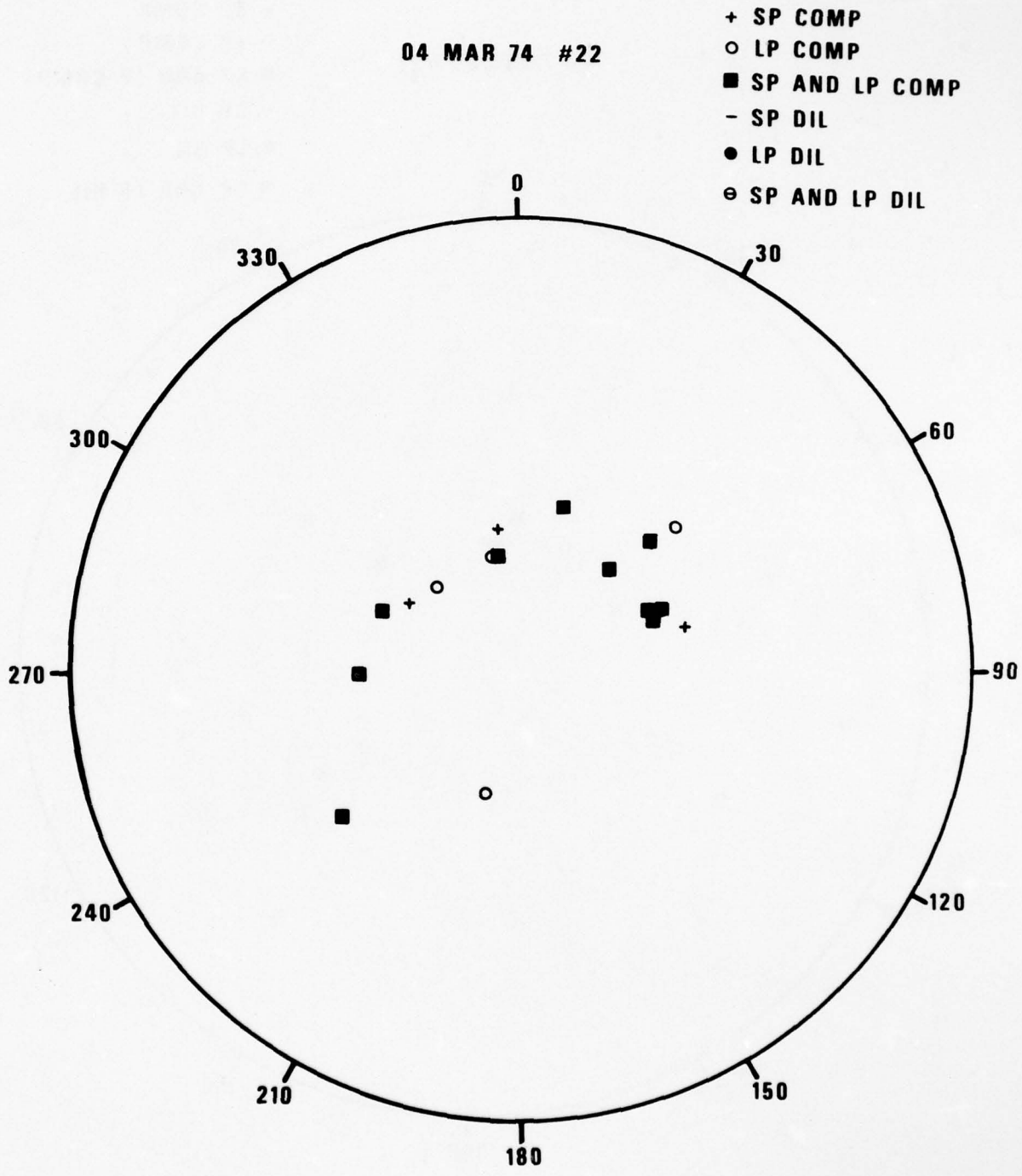

Figure 12 (Cont.) First motions for Kamchatka earthquakes in the lower half of the focal sphere (Wulff net).

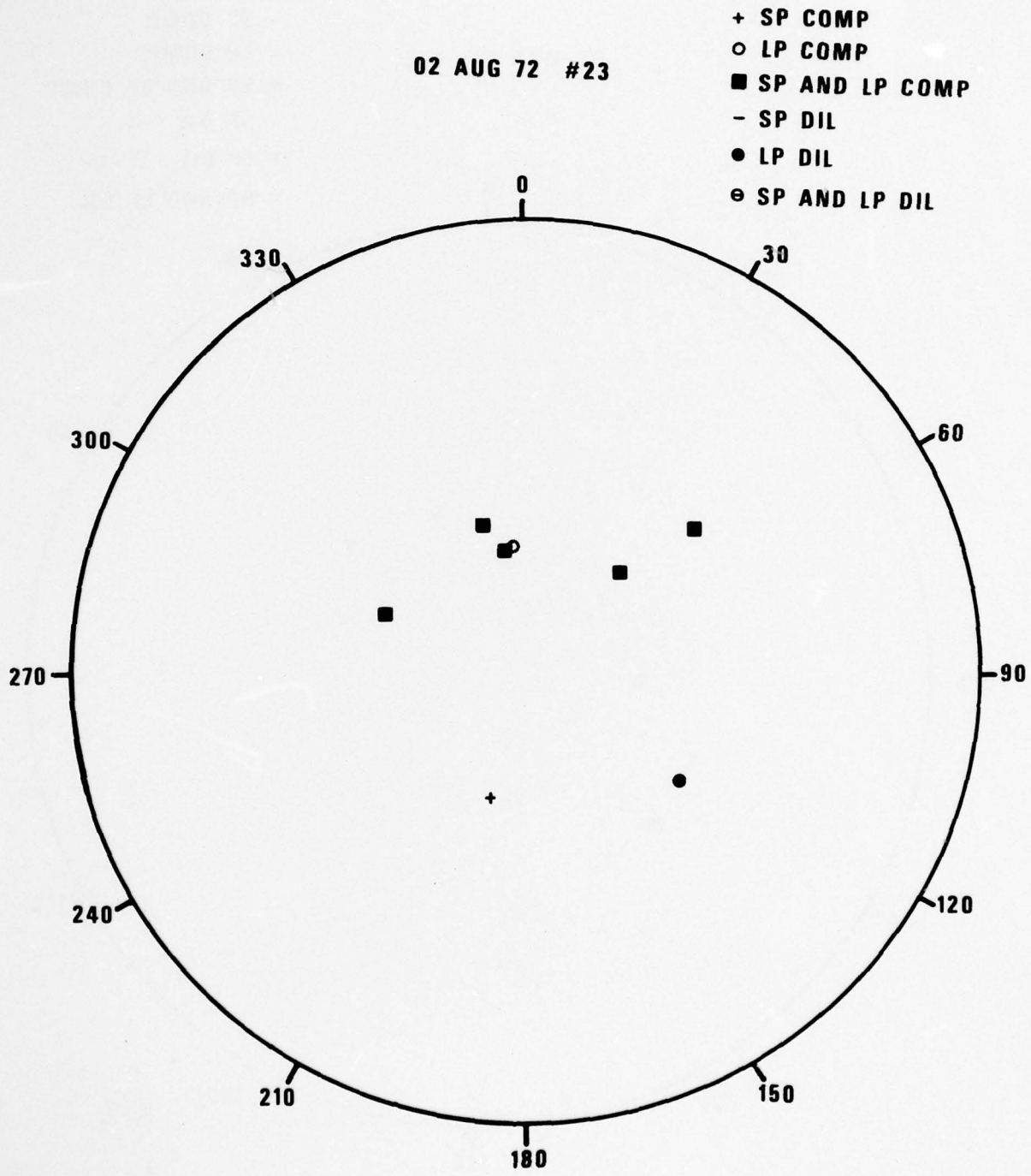

Figure 12 (Cont.) First motions for Kamchatka earthquakes in the lower half of the focal sphere (Wulff net).

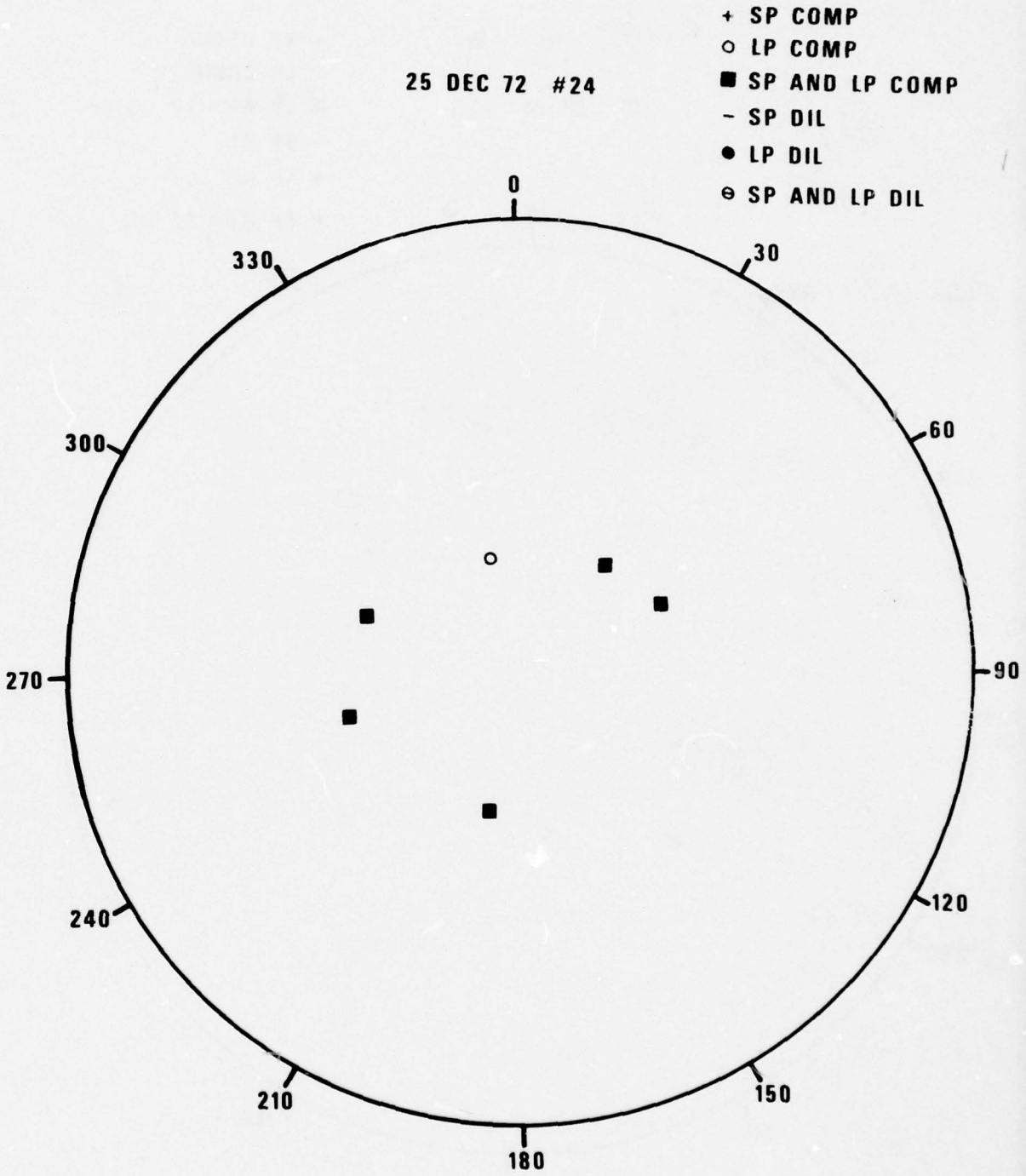

Figure 12 (Cont.) First motions for Kamchatka earthquakes in the lower half of the focal sphere (Wulff net).

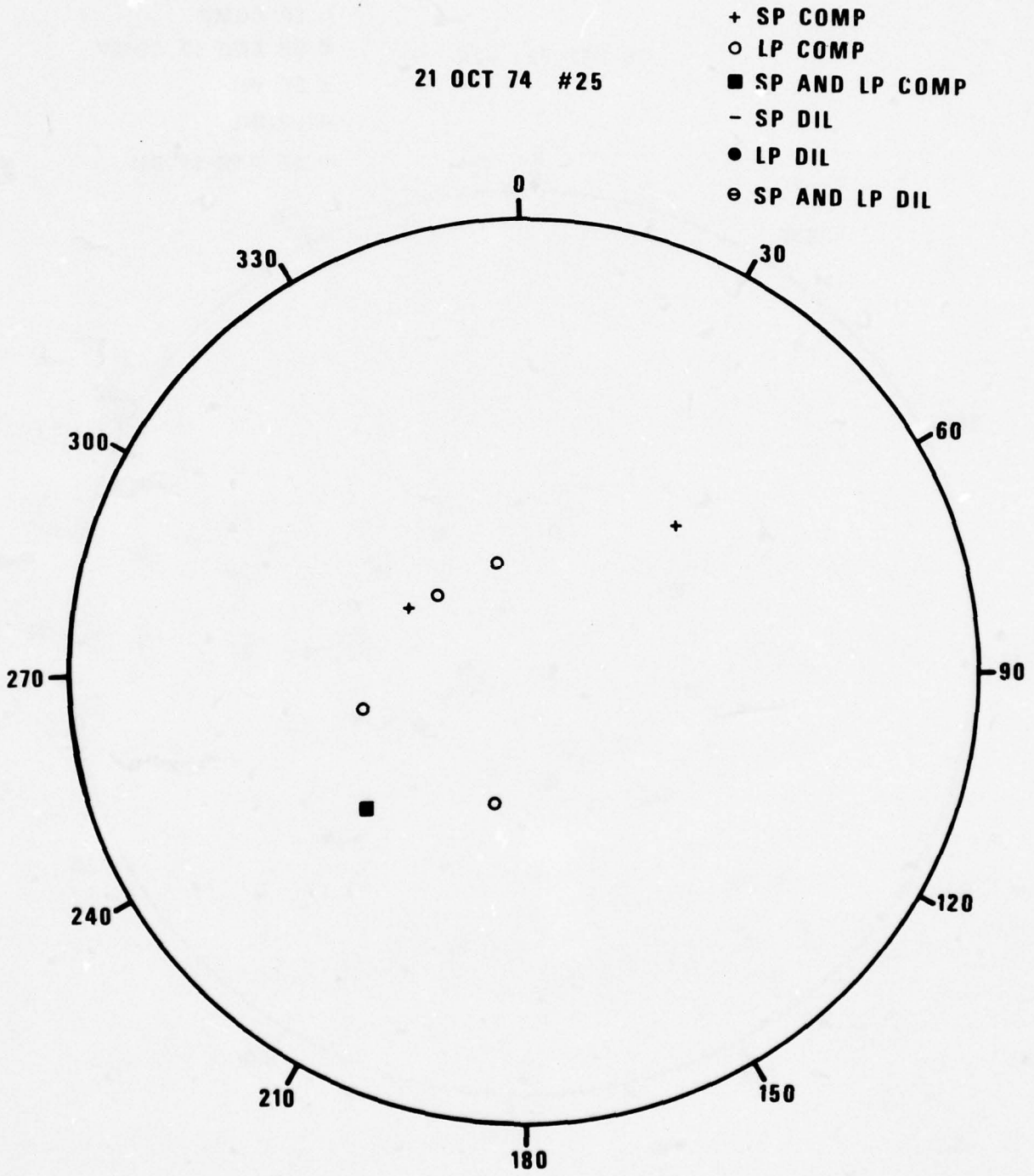

Figure 12 (Cont.) First motions for Kamchatka earthquakes in the lower half of the focal sphere (Wulff net).

We first consider the source mechanism among factors contributing to the observations made in a discrimination context. Presuming that our events are thrust type on shallow faults, having $\lambda = 90°$, $\delta = 25°$ with the fault strike aligned with the general tectonic trend at $\theta = 210°$, we can calculate theoretical M_s-m_b parameters and other signal properties as a function of receiver location. Calculations of the LR spectral displacement for a constant seismic moment at a period of 20 seconds for this mechanism, taken as a point source imbedded in the Kamchatka model given in Table I, a function of source depth as shown in Figure 13. We have also calculated the average excitation over all $0° < \delta < 90°$ for comparison. For each calculation, the azimuthal radiation pattern has been averaged using 5° increments of azimuth. Now we consider an explosion represented by three mutually orthogonal dipoles, with the moment of each equal to that of each of the two couples representing the earthquake and calculate its excitation at depths of 0 and 2.5 km in this same structure. Figure 13 indicates that the earthquake LR excitation at depths between 20 and 40 km (the depth range of events selected for this study) is roughly one-half of an explosion of equal moment. Considering P-waves, for excitation at frequencies lower than the corner frequency characteristic of the source dimensions, the spectral amplitude can be related to the seismic moment M_o as:

$$|\hat{u}_o| \simeq \frac{M_o}{4\pi\rho\alpha^3 r} R_{\theta\phi}$$

where ρ is density, α is compressional-wave velocity, and r is distance in a homogeneous full space. For an earthquake, $R_{\theta\phi}$ is a function of λ and δ and θ. For our selected events though, Figure 11 previously showed that the teleseismic stations lie near the maximum of a compressional quadrant of the focal sphere; and so $R_{\theta\phi} \simeq 1$ is a fair approximation for our purposes. Thus, on this simple basis, we predict that an explosion in Kamchatka would generate LR amplitude twice as large as an equivalent-moment earthquake such as we are considering.

We have neglected some important effects though, in this simple calculation. The interference of pP on explosion signals can change m_b by as much as as 0.2 (Douglas et al., 1971), the value of $\rho\alpha^3$ in the above equation will

---

Douglas, A., J. A. Hudson, and V. K. Kembhavi, 1971. The relative excitation of seismic surface and body-waves by point sources, J. Geophys. Res., v. 23, p. 451, 460.

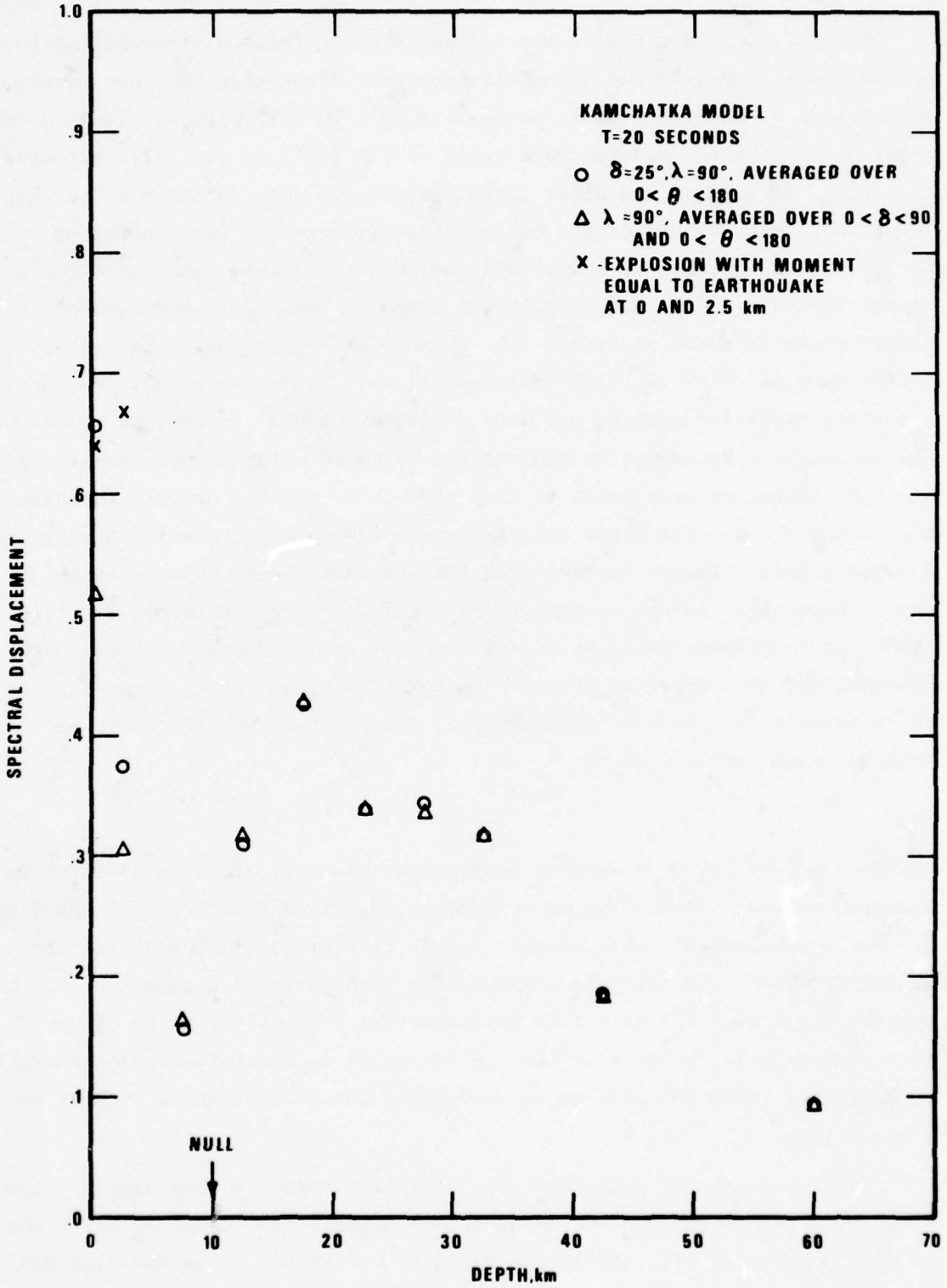

Figure 13 Theoretical LR excitation (T = 20 sec) for events of constant seismic moment at various depths in a Kamchatka earth model.

differ between an explosion at the surface and an earthquake at 30 km depth the intensity of the P-wave entering the mantle for the explosion detonated in rock of lower α will be less than the earthquake due to progressive refraction of the wavefront in the upper layers, i.e., a larger spreading effect, and the corner frequency of the earthquakes will undoubtedly be lower than that of an explosion with equivalent m_b. Although the precise quantification of all these effects requires more knowledge of this source region than we have been able to gather, we will attempt to estimate some of them as follows.

The effect of $\rho\alpha^3$ on the P-wave amplitude has been shown by Hudson and Douglas (1975) to be significant for the short-period band of the spectrum where m_b is usually measured. Using a program which generates synthetic seismograms (Der and McElfresh, 1976) for earthquakes and explosions, we have computed the P-wave amplitude in several seismometer passbands for pure dilatational sources of unit moment at various depths in our Kamchatka model. The measured amplitudes on synthesized WWSSN short-period, WWSSN long-period, and HGLP long-period seismograms are plotted in Figures 14, 15, and 16, respectively. The largest difference between surface sources and upper mantle sources is seen on the short-period WWSSN system although that on the long-period WWSSN is nearly as large because of its small negative slope in amplitude response vs. frequency. The important feature here is the one-half unit drop in m_b between a source near the surface in a medium with ρ = 2.2, α = 2.8, and any source in the basement rock or below. Without making the computations, we presume that such differences would also hold for double-couple sources. For the HGLP response, the dominant recorded period is nearly an order of magnitude larger than that on the WWSSN seismograms; and the m_b actually increases with depth of source, presumably due to the effects of pP modulation in the teleseismic spectrum.

Douglas, A., J. A. Hudson, and V. K. Kembhavi, 1971. The relative excitation of seismic surface and body-waves by point sources, J. Geophys. Res., v. 23, p. 451, 460.

Der, Z. A., and T. W. McElfresh, 1976. PSV--a program to compute synthetic seismograms, unpublished manuscripts, Teledyne Geotech, Alexandria, Virginia.

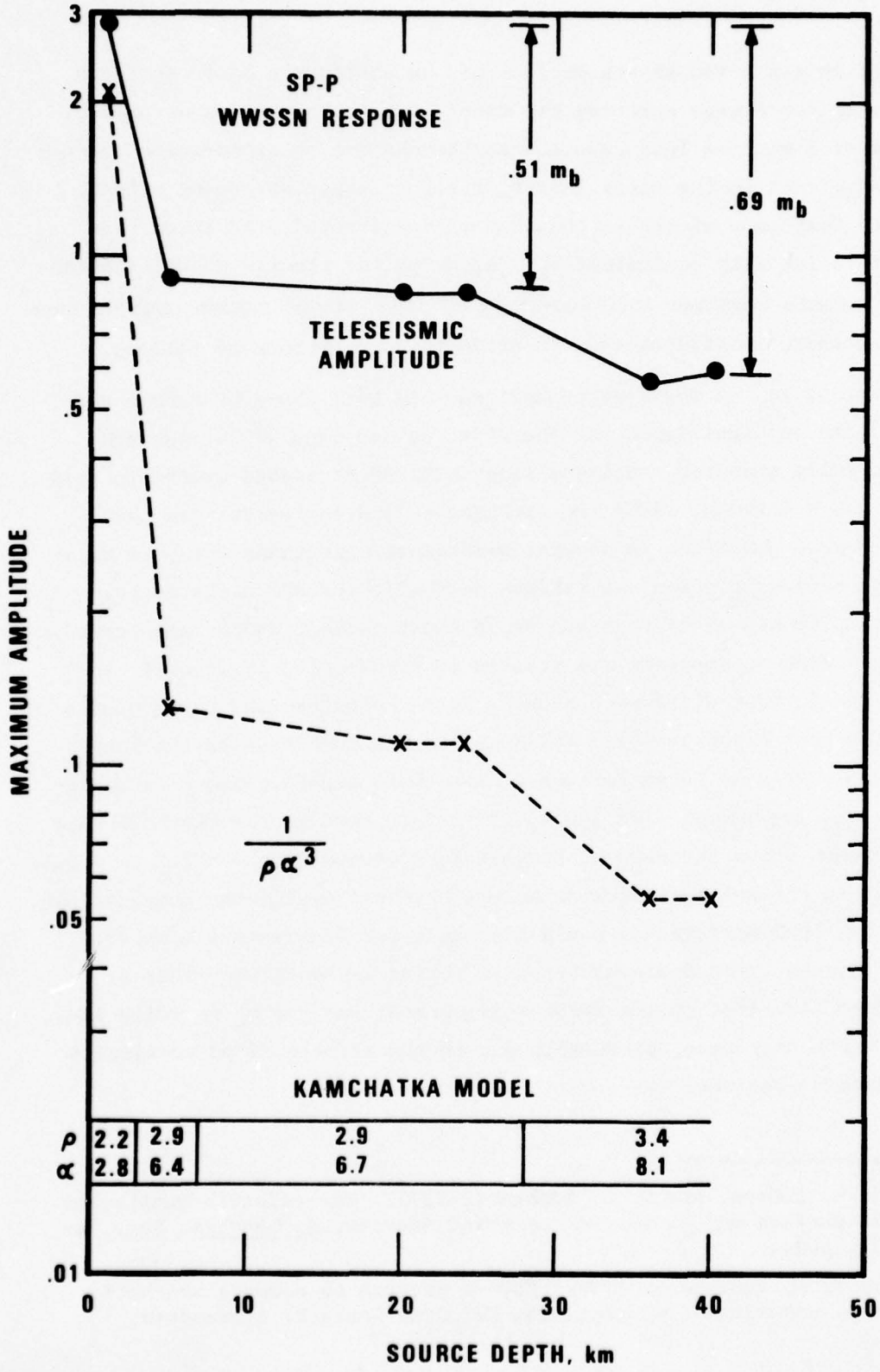

Figure 14 Teleseismic P-wave amplitude on WWSSN short-period recordings for dilatational sources at various depths in Kamchatka.

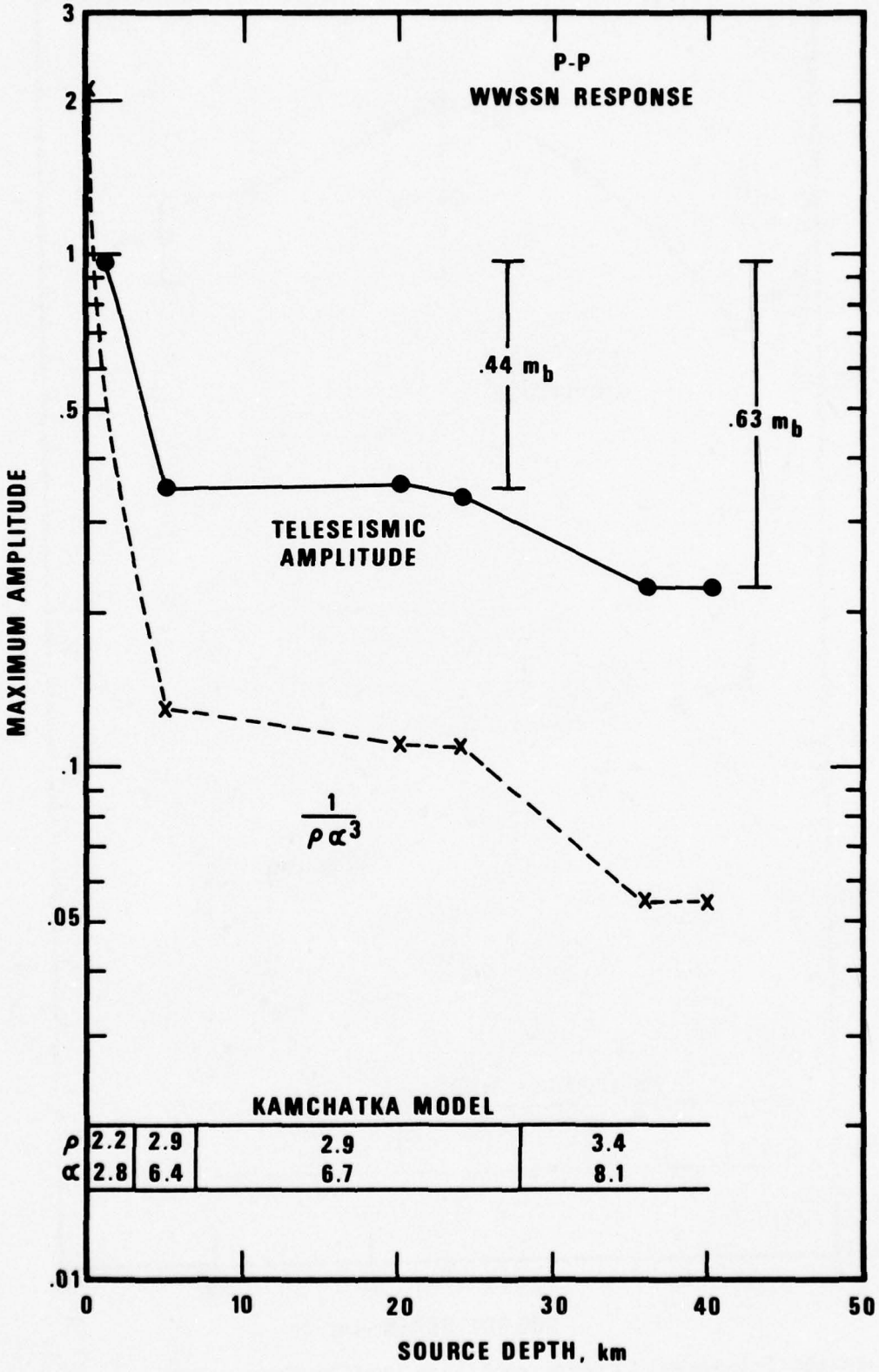

Figure 15 Teleseismic P-wave amplitude on WWSSN long-period recordings for dilatational sources at various depths in Kamchatka.

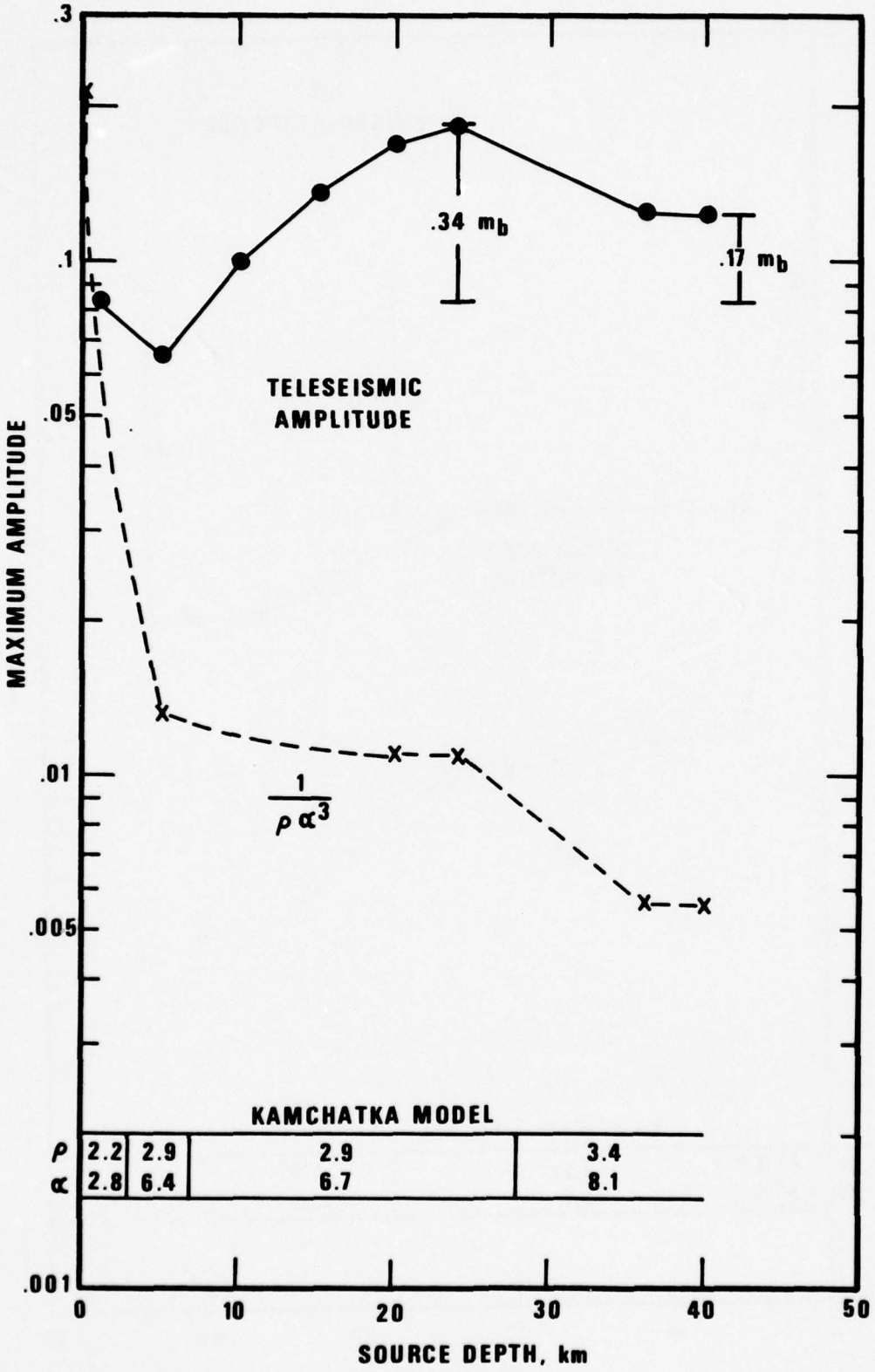

Figure 16 Teleseismic P-wave amplitude on HGLP long-period recordings for dilatational sources at various depths in Kamchatka.

Corner frequencies and moments for our Kamchatka events have also been estimated from LASA spectra which are shown in Figure 17. These spectra are composites from the long-period A0 seismometer and short-period A0 subarray; the frequency at which they were joined is .3 cps, and the short-period and long-period sample lengths were 6.4 and 64 seconds respectively. Only five of our events were of sufficient S/N ratio to determine the long-period P spectra. Attenuation was removed from the spectra by multiplying by the factor $\exp[\pi f t^*]$ with a t^* of .25, a value derived later in this report. Corner frequencies were estimated on the basis of complete stress drop and an f^{-3} asymptotic relation at high frequencies. Seismic moment was calculated using the relation

$$M_o = 4\pi\rho\alpha^3 r|\hat{u}_o|/R_{\theta\phi}$$

where $R_{\theta\phi}$ was assumed to be unity, values of $\rho\alpha^3$ from Table I appropriate to the source depth were used, and spherical divergence was substituted for r. We have estimated $|\hat{u}_o|$ essentially from the part of the spectrum at > .3 hz, choosing to ignore the longer periods where pP modulation may affect the level appreciably. A graph of moment vs. corner frequency is shown in Figure 18. In reference to constant stress-drop lines indicated by Hanks and Thatcher (1972), our events appear to be of intermediate stress drop.

We note the peculiar behavior of the Kamchatka spectra above the apparent corner frequency. The spectra generally drop rapidly at roughly $\hat{u} \propto f^{-3}$ and then level off to $\hat{u} \propto f^{-2}$ or less between 2 and 5 cps. The S/N ratio is adequate out to 5 hz to define the spectra; and unless the Q is frequency dependent, we may be seeing evidence of a number of subearthquakes with larger corner frequencies boosting the high-frequency portion of the spectra as suggested by Blandford (1975).

As a test of the adequacy of our earth model for our Kamchatka events, synthetic seismograms have been computed for the 03/04/73 earthquake using a computer program based on the reciprocity theorem (Lee and Teng, 1973;

Blandford, R. R., 1975. A source theory for complex earthquakes, Bull. Seism. Soc. Am., v. 65, p. 1385-1406.

Lee, T., and T. Teng, 1973. Polar radiation patterns of P and SV-waves in a multi-layered medium, Bull. Seism. Soc. Am., v. 63, p. 547.

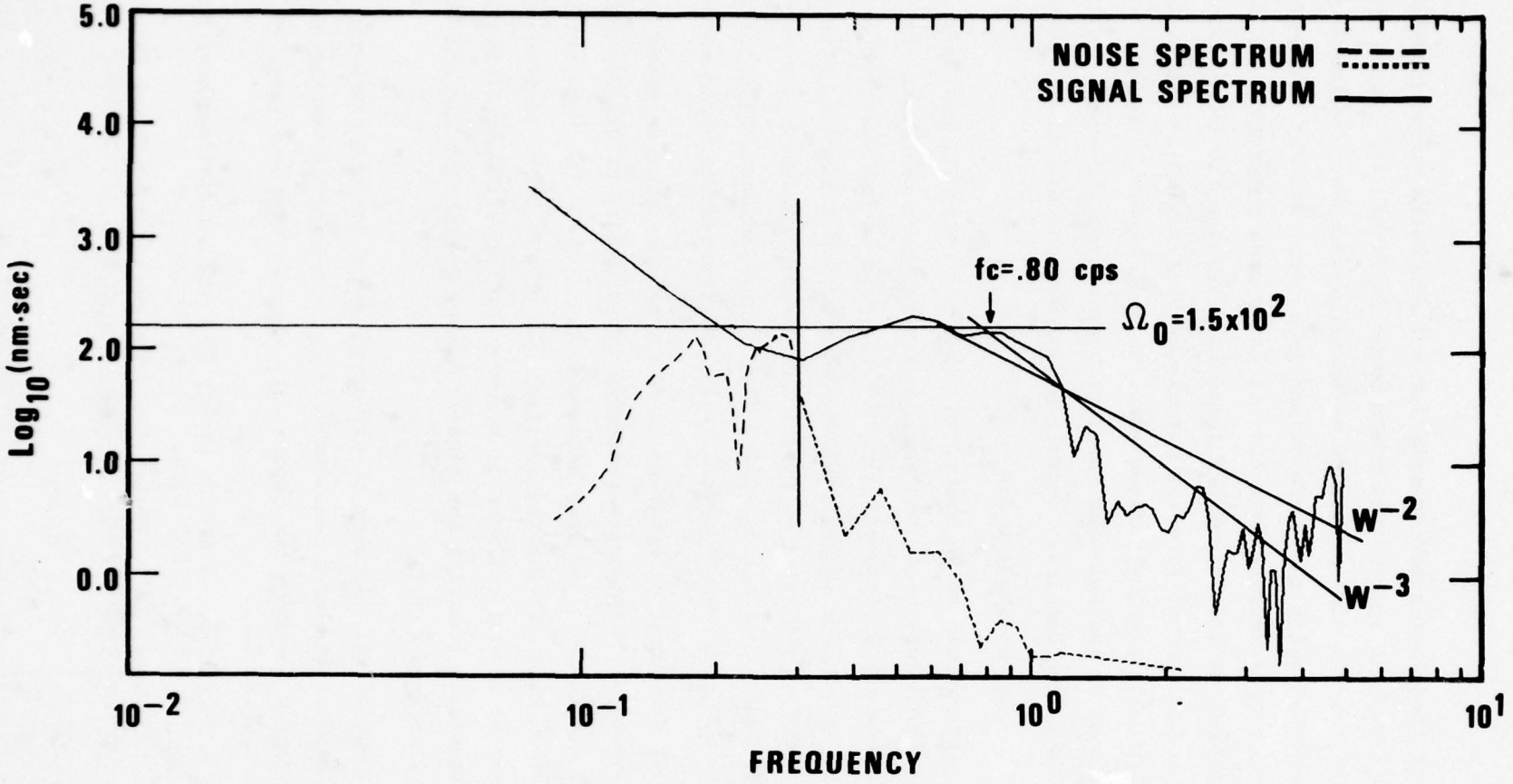

Figure 17 LASA AO subarray spectra of P-waves from Kamchatka earthquakes with instrument response and attenuation removed (t* = .25).

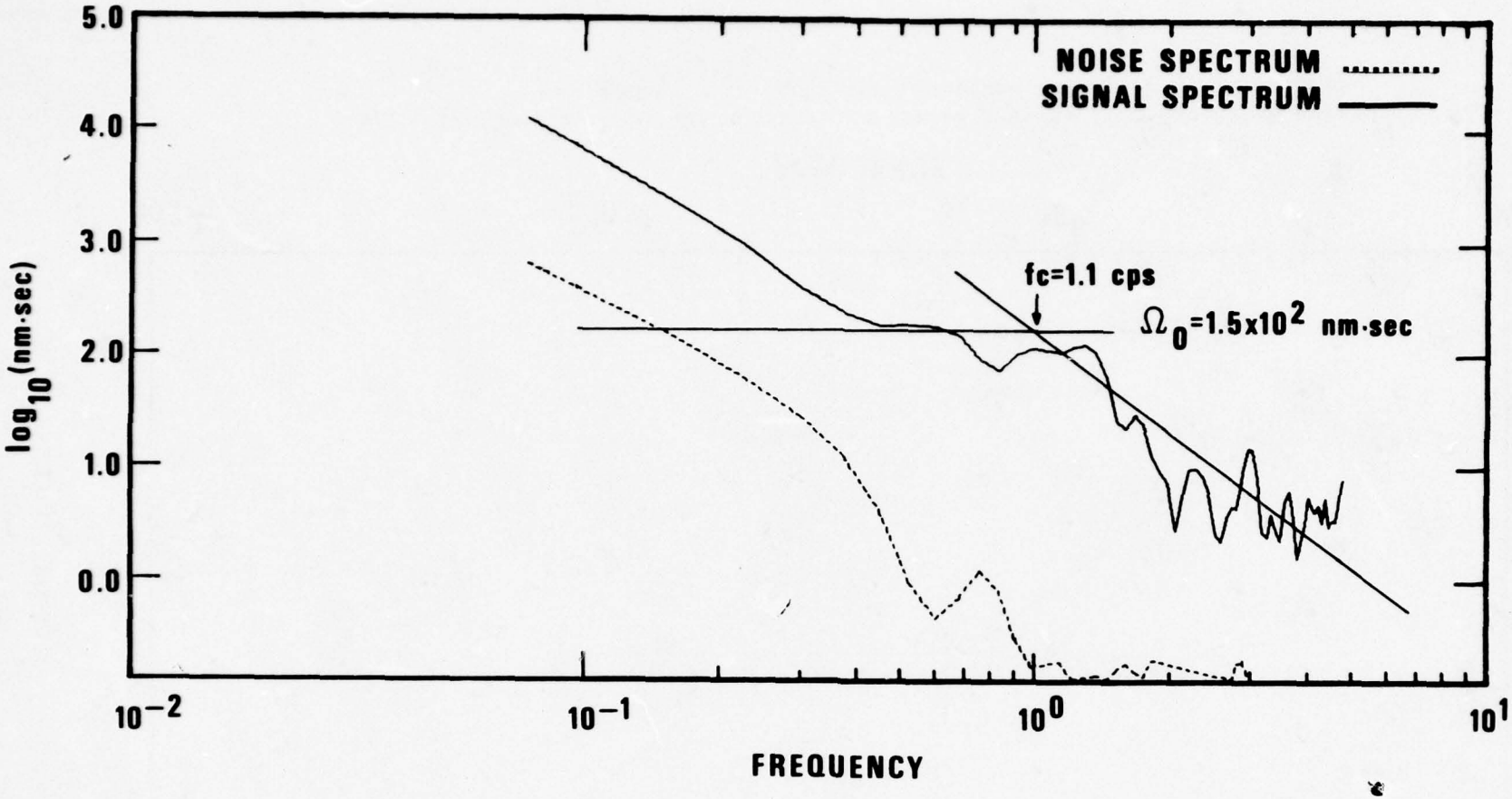

Figure 17 (Cont.) LASA AO subarray spectra of P-waves from Kamchatka earthquakes with instrument response and attenuation removed ($t^* = .25$).

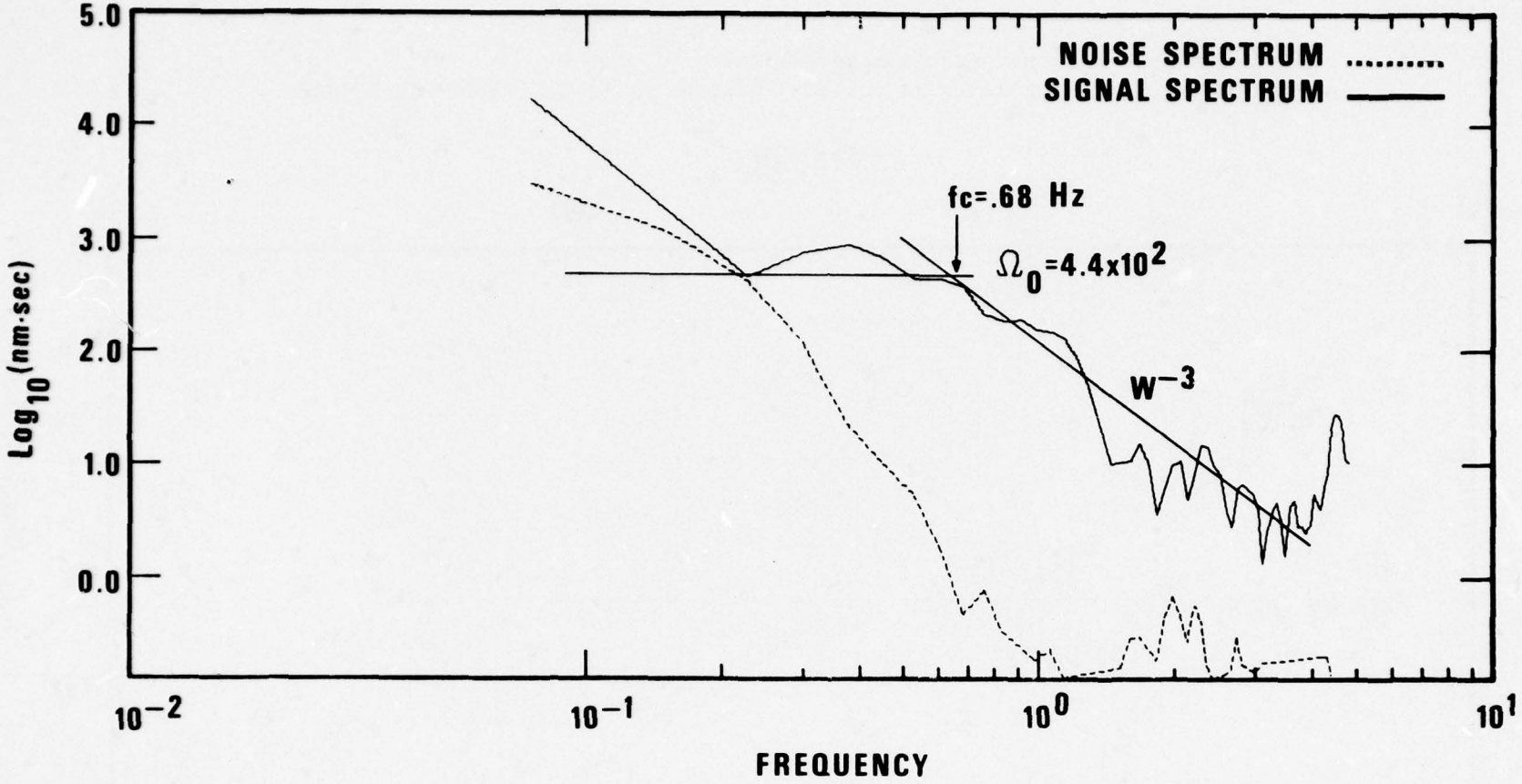

Figure 17 (Cont.) LASA A0 subarray spectra of P-waves from Kamchatka earthquakes with instrument response and attenuation removed (t* = .25).

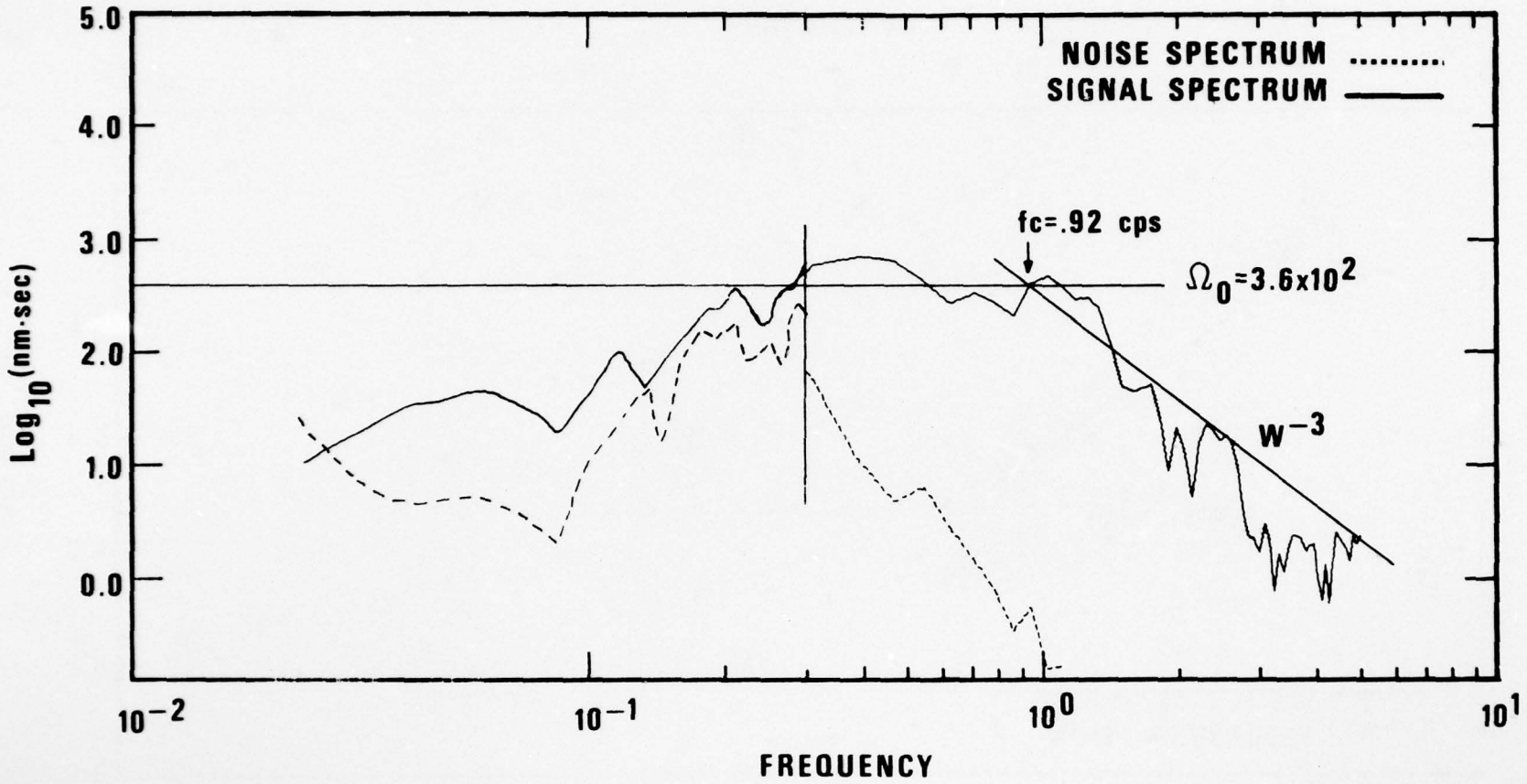

Figure 17 (Cont.) LASA A0 subarray spectra of P-waves from Kamchatka earthquakes with instrument response and attenuation removed ($t^* = .25$).

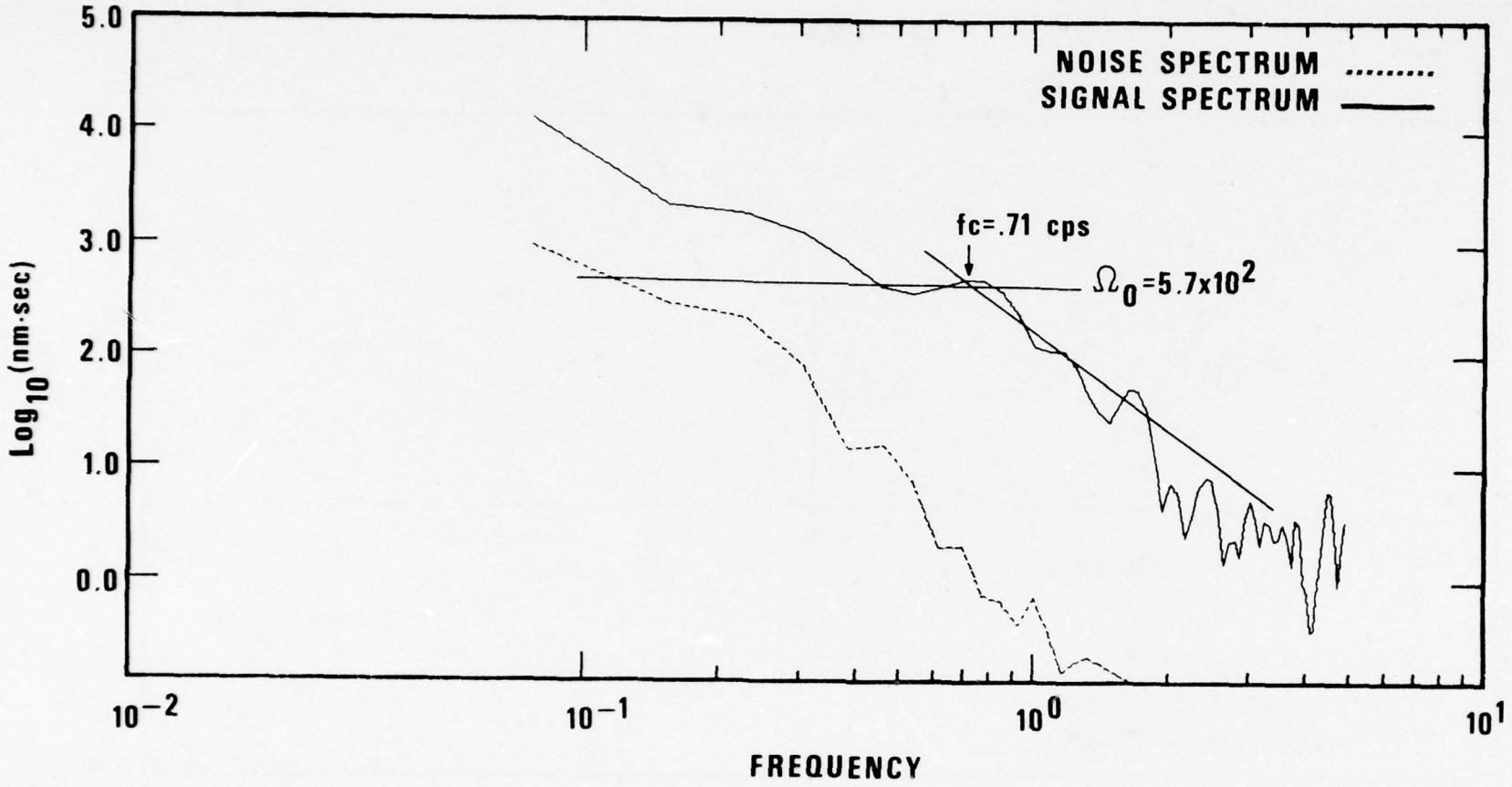

Figure 17 (Cont.) LASA A0 subarray spectra of P-waves from Kamchatka earthquakes with instrument response and attenuation removed (t* = .25).

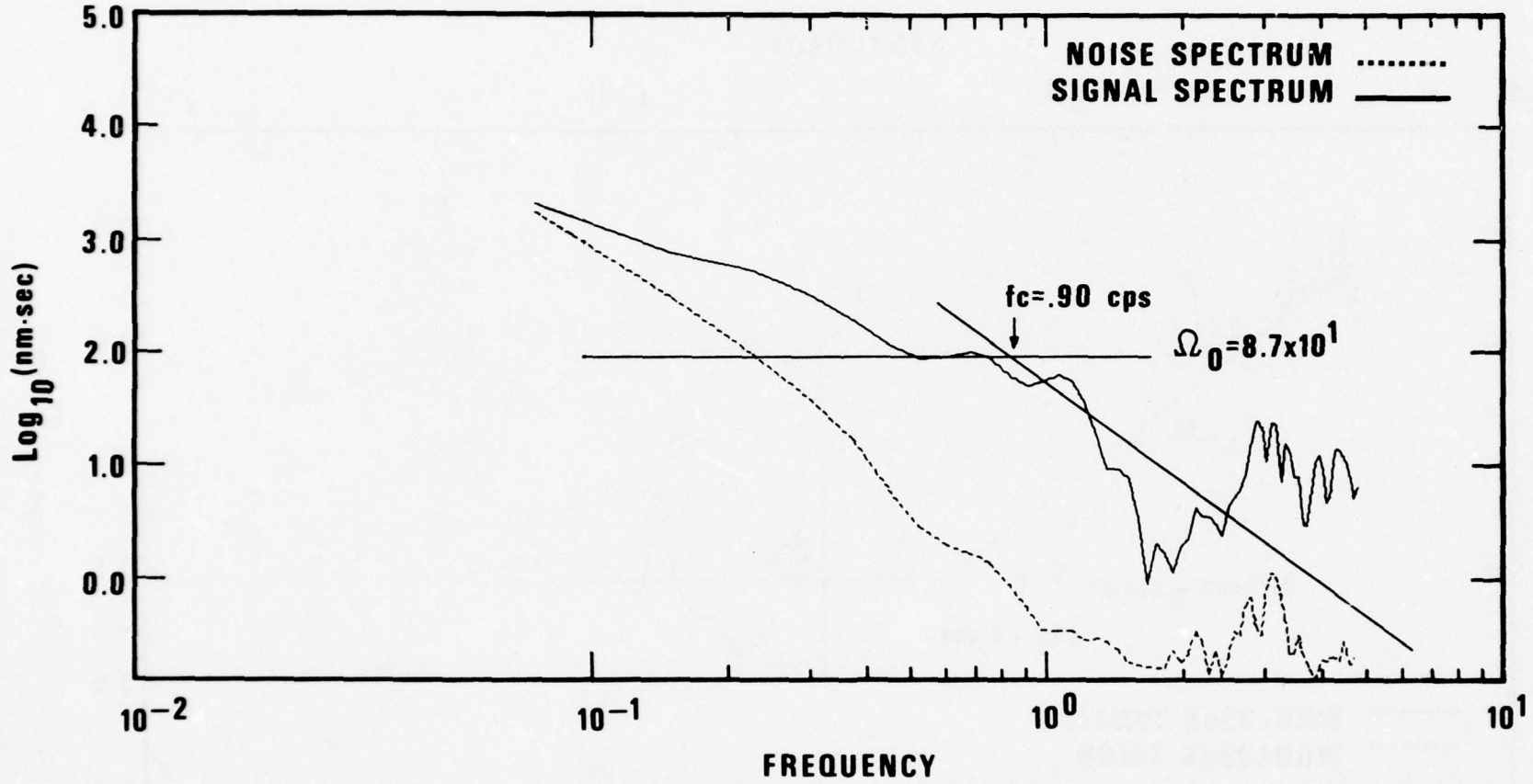

Figure 17 (Cont.) LASA A0 subarray spectra of P-waves from Kamchatka earthquakes with instrument response and attenuation removed ($t^* = .25$).

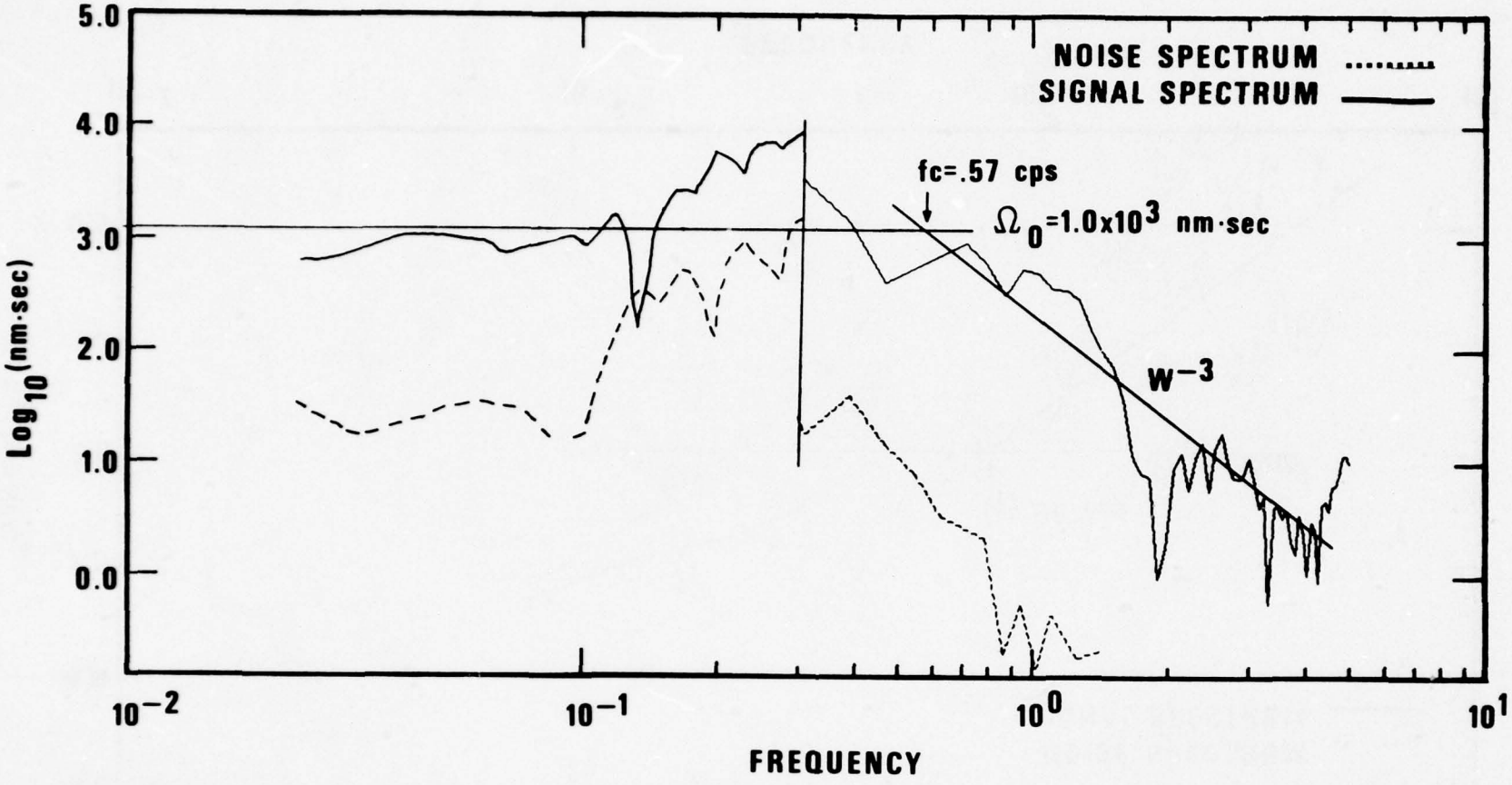

Figure 17 (Cont.) LASA A0 subarray spectra of P-waves from Kamchatka earthquakes with instrument response and attenuation removed (t* = .25).

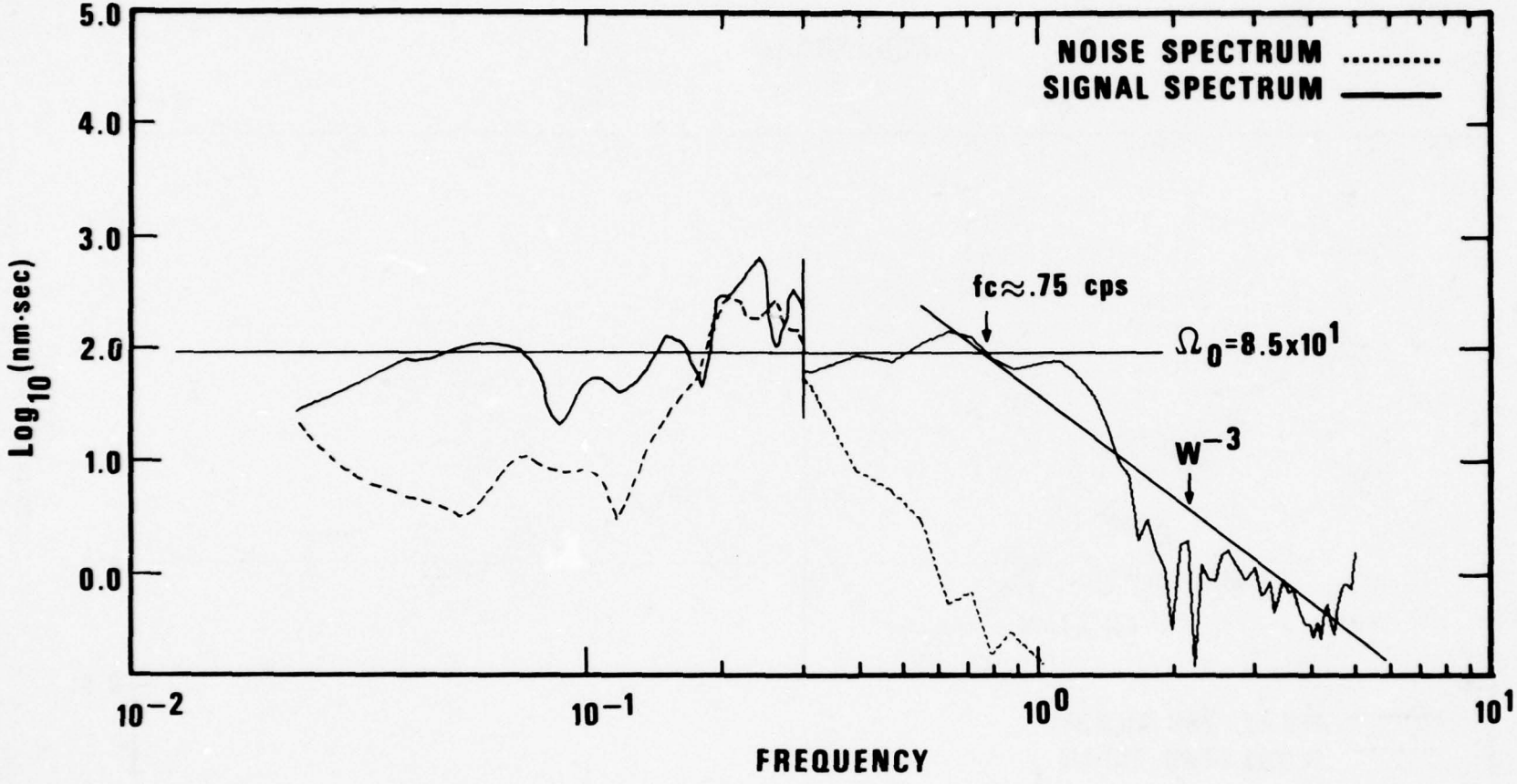

Figure 17 (Cont.) LASA A0 subarray spectra of P-waves from Kamchatka earthquakes with instrument response and attenuation removed (t* = .25).

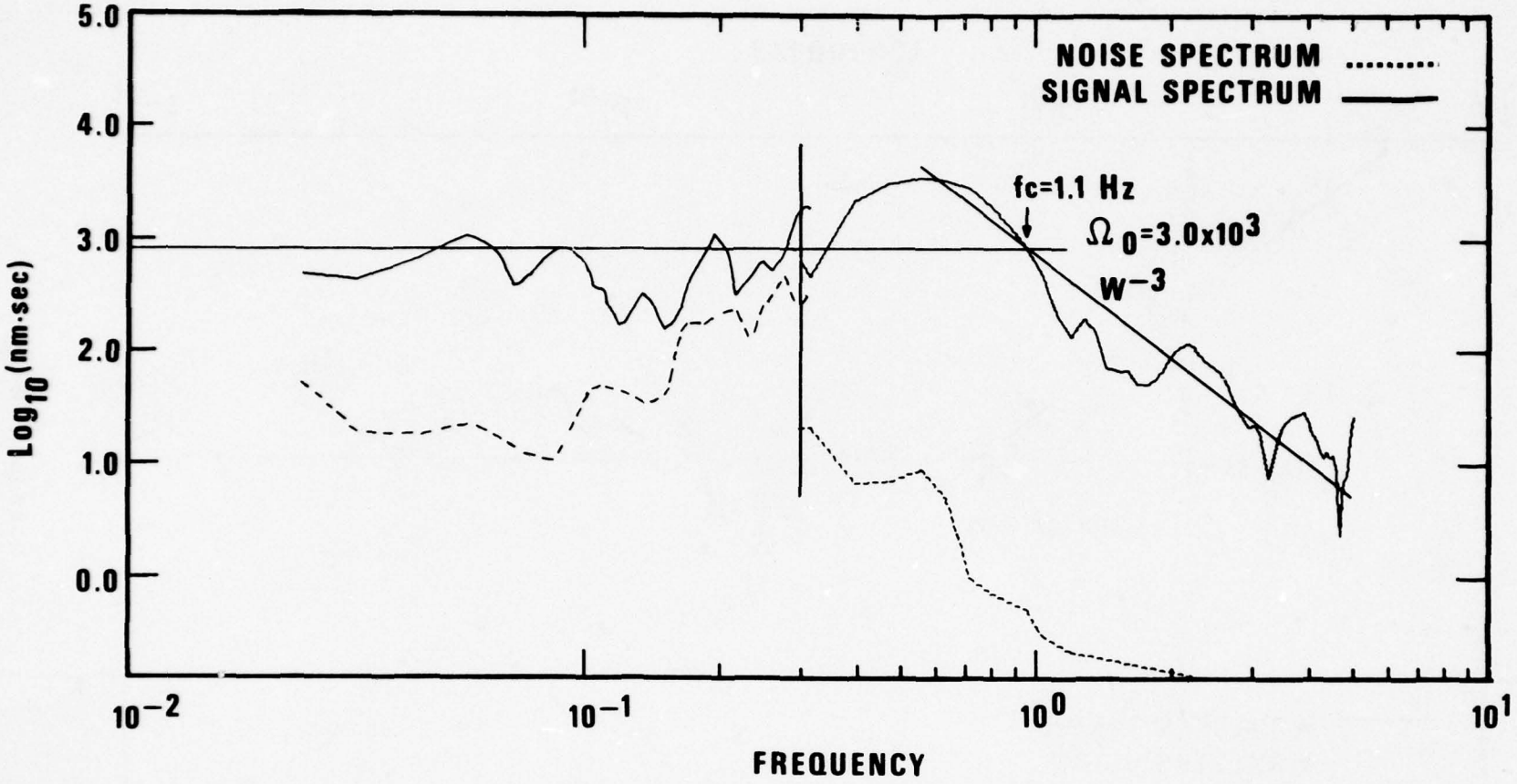

Figure 17 (Cont.) LASA A0 subarray spectra of P-waves from Kamchatka earthquakes with instrument response and attenuation removed (t* = .25).

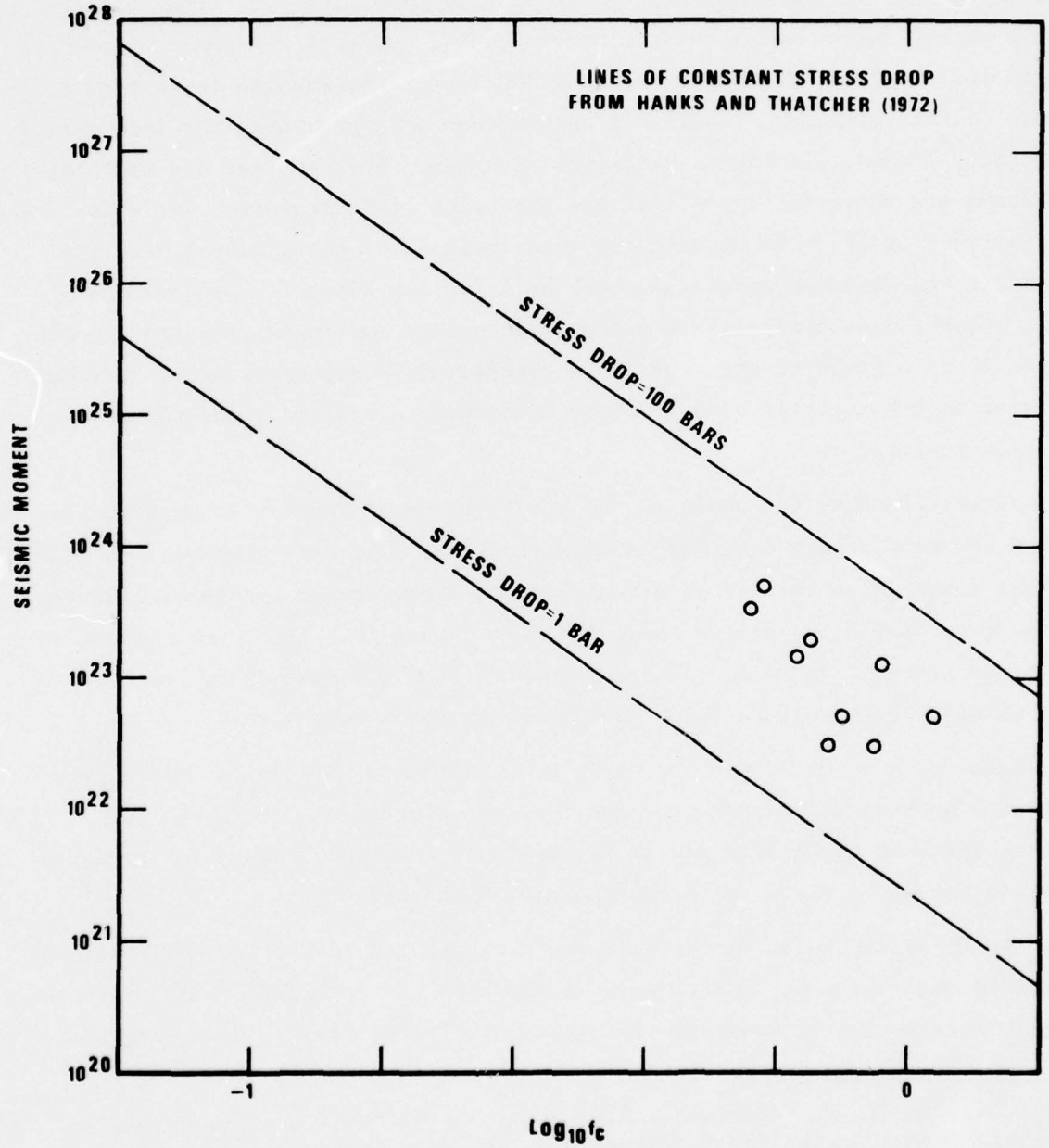

Figure 18 Seismic moment versus corner frequency for Kamchatka earthquakes from LASA P recordings.

Der and McElfresh (1976). Strains and displacements are computed in a layered medium due to an emergent P or S-wave from double-couple sources. The program requires as inputs the direction angles for the double couple, crustal parameters at the source and receiver, source depth, angle of incidence at the source and receiver, the mantle attenuation factor t*, and the instrument response of the recording. Synthetic seismograms were generated for long-period P at LASA, NORSAR, and eight world-wide stations. The observed and synthetic waveforms are shown in Figure 19. The direction of first motion for P and the arrival time of pP agree between the observations and the predictions. The synthetic and observed waveforms match well for the first few seconds and until other phases arrive which the program cannot duplicate, for example PcP. Figure 20 is a graph of observed versus predicted P-wave amplitudes. Except for station DAV there is a good linear relationship between predicted and observed amplitudes.

Figure 21 shows the observed and predicted waveforms for long-period S-phases recorded at the eight world-wide stations. The first motions and sS arrival times agree for most stations but the observed and synthetic S waveforms do not match as well as those for P in Figure 19. This could be due to either an increase in t* for S-waves since we used the same t* as for P-waves or to finite-fault rupture delays which effect the S-wave more.

Although the data comes from only one quadrant of the focal sphere, the synthetic seismograms support the fault plane orientation determined by Stauder and Mualchin (1976) and is representative of the average fault plane solution assumed for all the Kamchatka events in this study.

The focal mechanism just considered explains the lack of pP observations at NORSAR while LASA records pP well for most of our selected events as shown by the short-period seismograms in Figure 22. The pP raypath to the surface

---

Der, Z. A., and T. W. McElfresh, 1976. PSV--a program to compute synthetic seismograms, unpublished manuscripts, Teledyne Geotech, Alexandria, Virginia.

Stauder, W., and L. Mualchin, 1976. Fault motion in the larger earthquakes of the Kurile-Kamchatka Arc and of the Kurile-Hokkaido Corner, J. Geophys. Res., v. 81, p. 297-308.

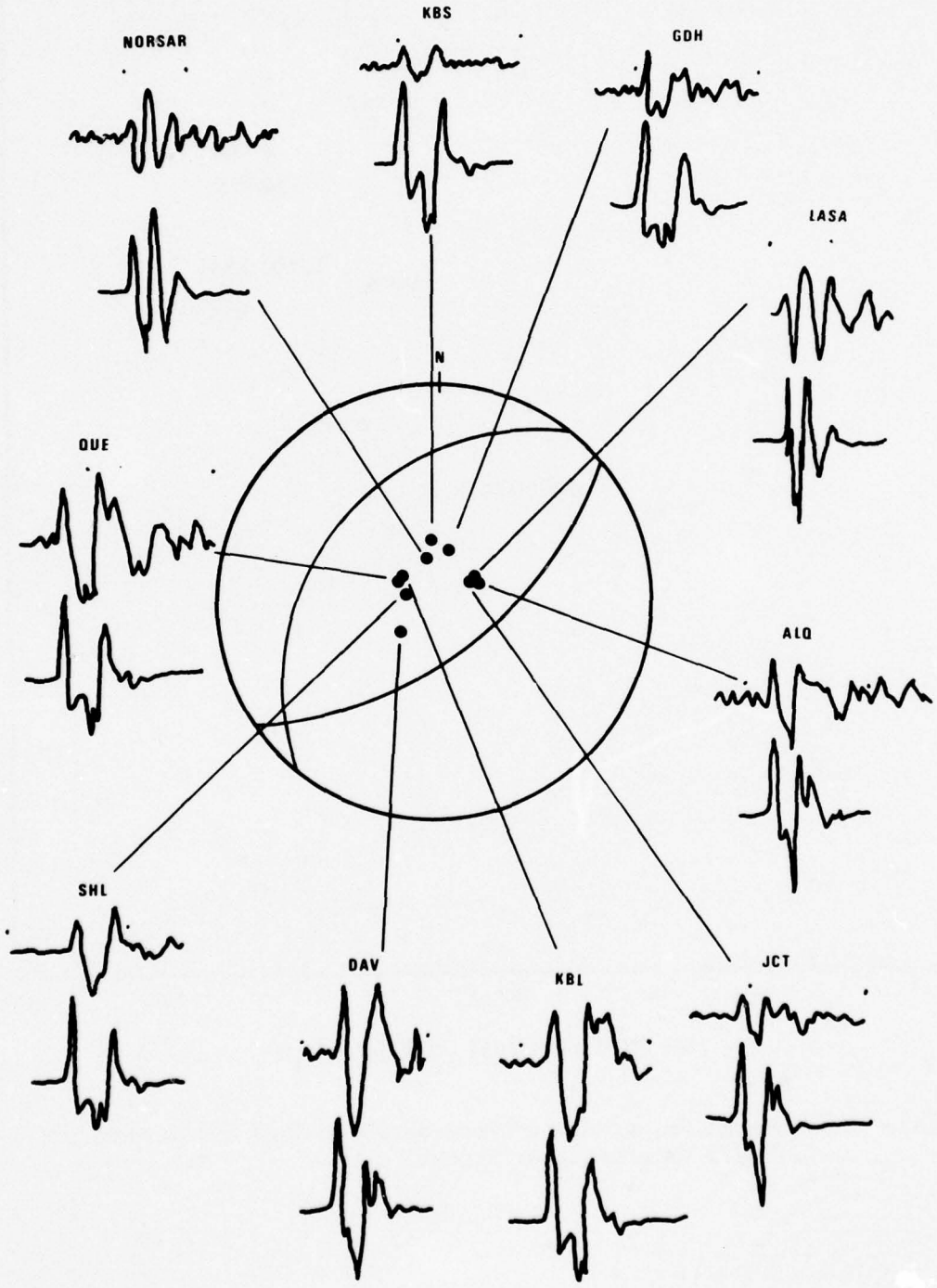

Figure 19 Synthetic and observed long-period vertical-component seismograms for P-waves from the 03/04/73 Kamchatka earthquake.

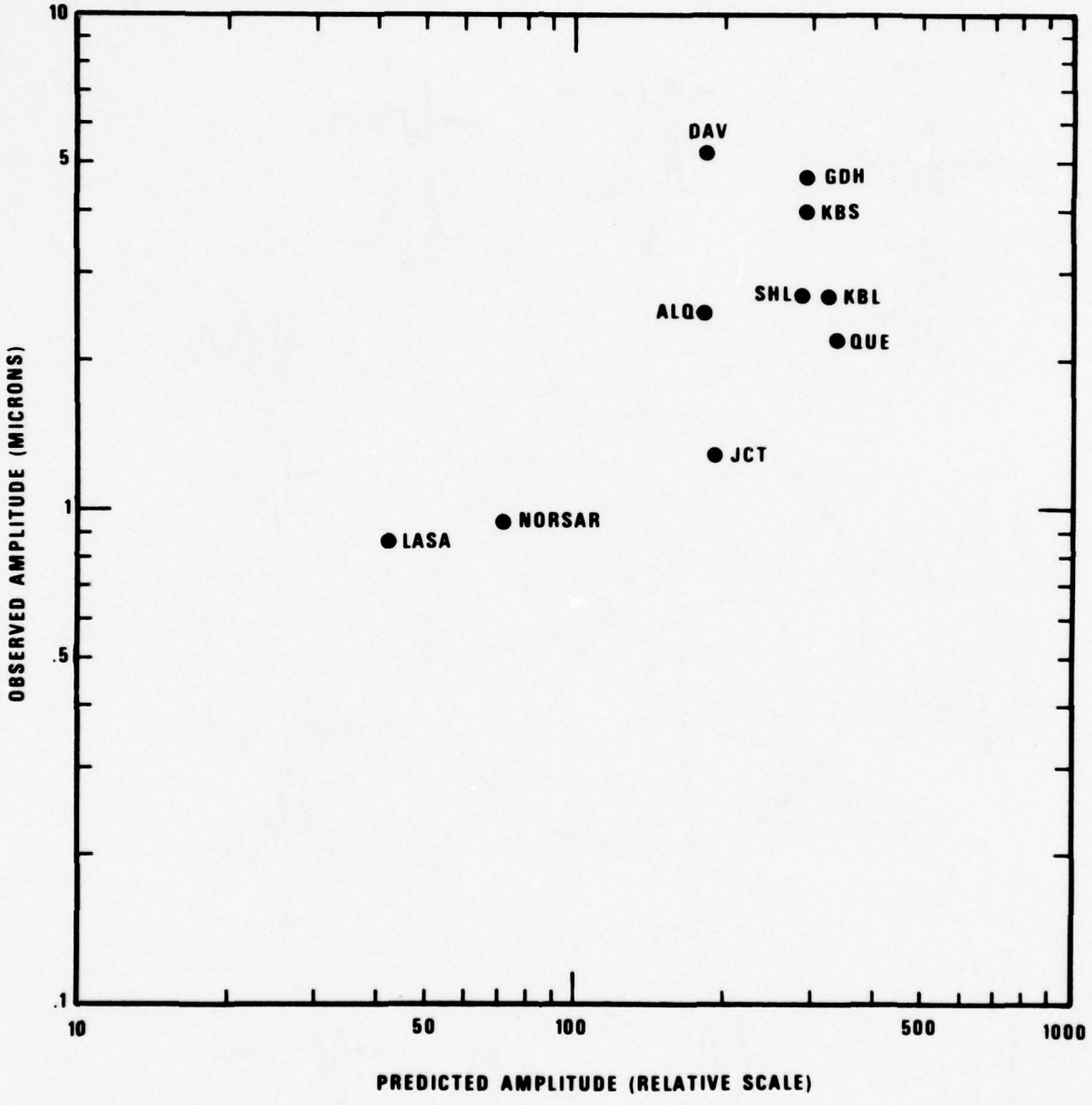

Figure 20 Observed vs. predicted long-period P-wave amplitudes for 03/04/73 Kamchatka earthquake.

Figure 21 Synthetic and observed long-period vertical-component seismograms for S-waves from the 03/04/73 Kamchatka earthquake.

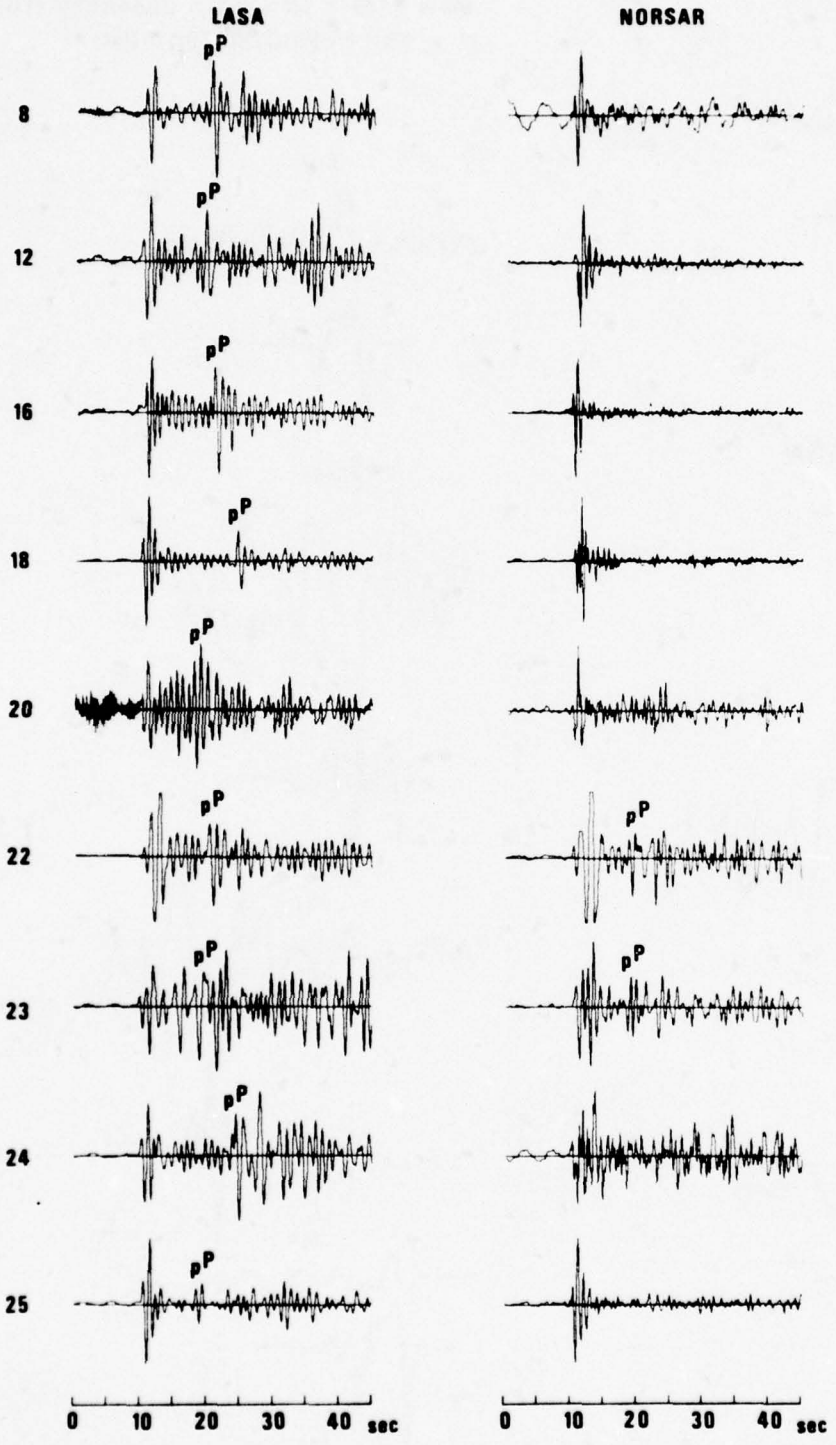

Figure 22 Short-period P-wave recorded at NORSAR (C3 subarray beam) and LASA (A0 subarray beam) for Kamchatka earthquakes.

for NORSAR lies near the auxiliary focal plane, and thus the amplitude should be low. For LASA, however, the pP amplitude is predicted to be roughly equivalent to that of the P-wave and of the same polarity.

Source effects on the LR amplitudes should be much easier to discern since we have analyzed a network of stations which covers all quadrants of the LR radiation pattern. In Figure 23 are plotted the antilogs of the M_s values for each event as listed in Table IV, except the masked 04/27/74 event, with the radiation pattern of the 03/04/73 earthquake superimposed such that its amplitude fits the observations in a least-squares sense. It can be seen that the observed distribution of amplitudes conforms to the calculated radiation pattern well in most cases and that no set of amplitudes from any one event seems to contradict this assumed excitation pattern. We have used the same pattern for all events even though their depths differ since additional calculations showed that the shape of the pattern did not depend on depth in the range 20 km < depth of focus < 50 km and that the effect of changing the dip angle was to increase or decrease the nodal amplitudes along the fault strike at $\theta \approx 210°$, which is the tectonic trend of this portion of the Kuril-Kamchatka Arc. Fluctuations of observed amplitudes about this radiation pattern are due to propagation effects which will be discussed in the next section.

Propagation Effects

Amplitudes of body-waves passing through the dipping lithospheric plate under Kamchatka are presumably effected differently than waves passing through the surrounding higher attenuation mantle. To study these differences, mantle attenuation along paths from Kamchatka to NORSAR was compared to attenuation along paths from Kamchatka to LASA, the only two sites for which we had short-period digital data.

One measurement of attenuation is the factor t*, which is the travel time along the ray path divided by the attenuation factor Q. Knowing t* for one ray path, t* for a second ray path can be found by finding the ratio of spectra for the two paths. Relative spectral amplitudes beyond the corner frequencies for the two paths can be expressed as

$$\log_e(A_1/A_2) = b + mf$$

TABLE IV

Magnitude Data for Selected Kamchatka Earthquakes

EVENT 25

21 OCT 74

STATION	DELTA	E-S AZ	S-E AZ	m_b	M_s
COL	27.67	466.	272.	5.58	4.45
MAT	23.25	231.	35.	6.11	4.46
SHI	76.23	302.	35.	0.0	5.04
TLO	85.63	348.	9.	0.0	4.67
CHG	58.30	258.	38.	0.0	4.83
CTA	74.73	194.	9.	0.0	4.21
EIL	84.48	315.	29.	0.0	5.01
KIP	45.13	120.	326.	0.0	4.87
KON	64.38	344.	19.	0.0	4.76
OGD	74.22	40.	330.	0.0	4.63
ALP	27.69	45.	271.	0.0	4.28
LAS	55.84	56.	314.	5.27	4.43
NOR	63.07	344.	20.	6.19	4.53
Mean				5.79	4.63

EVENT 8

25 JAN 73

STATION	DELTA	E-S AZ	S-E AZ	m_b	M_s
MAT	24.17	231.	34.	5.51	4.39
COL	26.75	47.	272.	4.72	4.48
BKS	52.61	75.	315.	-5.00	-4.67
CHG	59.07	259.	37.	5.36	4.63
GDH	53.85	15.	335.	5.23	-4.59
DAV	55.46	225.	25.	-5.40	-4.68
KBL	64.01	293.	40.	0.0	4.69
QUE	68.54	292.	39.	5.44	5.01
OGD	73.31	41.	330.	0.0	4.49
ALQ	63.43	67.	319.	4.99	4.60
SHL	57.91	270.	40.	4.46	4.91
SHK	28.41	237.	36.	5.68	4.33
KIP	44.89	121.	328.	5.54	-5.43
SHI	76.45	302.	34.	5.47	-4.37
KON	63.94	345.	18.	0.0	4.36
TLO	85.13	349.	8.	0.0	4.56
ALP	26.77	46.	271.	0.0	4.34
LAS	54.94	57.	315.	5.49	4.62
NOR	62.63	344.	19.	5.89	0.0
Mean				5.25	4.52

EVENT 12

9 JUN 73

STATION	DELTA	E-S AZ	S-E AZ	m_b	M_s
ALQ	64.93	65.	318.	5.00	0.0
COL	28.56	45.	270.	4.96	4.25
KIP	44.85	118.	325.	-5.41	4.34
KBL	63.84	293.	42.	5.61	4.86
MAT	22.43	232.	36.	5.68	4.42
SHI	76.56	301.	36.	5.90	0.0
OGD	75.16	40.	329.	0.0	4.57
CTA	73.68	194.	9.	0.0	4.23
EIL	85.02	314.	30.	0.0	4.90
TLO	86.58	348.	10.	0.0	4.10
ALP	28.58	44.	270.	0.0	4.34
LAS	56.61	55.	314.	5.33	4.82
NOR	63.98	344.	20.	5.47	0.0
Mean				5.39	4.52

EVENT 16

3 NOV 73

STATION	DELTA	E-S AZ	S-E AZ	m_b	M_s
MAT	24.13	231.	34.	5.50	3.91
COL	26.79	47.	272.	5.02	3.86
SHK	28.36	237.	36.	5.75	0.0
CHG	58.99	259.	37.	5.29	4.56
QUE	68.44	292.	39.	5.23	4.68
SHI	76.35	302.	34.	5.57	-4.05
KIP	44.99	121.	328.	5.63	4.44
BKS	52.68	75.	315.	-4.97	-4.48
GDH	53.83	15.	336.	-5.26	-4.57
DAV	55.43	225.	24.	-6.00	-4.36
OGD	73.33	41.	330.	-4.87	-4.42
ALQ	63.49	67.	320.	-5.19	4.27
KON	63.87	345.	18	0.0	3.92
CTA	75.53	195.	9.	0.0	4.18
TLO	85.07	349.	8.	0.0	4.35
LAS	54.99	57.	315.	5.38	4.05
NOR	62.56	344.	19.	5.41	3.78
Mean				5.25	4.14

EVENT 18

26 FEB 74

STATION	DELTA	E-S AZ	S-E AZ	m_b	M_s
MAT	22.50	230.	35.	5.99	4.17
COL	28.43	45.	271.	5.38	4.09
BKS	54.03	73.	314.	5.10	-4.64
ALQ	64.97	65.	319.	5.53	4.47
DAV	53.78	224.	25.	-5.98	-4.57
SHI	76.15	301.	36.	0.0	4.52
KBL	63.46	293.	42.	0.0	4.62
KON	64.84	344.	19.	0.0	4.50
OGD	74.99	39.	330.	0.0	4.17
CTA	74.02	193.	8.	0.0	4.34
TLO	86.13	348	10.	0.0	4.43
ALP	28.45	45.	271.	0.0	4.23
LAS	56.57	55.	314.	5.98	4.52
NOR	63.52	344.	20.	5.65	4.45
Mean				5.59	4.36

EVENT 22

4 MAR 73

STATION	DELTA	E-S AZ	S-E AZ	m_b	M_s
COL	26.58	47.	272.	5.85	5.72
KIP	45.02	121.	328.	6.04	6.11
KBS	45.29	352.	24.	6.24	5.84
HKC	47.91	247.	35.	5.68	5.82
KEV	51.45	342.	32.	5.70	5.80
BKS	52.55	75.	315.	5.91	5.95
GDH	53.60	15.	336.	6.49	5.78
DAV	55.64	225.	24.	6.35	5.59
AKU	59.81	0.	0.	6.34	5.94
ALO	63.33	67.	320.	5.84	5.84
QUE	68.44	292.	38.	5.80	6.30
ESK	69.51	351.	9.	6.67	5.92
JCT	70.31	65.	323.	5.85	5.89
OGD	73.11	41.	330.	5.68	5.85
LEM	76.03	236.	29.	5.73	5.32
TOL	84.86	349.	8.	7.28	5.40
SHI	76.31	302.	34.	6.00	0.0
SHL	57.91	270.	40.	4.86	6.19
ADE	91.58	199.	13.	5.89	5.92
MAT	24.33	231.	34.	0.0	5.63
GUA	43.22	204.	14.	0.0	5.38
KBL	63.90	293.	40.	0.0	5.86
MSH	67.44	301.	38.	0.0	6.33
CTA	75.76	195.	9.	0.0	5.57
ALP	26.59	47.	271.	0.0	5.74
LAS	54.80	57.	315.	6.30	6.09
Mean				6.02	5.83

EVENT 23

2 AUG 72

STATION	DELTA	E-S AZ	S-E AZ	m_b	M_S
COL	25.07	49.	273.	5.58	5.53
KIP	44.91	124.	330.	5.46	5.30
ALQ	62.00	69.	321.	5.17	5.21
KON	62.75	345.	16.	5.70	5.42
OGD	71.58	42.	330.	5.53	5.55
CTA	77.19	196.	10.	5.57	5.33
TOL	83.84	350.	7.	6.25	5.43
KBL	64.27	294.	38.	0.0	5.71
LAS	53.36	59.	316.	5.48	0.0
NOR	61.45	345.	17.	5.36	0.0
Mean				5.57	5.43

EVENT 24

25 DEC 72

STATION	DELTA	E-S AZ	S-E AZ	m_b	M_S
KIP	45.27	117.	325.	5.93	-5.61
CHG	57.46	258.	39.	5.60	5.52
OGD	75.35	39.	330.	5.38	5.12
CTA	73.68	193.	8.	5.72	5.21
COL	28.79	45.	271.	0.0	5.27
KBL	63.41	293.	43.	0.0	5.56
ALQ	65.28	64.	318.	0.0	5.34
TLO	86.39	347.	10.	0.0	5.51
ALP	28.80	44.	271.	0.0	5.08
LAS	56.90	55.	314.	5.98	5.44
NOR	63.77	344.	21.	5.27	5.25
Mean				5.65	5.33

---

*mean estimated by method of Ringdal (1976)

- indicates upper bound to magnitude established by noise level when no signal detected

0.0 indicates no measurement

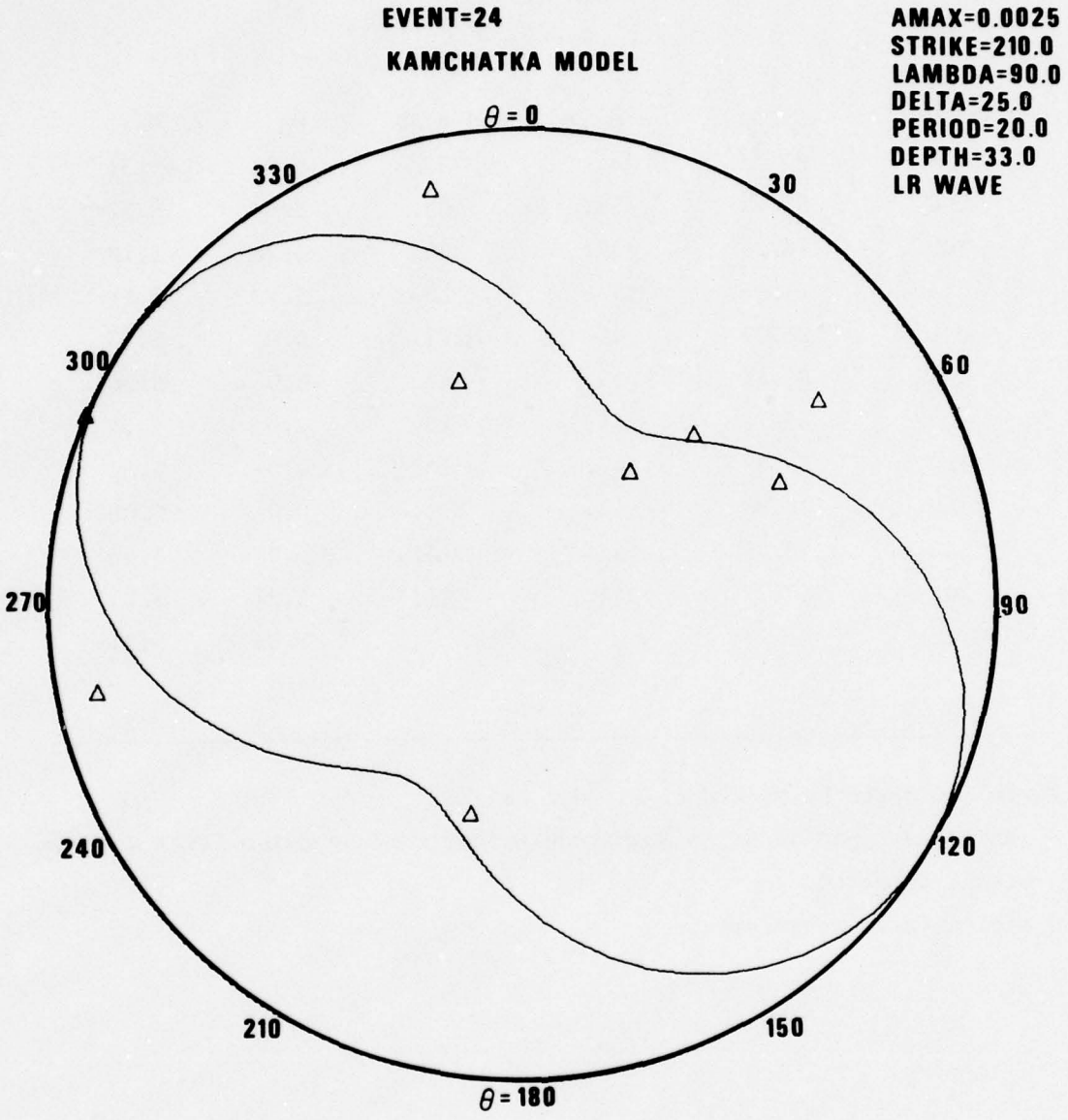

Figure 23 Theoretical and observed LR amplitude (T = 20 sec) for Kamchatka earthquakes of this study.

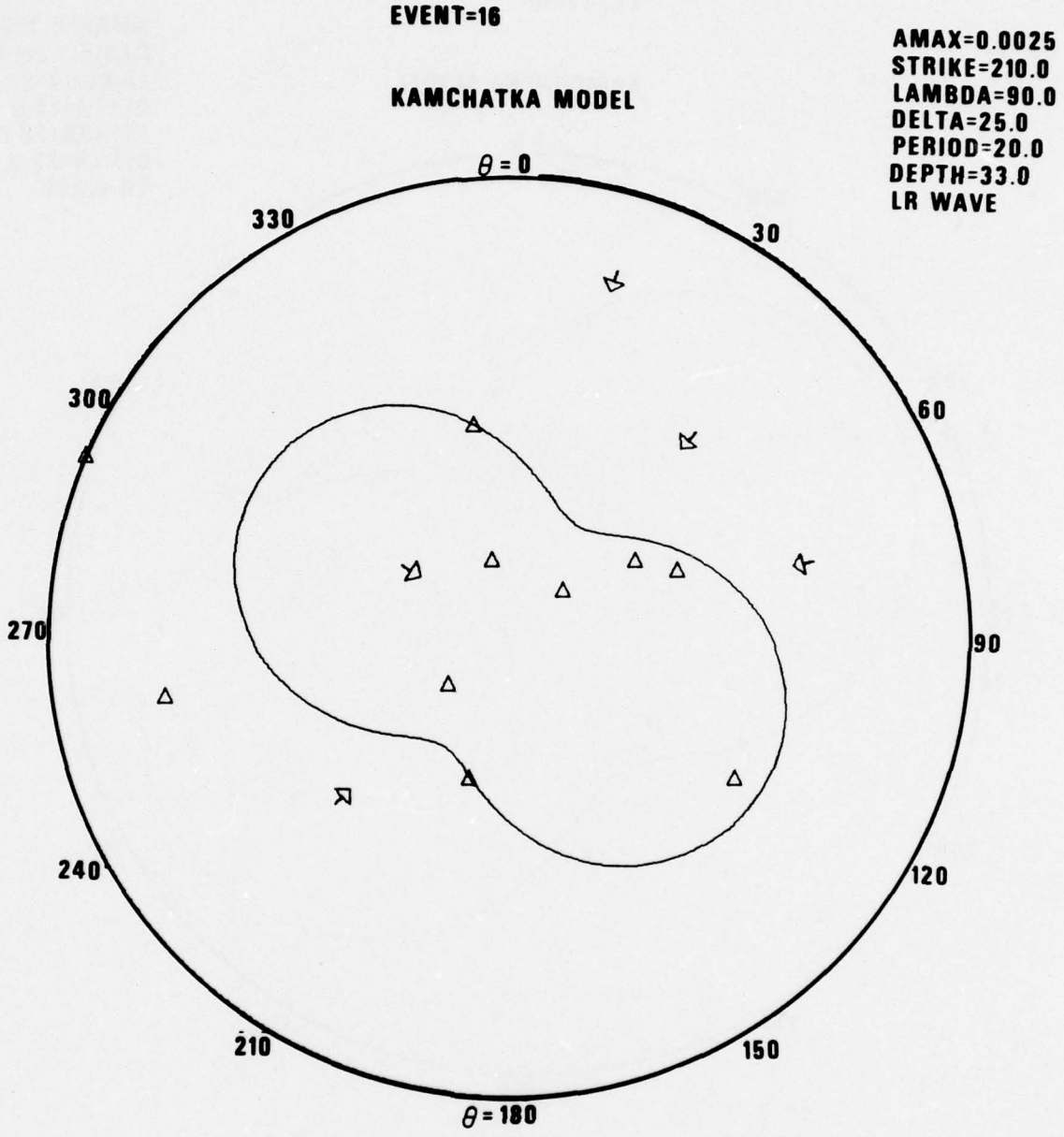

Figure 23 (Cont.) Theoretical and observed LR amplitude (T = 20 sec) for Kamchatka earthquakes of this study.

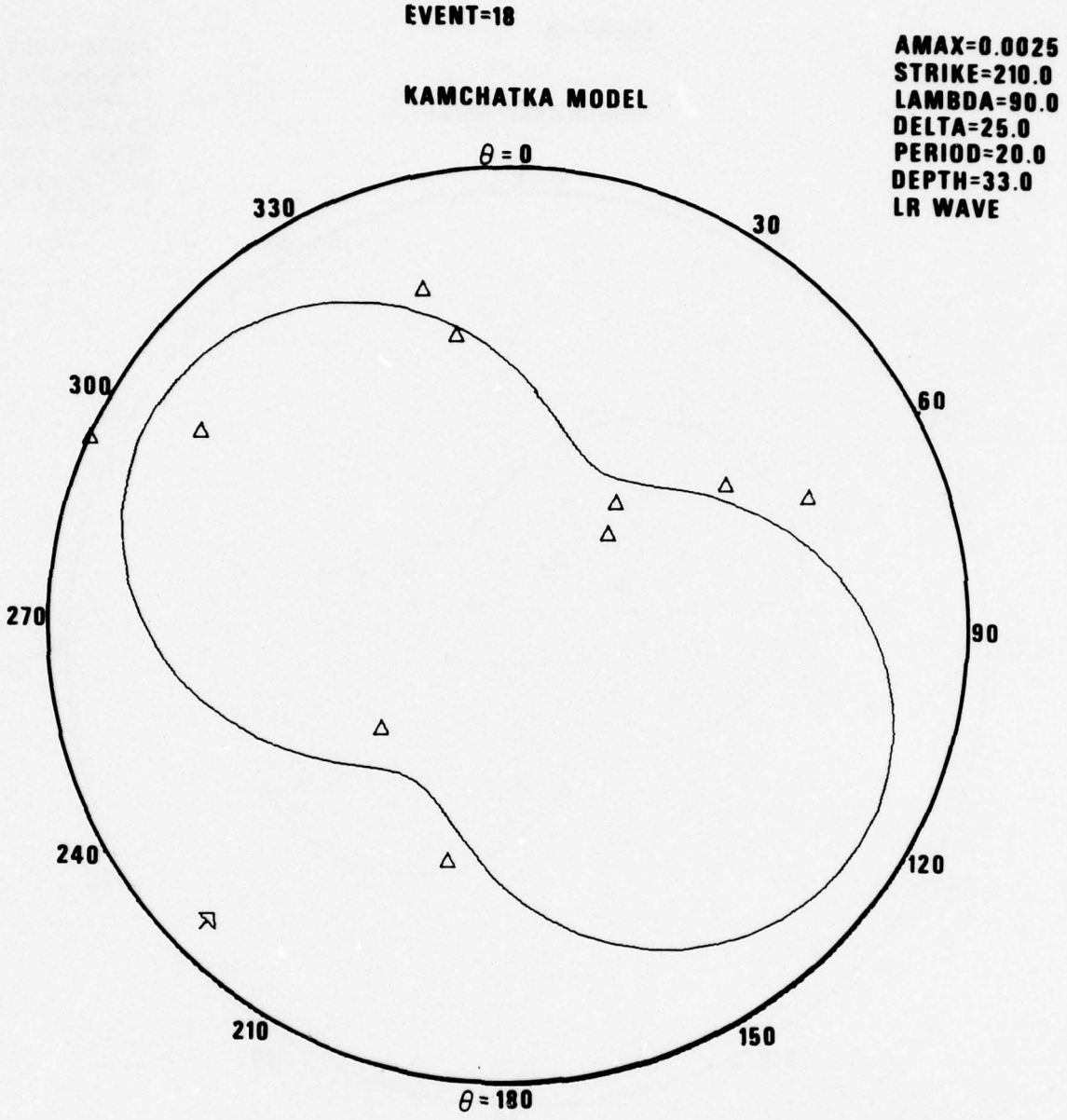

Figure 23 (Cont.) Theoretical and observed LR amplitude (T = 20 sec) for Kamchatka earthquakes of this study.

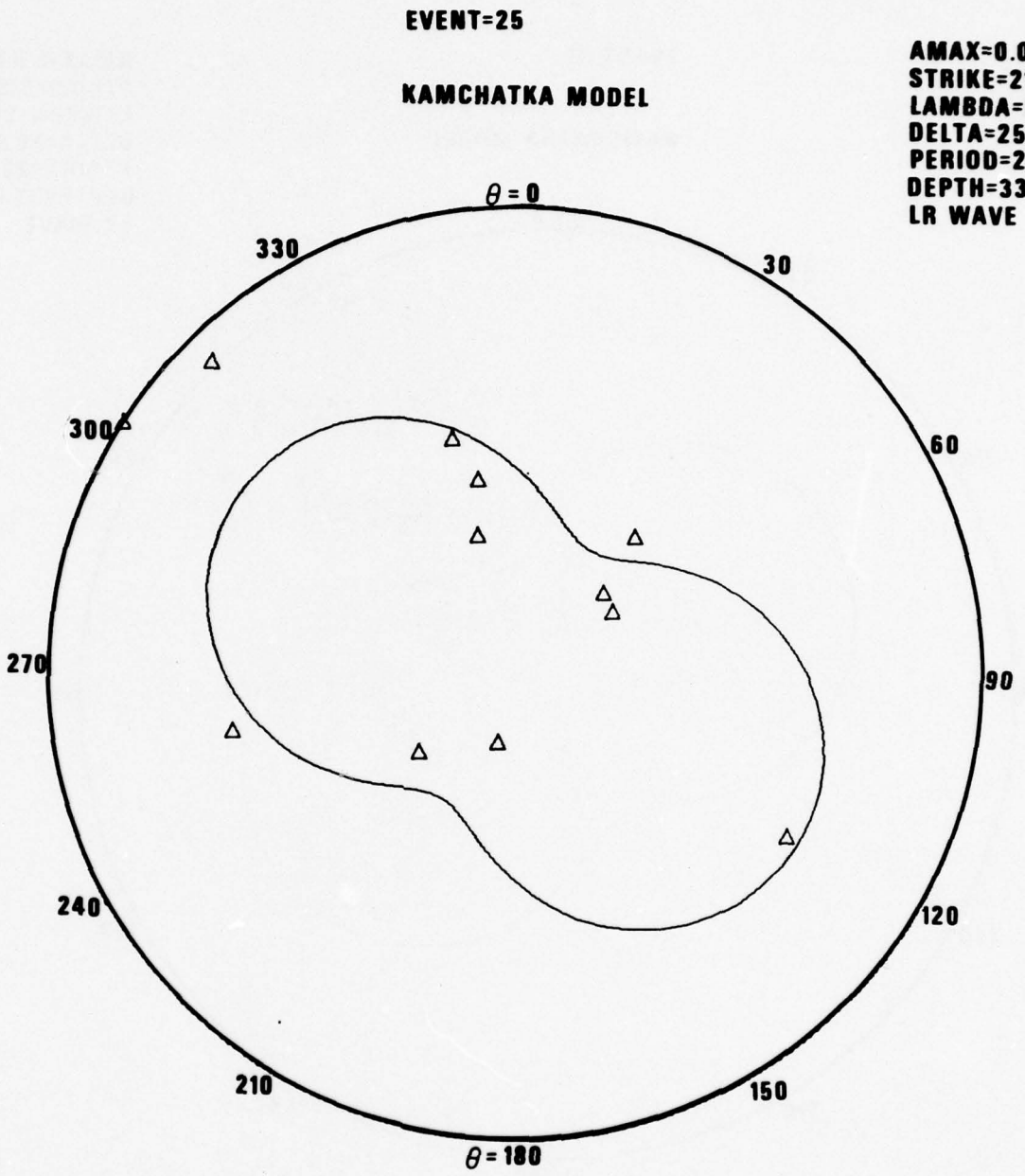

Figure 23 (Cont.) Theoretical and observed LR amplitude (T = 20 sec) for Kamchatka earthquakes of this study.

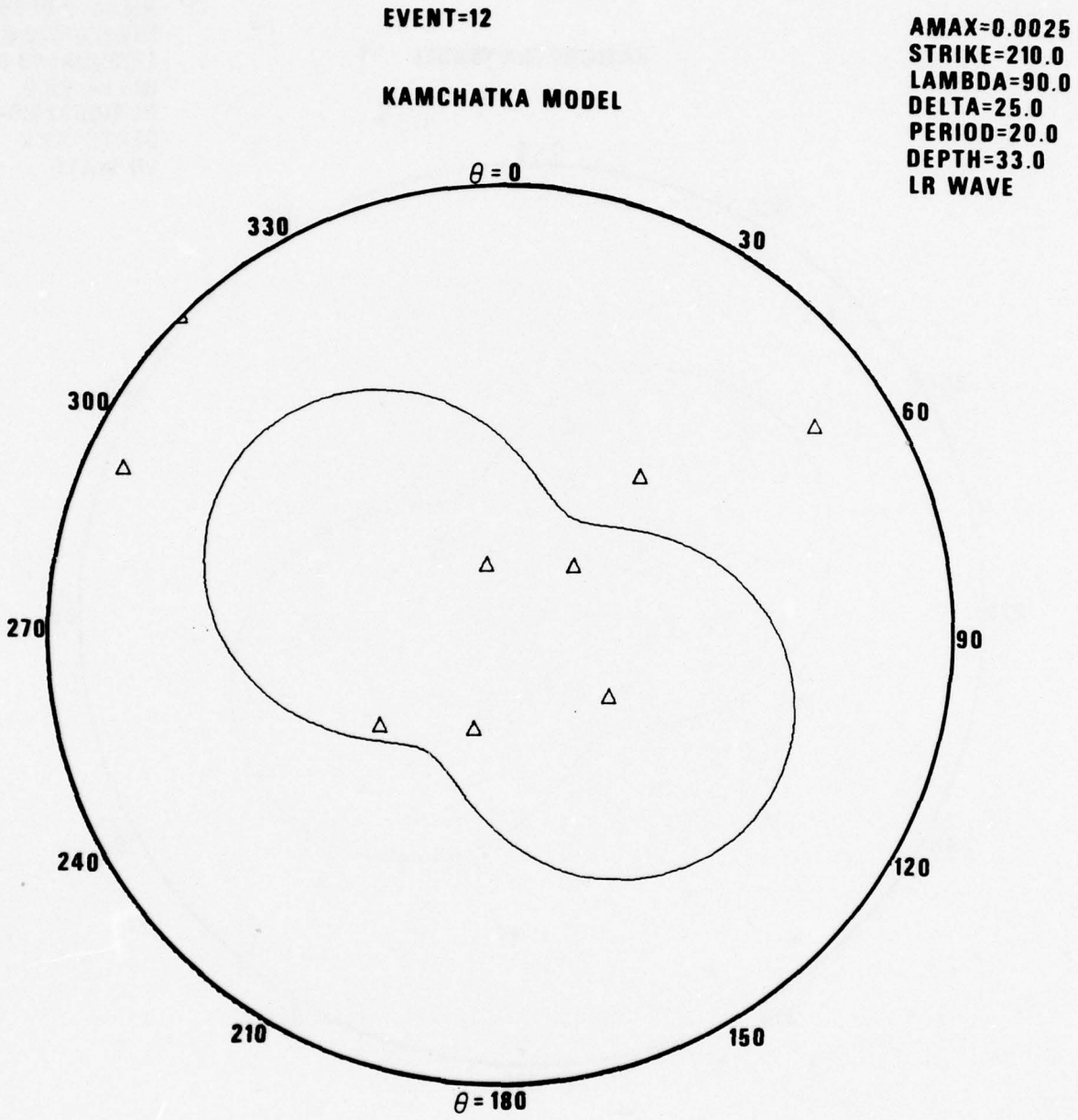

Figure 23 (Cont.) Theoretical and observed LR amplitude (T = 20 sec) for Kamchatka earthquakes of this study.

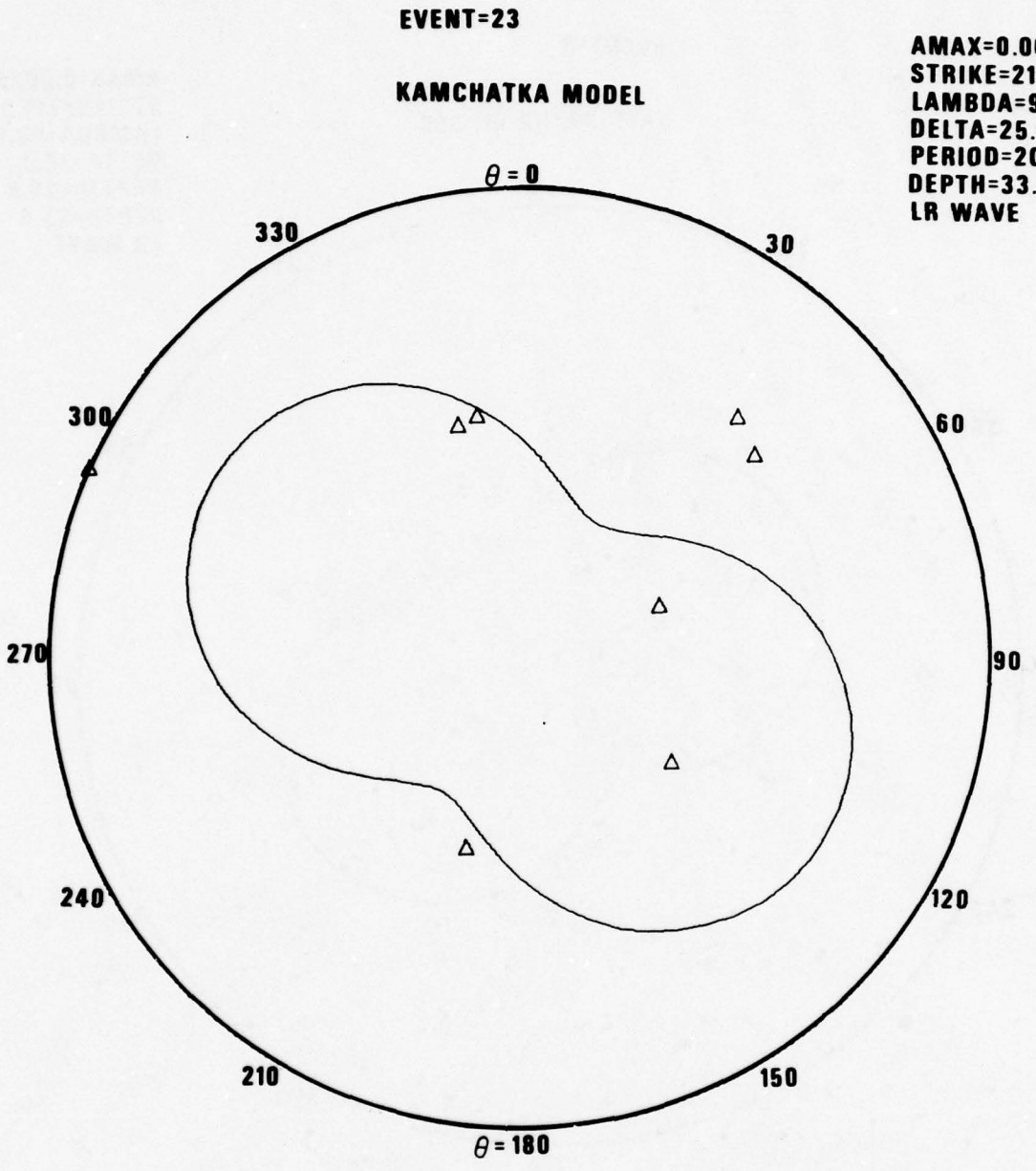

Figure 23 (Cont.) Theoretical and observed LR amplitude (T = 20 sec) for Kamchatka earthquakes of this study.

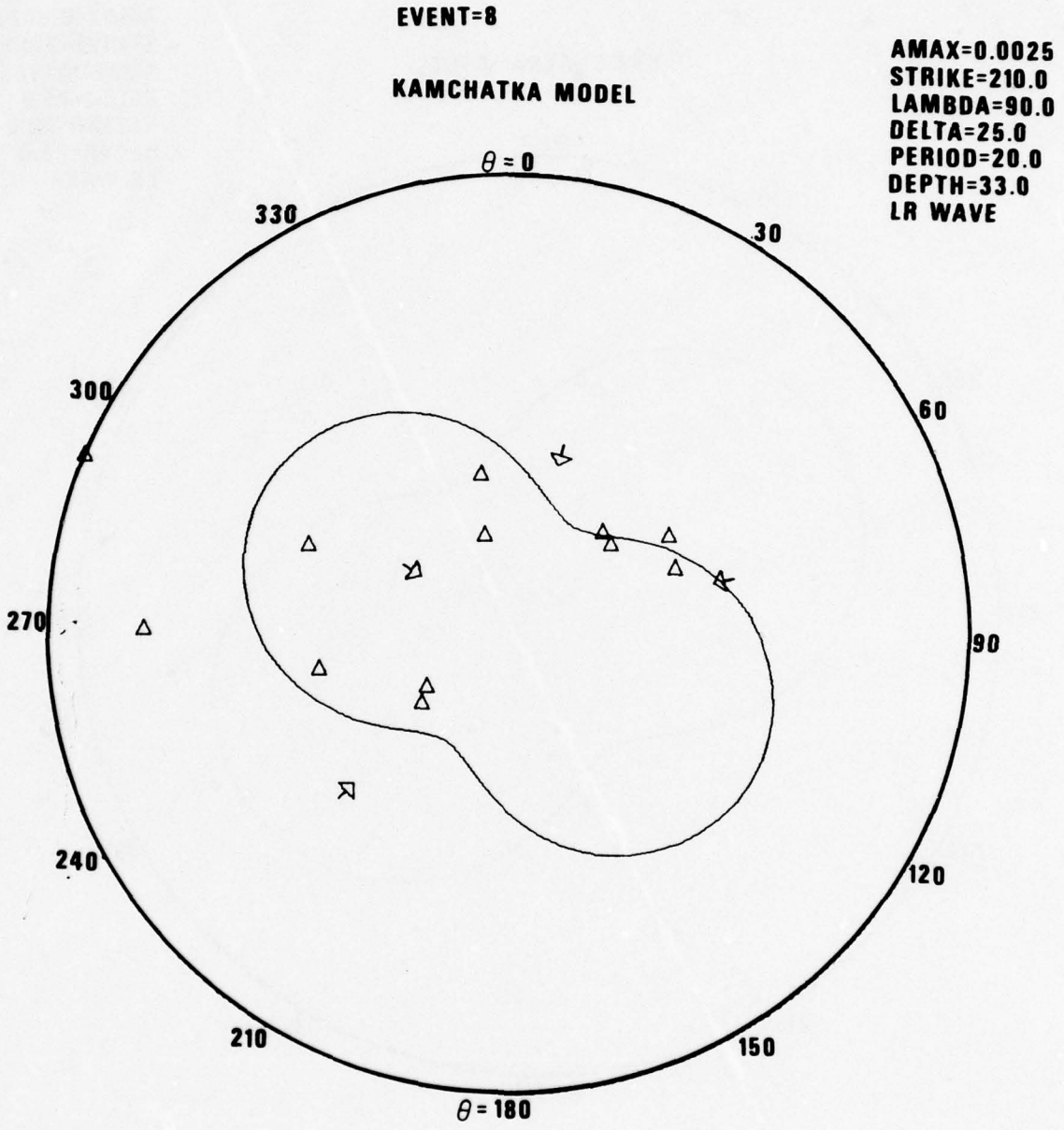

Figure 23 (Cont.) Theoretical and observed LR amplitude (T = 20 sec) for Kamchatka earthquakes of this study.

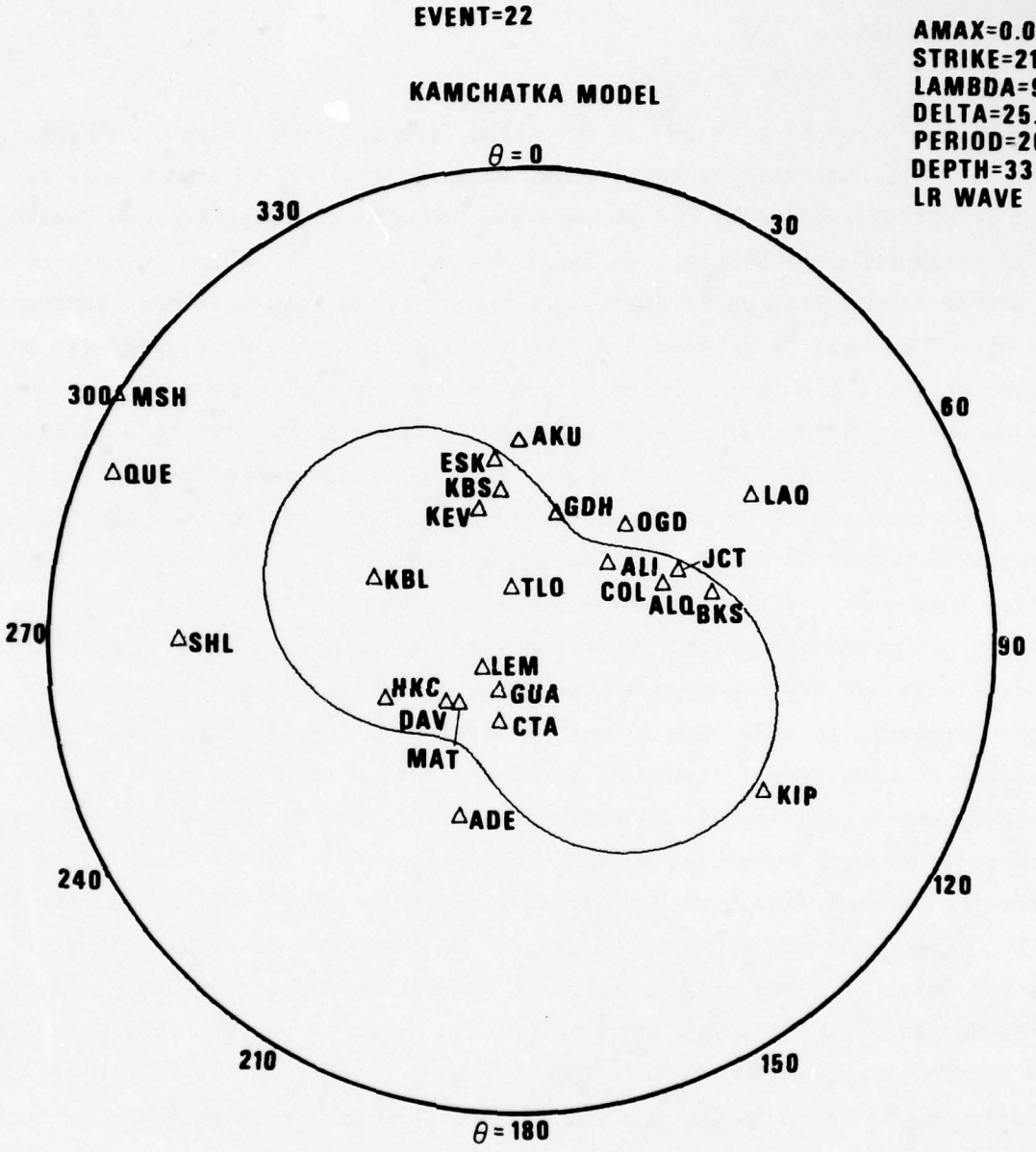

Figure 23 (Cont.) Theoretical and observed LR amplitude (T = 20 sec) for Kamchatka earthquakes of this study.

where b is a constant and

$$m = -\pi(t_1^* - t_2^*).$$

Noponen (1975) reports a t* of .20 for paths from Eastern Kazakh to NORSAR. Figure 24 shows the ratio of the average spectra of the Kamchatka events recorded at NORSAR divided by the average spectra of four large Eastern Kazakh explosions recorded at NORSAR. We first assumed the earthquakes to have the same source spectral shape as explosions, namely, the high-frequency asymtotic slope of ω^{-2} as used by Noponen. A line was fitted to the data points at high frequencies where S/N ratio was high even to 5 Hz, taking care to be beyond the corner frequencies for these events, probably at <2 Hz. On this semilogarithmic plot (base 10) the slope of the line is -.143. After converting to a base e y-axis, the slope of the line is -.330. Then t* for the path from Kamchatka to NORSAR is found from the above relation (use $t_2^* = .20$) to be $t_1^* = 0.31$. This value of t* corresponds to an average Q of 2100; that is, a relatively low attenuation path. Note that, if we had assumed an ω^{-3} slope for the earthquake spectra, an even higher Q would result. In order to find t* for the Kamchatka to LASA path it was necessary to first find t* for the Eastern Kazakh to LASA path. Figure 25 shows the ratios of the average of four Eastern Kazakh signal spectra recorded at LASA divided by the average spectra of the same events recorded at NORSAR. Using Noponen's result again of t* = .20 for the Eastern Kazakh to NORSAR path, the value of t* for the Eastern Kazakh to LASA path was found to be .44, or an average Q of 1700. Figure 26 shows the ratio of the average spectra of Kamchatka events recorded at LASA. Then t* for the path from Kamchatka to LASA is found to be t* = .25, using t* = .44 for Eastern Kazakh to LASA. This value of t* corresponds to a Q of 2300, or nearly equally attenuating path as the one from Kamchatka to NORSAR. Nearly identical Q for the two paths is reflected in the similar frequency content of P-waves at LASA and NORSAR as seen visually in Figure 22.

Noponen, I., 1975. Compressional wave power spectrum from seismic sources, Report to the Advanced Research Project Agency, ARPA Order Number AO 2131-1, 64 p.

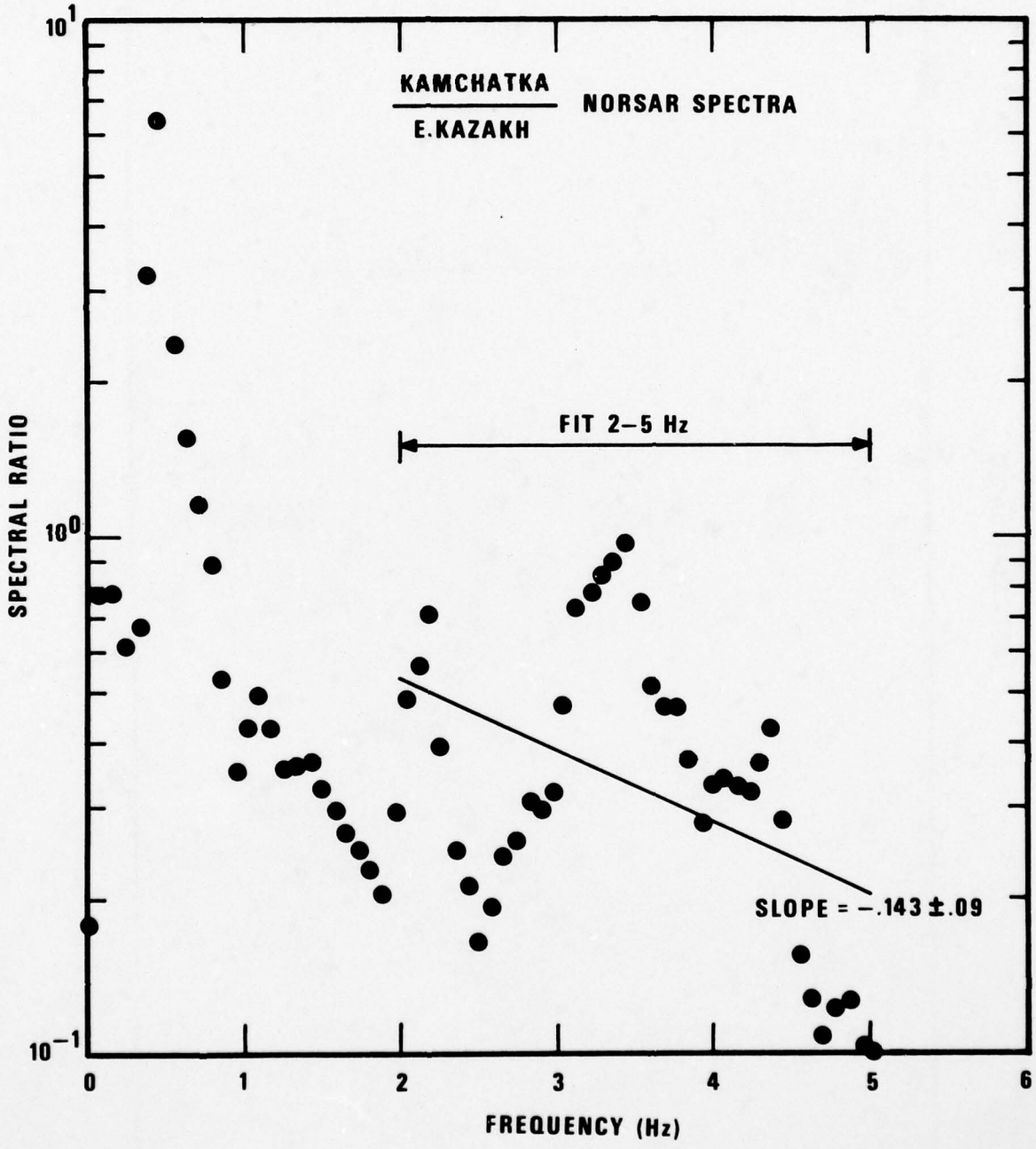

Figure 24 Ratio of average Kazakh explosion spectra to average Kamchatka earthquake spectra recorded at NORSAR.

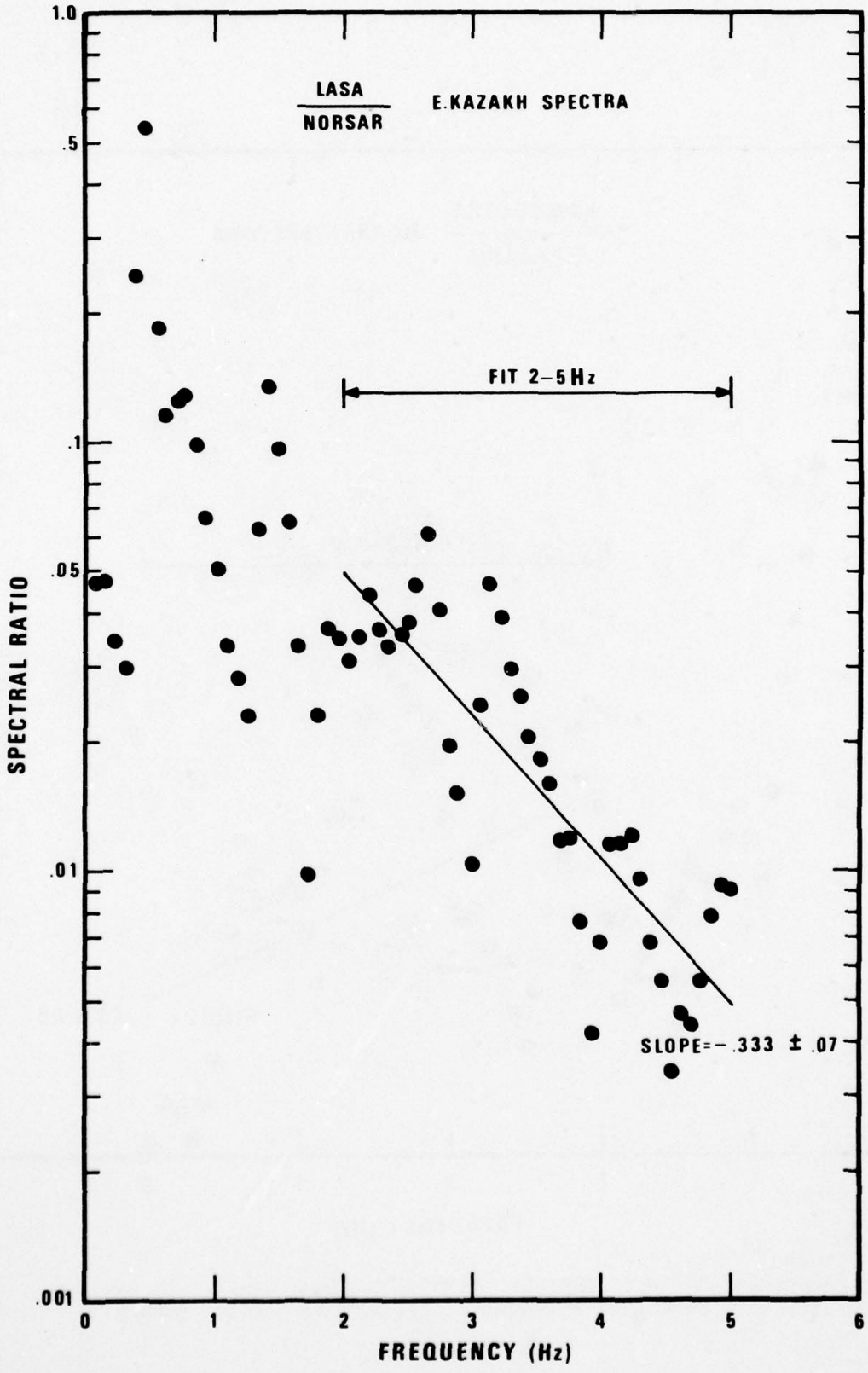

Figure 25 Ratio of average LASA spectra to average NORSAR spectra for four Eastern Kazakh explosions.

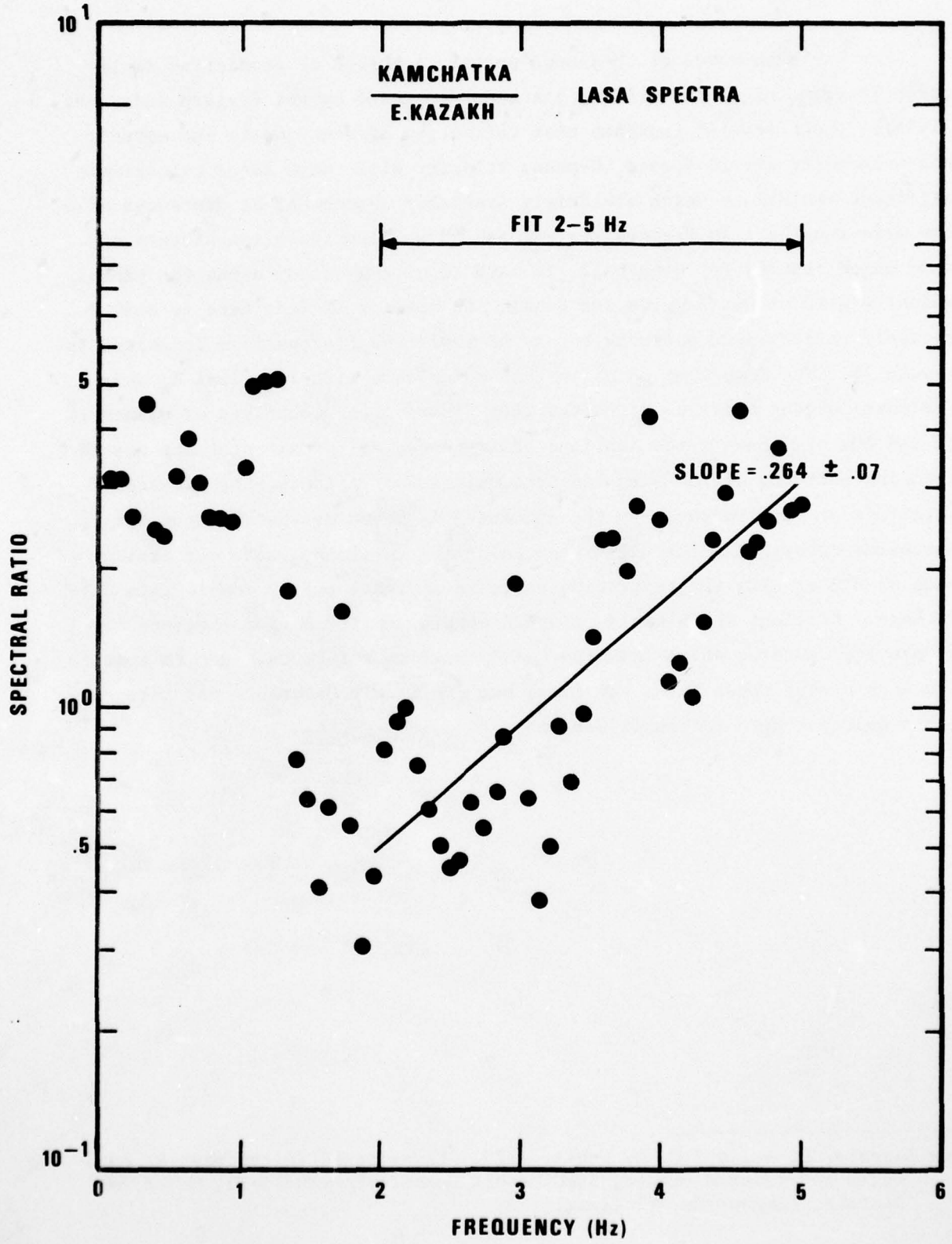

Figure 26 Ratio of average Kamchatka earthquake spectra to average Kazakh explosion spectra recorded at LASA.

For Rayleigh-waves of 20-second period, a method of predicting amplitudes by geometrical ray tracing has been presented by von Seggern and Sobel (1975). Their results indicate that refraction effects due to the earth's non-uniformity for 20-second LR-phase velocity will cause large teleseismic amplitude variations which are fairly spatially incoherent at distances of a few wave-lengths. In Figures 27, 28, and 29 we illustrate the pattern of rays which results for events 12, 16, and 20 of this study using the global velocity grid of von Seggern and Sobel. No attempt is made here to quantitatively relate these patterns to the LR amplitude fluctuations indicated in Figure 23. The important point is that epicenters with identical M_s only a few wave-lengths apart on Kamchatka (see Figure 1 for locations of events 12 16 and 20) will have large amplitude differences at certain stations due to changing patterns of focusing and defocusing. For instance, the predicted amplitude at KIP increases as the epicenter is moved southward along the Kamchatka coast, with the difference amounting to .25 M_s unit. At stations such as BKS or EIL, the raytracing patterns indicate nearly double this difference. Stations which would record a stable amplitude from these three events lie on paths which traverse nearly uniform structure, such as that to the ALPA array; these paths are rare, but are highly desirable for calibrating a source region for amplitude.

---

von Seggern, D. H., and P. A. Sobel, 1975. Experiments in refining M_S estimates for seismic events, SDAC Report Number SDAC-TR-75-17, Teledyne Geotech, Alexandria, Virginia.

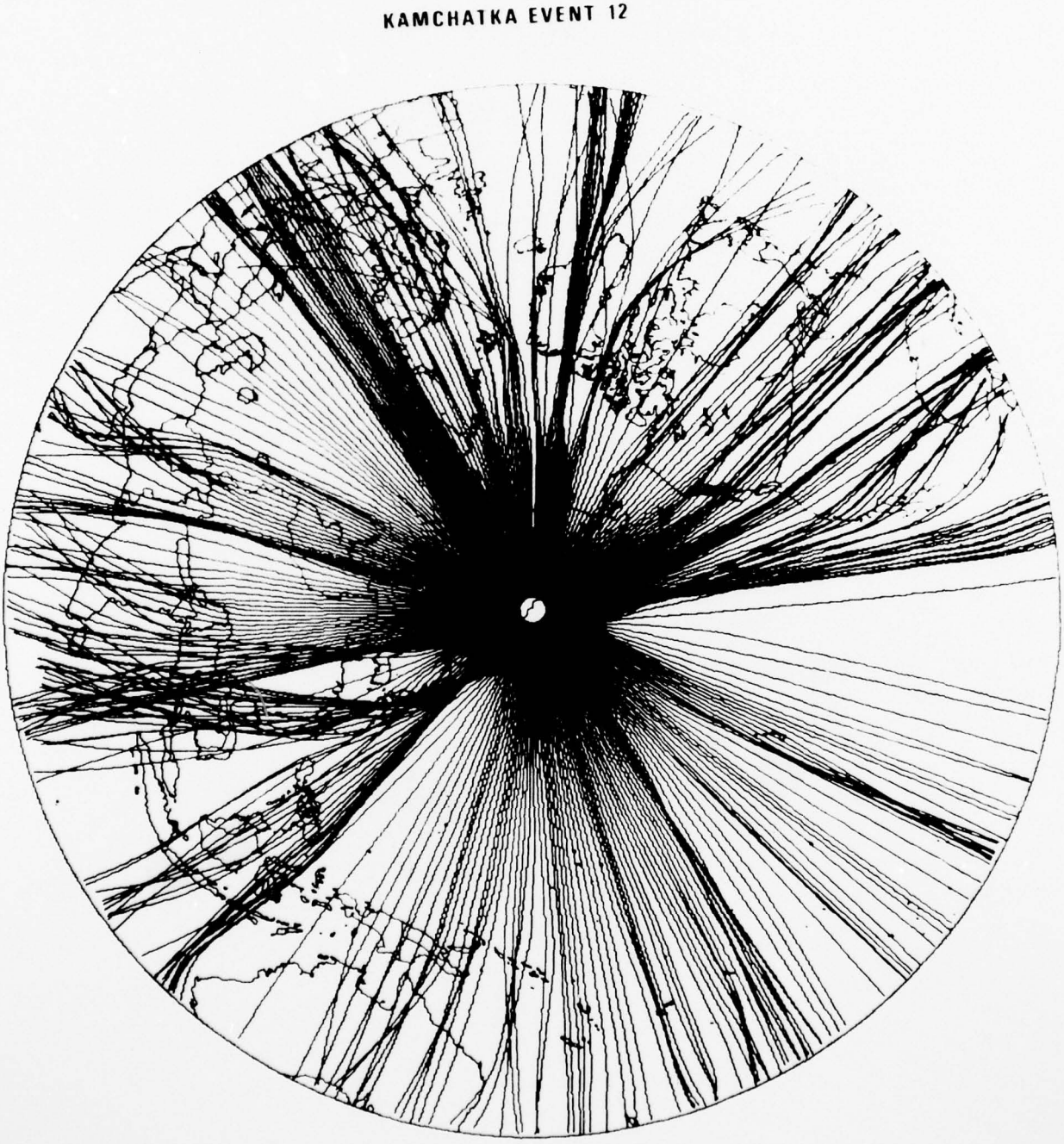

Figure 27 Predicted LR raypaths (T = 20 sec) from event 12.

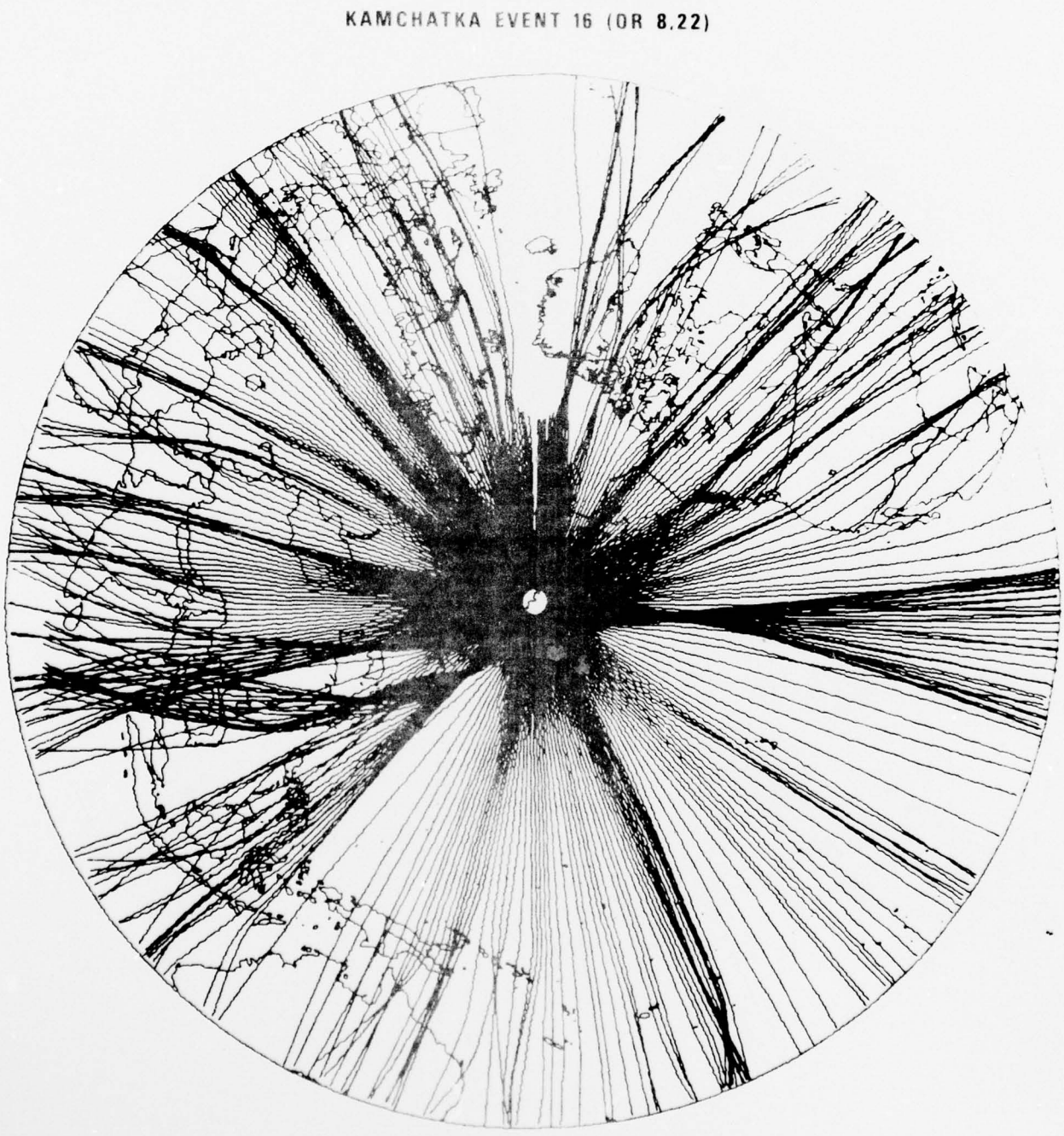

Figure 28 Predicted LR raypaths (T = 20 sec) from event 16.

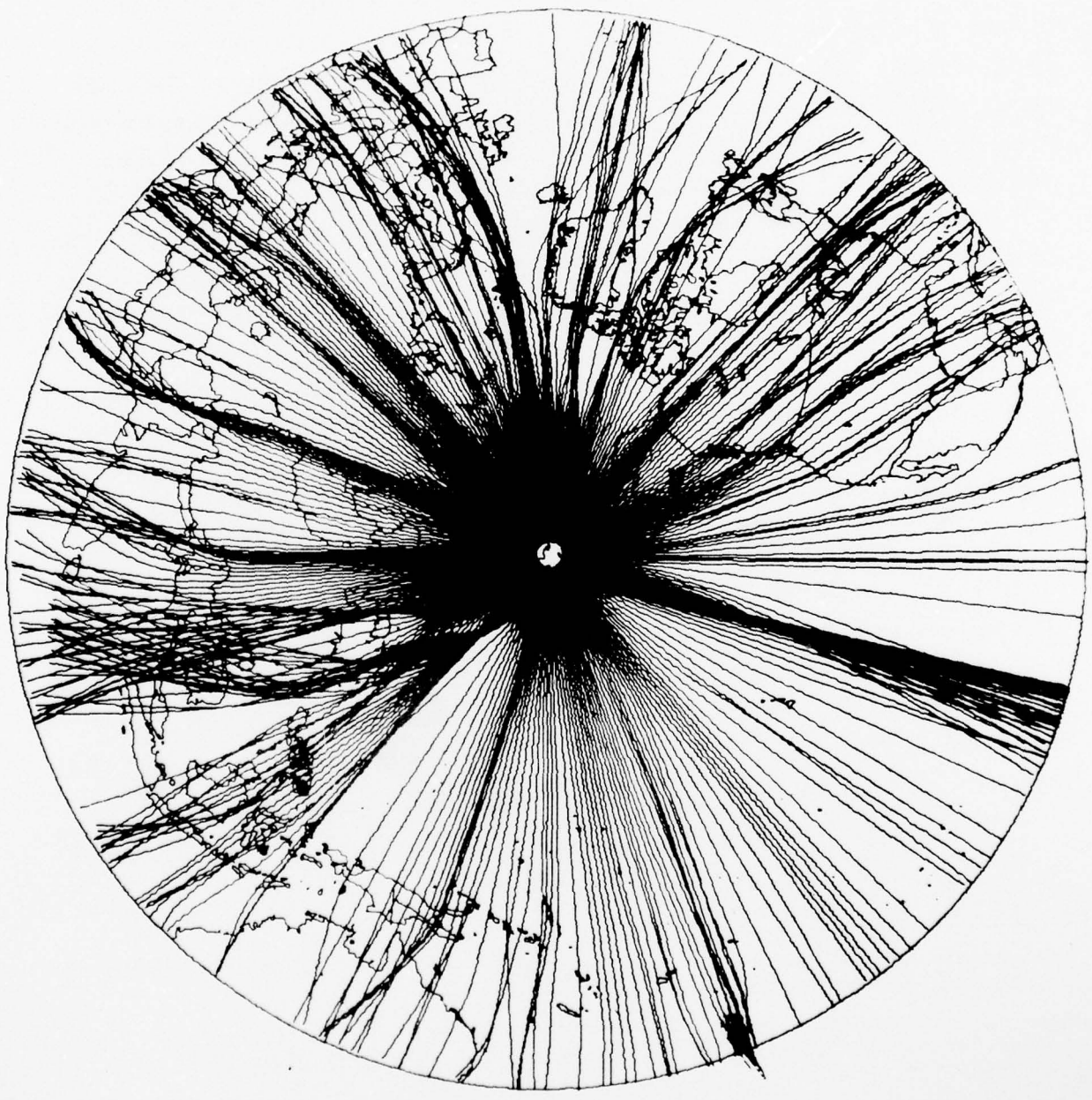

Figure 29 Predicted LR raypaths (T = 20 sec) from event 20.

DISCRIMINATION ASPECTS

As stated early in this report, the purpose of our Kamchatka study has been to describe its seismic source characteristics and propagation path effects with a view toward discrimination. In this section we will present several of the commonly employed discriminants between earthquakes and explosions as extracted from the signals of the nine events considered. With the lack of any large explosions in this region, we can only speculate on the true worth of these discrimination parameters, but hopefully our study has added some insights which will put these speculations on a firmer basis. Also, we are able to draw on the Amchitka Island tests LONG SHOT, MILROW, and CANNIKIN in a limited way. There is a good similarity between the tectonic setting of the Amchitka explosions and our Kamchatka earthquakes, and so extrapolation of these explosions to Kamchatka is not unreasonable, especially since the distance between the two regions involved is not great in regard to teleseismic recording distances. Several studies of the Amchitka source region have already shown that the three explosions there are in a non-evasive context easily distinguished from natural seismic events nearby (von Seggern and Lambert, 1972; Wyss et al., 1971; Liebermann and Pomeroy, 1969).

$M_s - m_b$

We have independently determined average M_s and m_b values for the Kamchatka events in Table II using selected WWSSN stations, HGLP stations, and the NORSAR and LASA arrays. The data contributing to the average estimates are listed in Table IV. In this study, we have used the following forms for magnitude computation:

$$m_b = \log\left(\frac{A}{T}\right) + B(\Delta)$$

$$M_s = \log\left(\frac{A}{T}\right) + 1.66 \log\Delta + 0.3$$

---

von Seggern, D. H., and D. G. Lambert, 1972. Analysis of teleseismic data for the nuclear explosion Milrow, SDL Report Number 258.

Wyss, M., T. C. Hanks, and R. C. Liebermann, 1971. Comparison of P-wave spectra of nuclear explosions and earthquakes, J. Geophys. Res., v. 76, p. 2716-2729.

Liebermann, R. C., and P. W. Pomeroy, 1969. Relative excitation of surface waves by earthquakes and underground explosions, J. Geophys. Res., v. 74, p. 1575-1590.

where

A = one-half the peak-to-peak maximum recorded amplitude reduced to nm ground displacement,

T = period in seconds (restricted to 17-23 sec for M_s calculation),

Δ = epicentral distance in degrees,

$B(\Delta)$ = Gutenberg-Richter correction term for P-waves.

We have used a method of magnitude averaging, proposed by Ringdal (1976), which includes noise measurements as upper bounds of M_s measurement to produce the M_s-m_b plot in Figure 30. Note that in Table IV only a few noise measurements are listed, and so the averages should be very close to what would result if only measured signal amplitudes were used. This was confirmed by actual computations. The M_s of one event, the 4/27/74 earthquake, could not be reliably determined due to the interference by the long-period coda of a larger earthquake prior to it, and it has not been plotted. Since we had purposely chosen those events which, in preliminary analysis, were of low M_s for their m_b (except the 03/04/73 event, with largest M_s and m_b), we feel that Figure 30 shows M_s-m_b values representative of the most anomalous coastal Kamchatka earthquakes down to $m_b = 5$. Support for this statement is contained in an M_s-m_b plot of von Seggern (1976) for shallow activity in Seismic Region 19 (Kurils-Kamchatka-Japan) during 1972 since the line $M_s = m_b - 1.0$ in Figure 30 would easily lie below all events in von Seggern's plot down to $m_b \approx 4.0$; thus M_s-m_b discrimination for Kamchatka events would most likely effectively persist down to this magnitude level.

In Figure 30 we have also plotted the magnitudes of the three Amchitka Island explosions. The m_b's for these events are taken from the ISC list. The M_s of CANNIKIN was averaged from recordings from a well-distributed set of 10 WWSSN stations, and those of MILROW and LONG SHOT have been scaled from CANNIKIN according to $M_s \propto \log$ (yield) with the published yields of 80, 1000,

---

Ringdal, F., 1976. Maximum-likelihood estimate of event magnitude, Bull. Seism. Soc. Am., v. 66, p. 789-802.

von Seggern, D. H., 1976. (U) Final report on the analysis of the VLPE network, SDAC Report Number SDAC-TR-76-1, Teledyne Geotech, Alexandria, Virginia. Classified

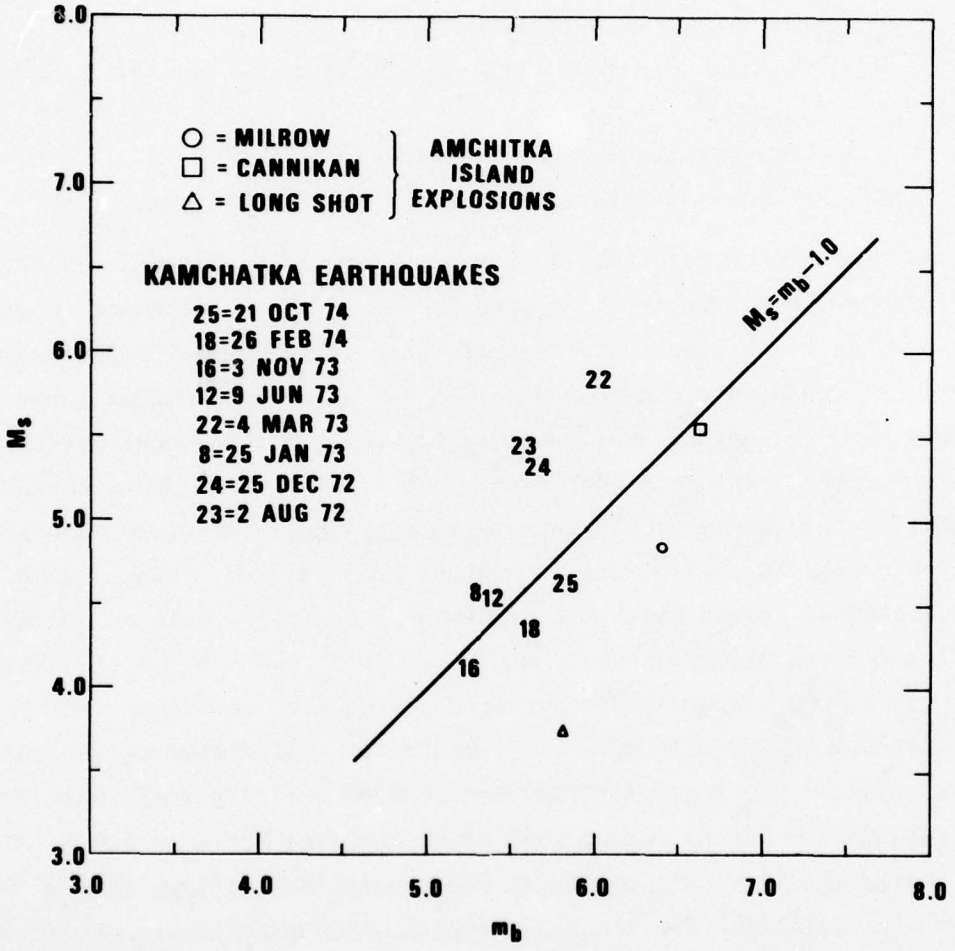

Figure 30 M_S vs. m_b for selected Kamchatka earthquakes of thrust-type mechanism.

and 5000 kt. A M_s separation of about 0.6 magnitude units is observed between the Long Shot explosion and the lowest Kamchatka events in our limited sample and, by inference, this would be the minimum separation observed for any sample of shallow kamchatka activity. This difference is slightly greater than may be easily obtained by an evasion scheme which had shots fired in an array if m_b is measured in the first ten seconds as suggested by Blandford and Clark (1975).

Corner Frequency

The spectrum for MILROW, reduced back to the source in the same manner as for Kamchatka earthquakes in Figure 17, is shown in Figure 31. Note that the MILROW spectrum exhibits a fairly constant high-frequency falloff of $A \propto f^{-2}$. Figure 32 is a plot of $|\hat{u}_o|$ versus corner frequency for the five earthquakes for which such data could be obtained with adequate S/N ratio and for the explosion MILROW on Amchitka Island. These data, presented earlier in the form of seismic moment vs. f_c (except for MILROW), suggests roughly an order of magnitude difference in long-period level between earthquakes and explosions for a given f_c and basically agrees with some data presented by Hanks and Thatcher (1972) for Aleutian events only.

Long-Period Body-Wave Excitation

For the nine earthquakes of this study, we have compiled in histogram form the ground displacement ratios of long-period S and P-waves to LR waves in Figures 33 to 35. No distance corrections have been applied to these ratios, but only the gross statistics of the ratios are considered here. These distributions of ratios may be compared to the distributions obtained from LRSM stations using worldwide events in Von Seggern (1972). The median log (SH/LR) at roughly -.4 in Figure 33 agrees well with -.3 in Von Seggern. The median log (SV/LR) in Figure 34 lies at roughly -.6, indicating SV/SH < 1. In either case, the Kamchatka log (S/LR) values are higher than those of typical NTS explosions recorded at LRSM stations, which lie at roughly -1.2 in Von Seggern's histogram; but there is some overlap between the two populations. In Figure 35, the median log (P/LR) lies at roughly -.4, indicating roughly

---

Hanks, T. C., and W. Thatcher, 1972. A graphical representation of seismic source parameters, J. Geophys. Res., v. 77, p. 4393-4406.

von Seggern, D. H., 1972. Seismic shear waves as a discriminant between earthquakes and underground nuclear explosions, SDL Report Number 295, Teledyne Geotech, Alexandria, Virginia.

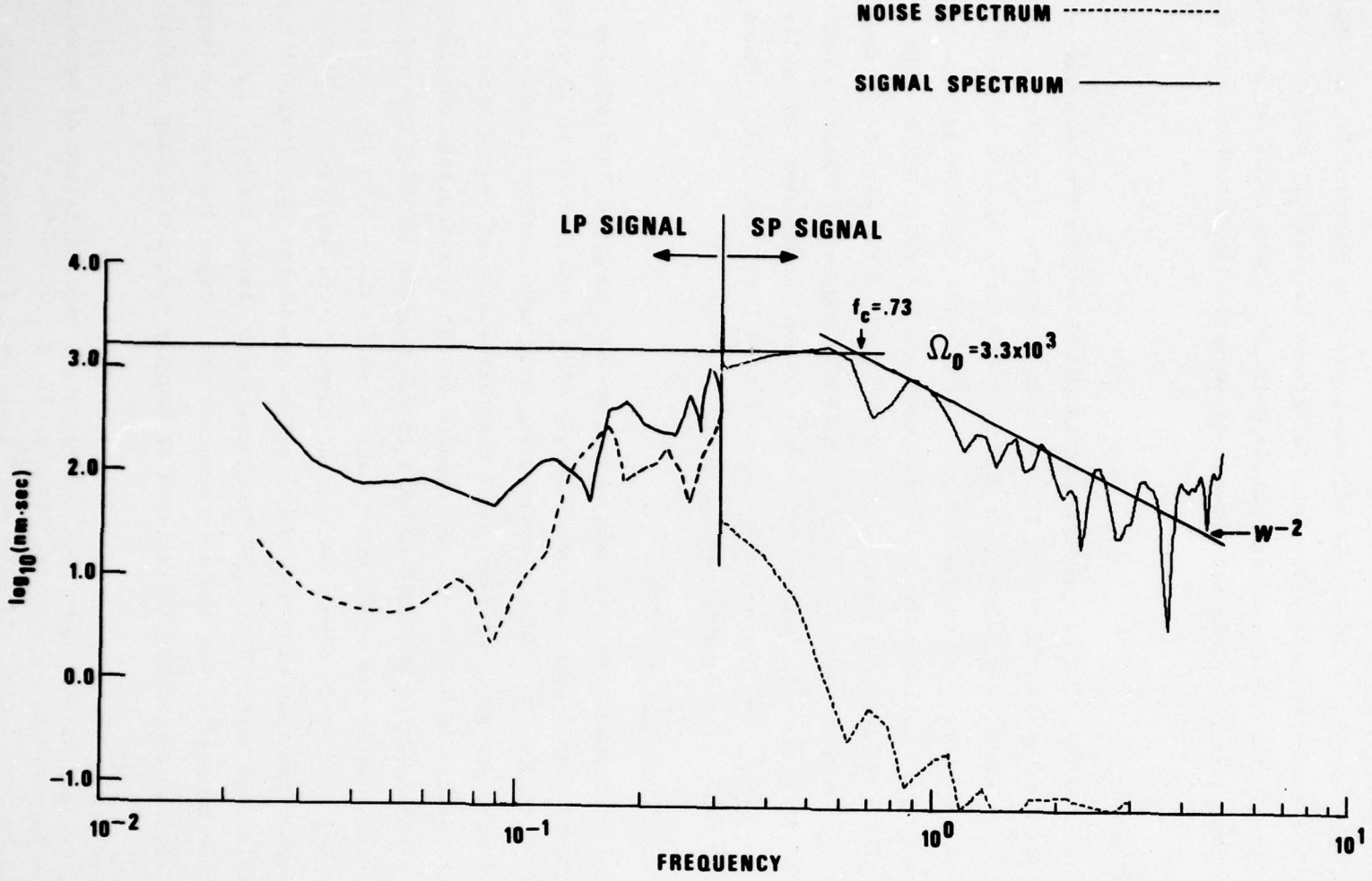

Figure 31 LASA A0 subarray spectra of P-wave from MILROW with instrument response and attenuation removed (t* = .25).

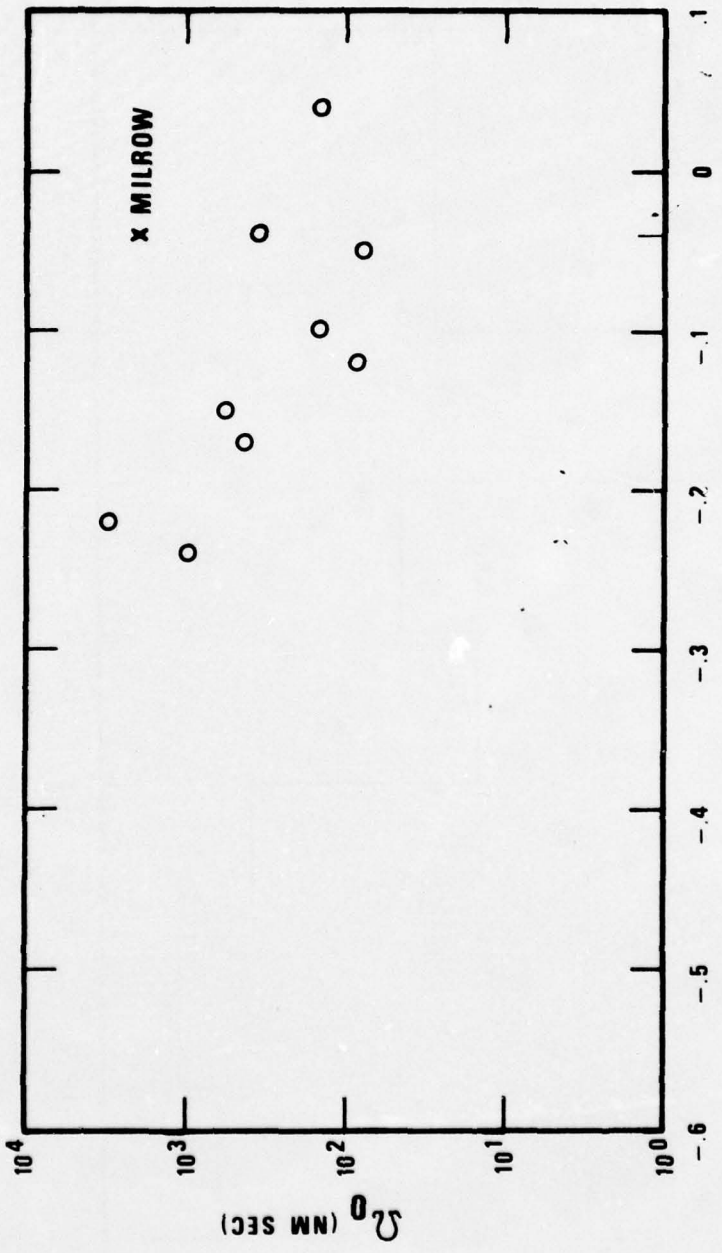

Figure 32 Long-period spectral level vs. corner frequency for Kamchatka earthquakes from LASA P recordings.

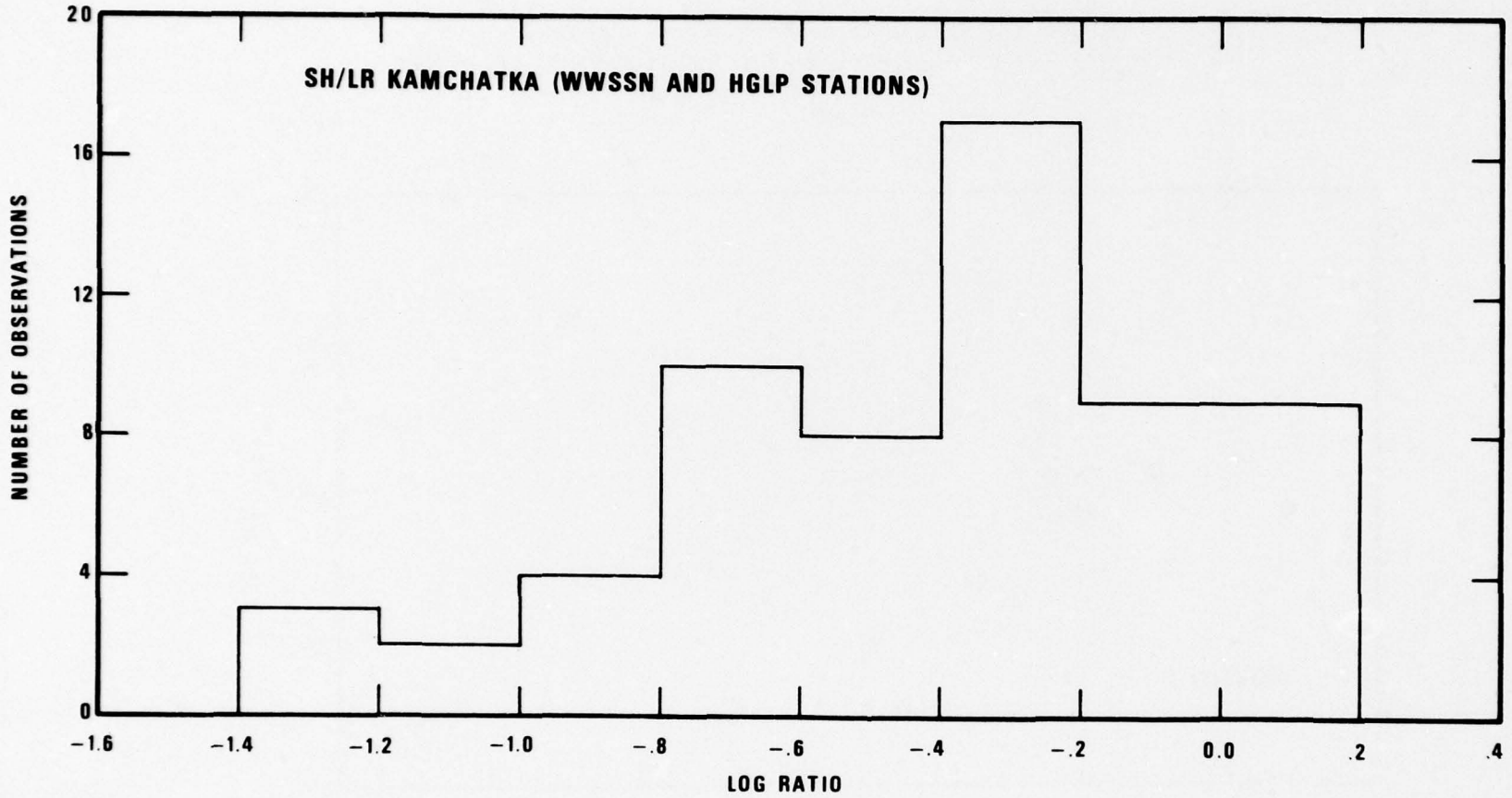

Figure 33 Distribution of log (SH/LR) for ratios of ground displacements from Kamchatka earthquakes.

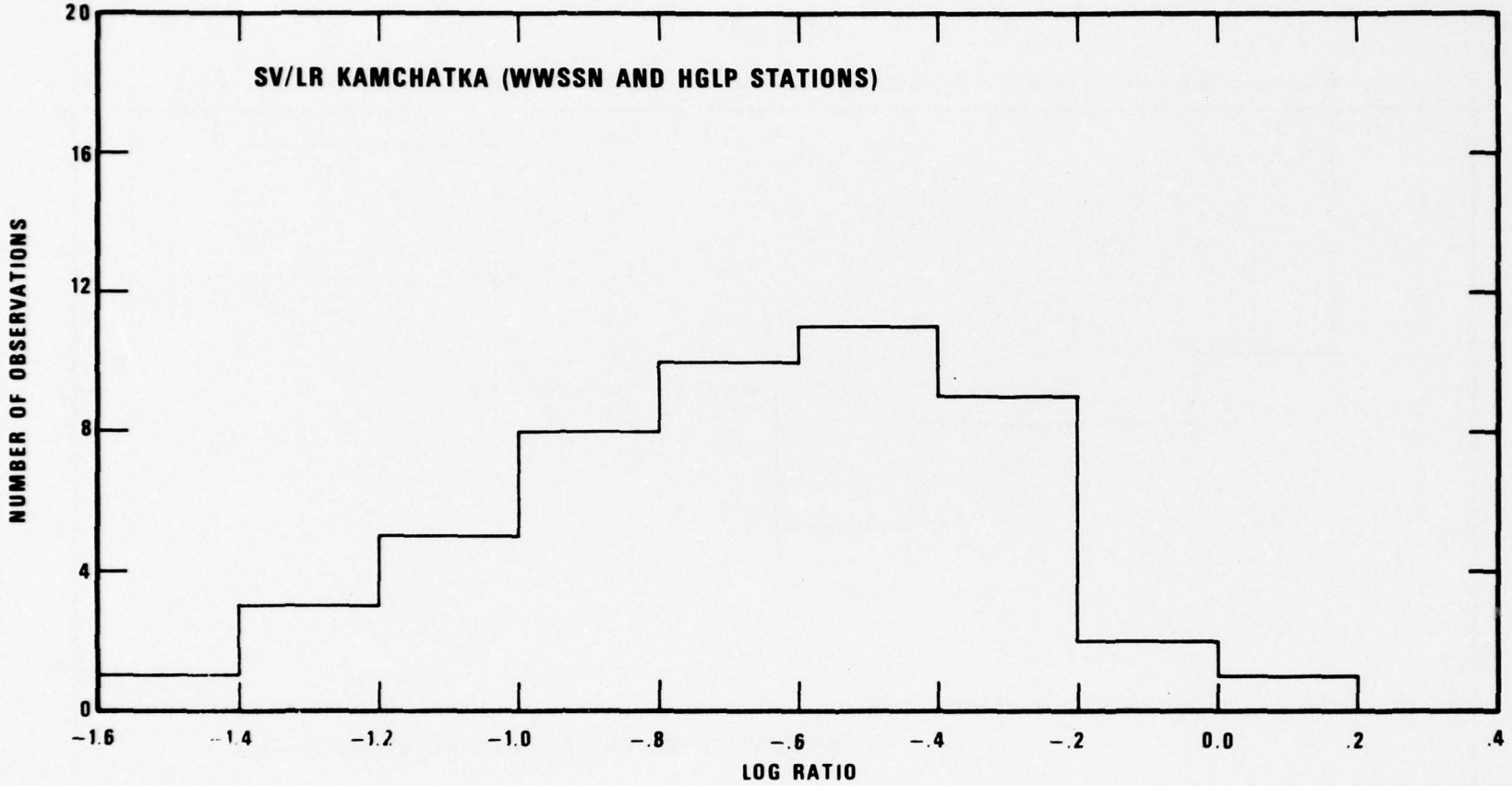

Figure 34 Distribution of log (SV/LR) for ratios of ground displacements from Kamchatka earthquakes.

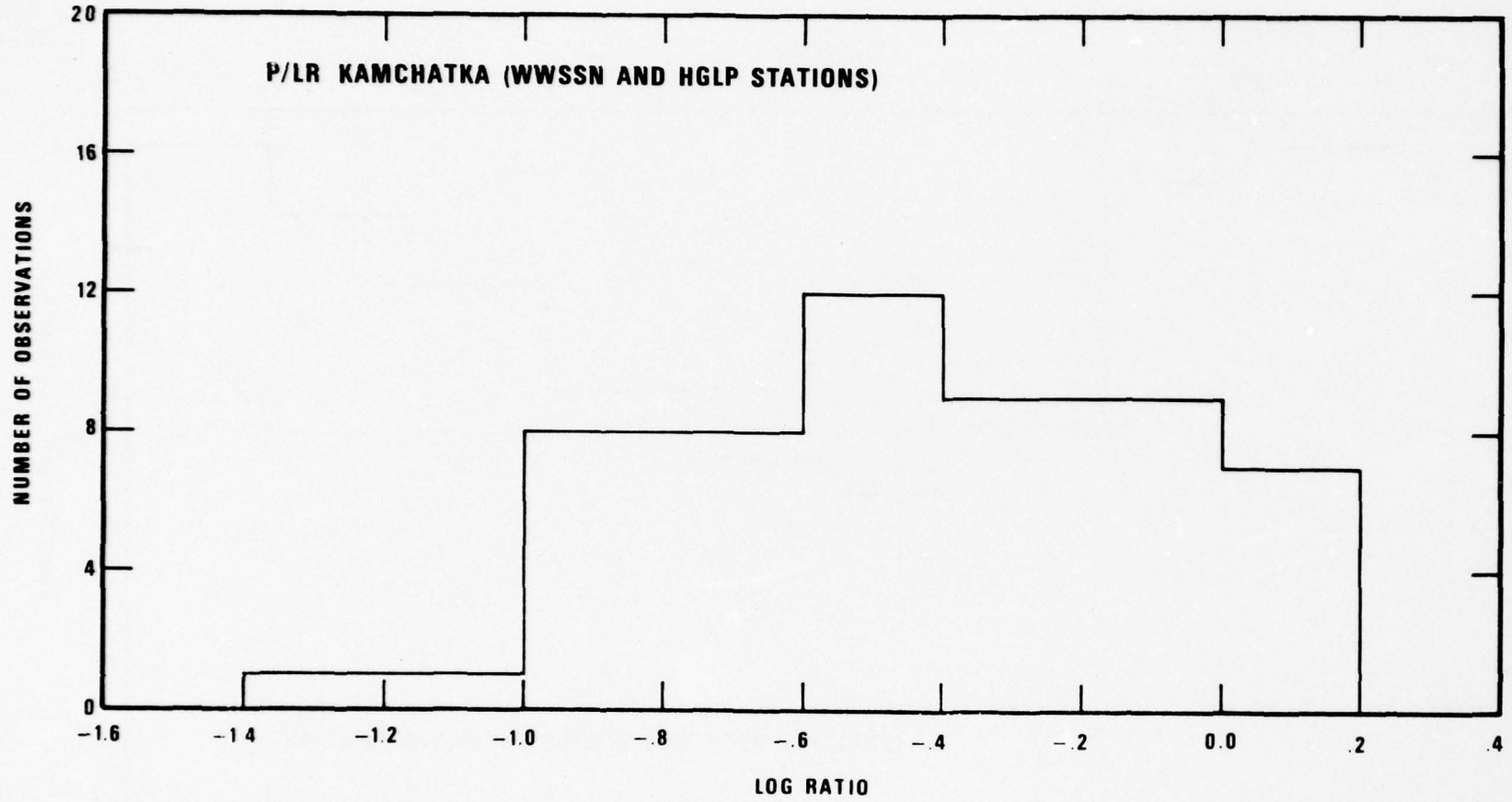

Figure 35 Distribution of log (P/LR) for ratio of ground displacements from Kamchatka earthquakes.

equal P and SH amplitude for these Kamchatka earthquakes; this again would be higher than typical explosion values inferred from Von Seggern's histograms. Limited data for long-period body-waves from Amchitka explosions (Blandford and Clark, 1974) indicated that values for these explosions lie to the left of the large majority of Kamchatka earthquake values given here.

A more useful discriminant based on long-period body-waves is obtained when distance effects are removed by computing magnitude. Table V lists the average parameters $\overline{m_b(LPP)} - \overline{M_s}$ and $\overline{m_b(LPS)} - \overline{M_s}$ for the eight Kamchatka earthquakes having observable long-period phases. Unless indicated, each average is based on observations at four or more stations. The maximum shear-wave component (SH or SV) was used in every case to compute $m_b(LPS)$. The $\overline{m_b(LPS)} - \overline{M_s}$ are all well above the mean of roughly zero for Aleutian earthquakes as reported by Blandford and Clark (1974) and therefore should offer good discrimination capability for the Kamchatka region. Also, the parameter corresponding to P-waves in Table V is well above that expected for nuclear explosions. These discriminants should work equally well for shot arrays. Use of Ringdal's (1976) method for computing m_b (LPP) would probably improve discrimination.

Depth of Focus

On the basis of P-arrival times only, a considerable number of Kamchatka events would probably have error ellipses such that very shallow depth could not be rejected with high confidence even after application of known travel-time residuals (Evernden, 1975; Veith, 1974). However, of the nine events studied here, eight of them had apparent pP phases recorded at LASA; as noted earlier, this is undoubtedly a result of the favorable radiation pattern for pP to this array. Thus we feel that many low M_s-m_b events in this source region could be identified as earthquakes on the basis of pP, assuming that

---

Blandford, R. R., and D. M. Clark, 1974. Detection of long-period S from earthquakes and explosions at LASA and LRSM stations with application to positive and negative discrimination of earthquakes and underground explosions, SDAC Report Number SDAC-TR-74-15, Teledyne Geotech, Alexandria Virginia.

Evernden, J. F., 1975. Further studies on seismic discrimination, Bull. Seism. Soc. Am., v. 65, p. 359-392.

Veith, K., 1974. The relationship of island arc seismicity to plate tectonics, Ph.D. Thesis, Southern Methodist University, Dallas, Texas.

TABLE V

Long-Period Body-Wave Minus Rayleigh-Wave

Magnitudes for Selected Kamchatka Earthquakes

Event	$\overline{m_b(LPP)}-\overline{M_s}$	$\overline{m_b(LPS)}-\overline{M_s}$
8	.57	.31
12	.62	.26
16	-.26 (1)*	.49 (2)
18	.40	.39
22	.46	.32
23	.51	.51
24	.67	.34
25	.31	.29

*number of observations of P or S $\geq$ 4 unless indicated

other suitably located stations would corroborate LASA pP detection by showing the characteristic move-out of the pP phase with epicentral distance. This move-out was, in fact, observed with the use of the WWSSN for several of the events. In addition, the absence of pP at NORSAR for most events is in accordance with the regional focal mechanism and would fail an attempt to model pP by a shot array.

Complexities

We have computed the "complexity" parameter as seen by NORSAR and LASA for the Kamchatka earthquakes in the manner given by Lambert et al. (1969). Table VI lists the computed values. Except for one event, LASA beams show clear pP signals whose amplitudes range from 30 to 140 percent of the main phase. NORSAR beams have pP signals in only 2 of the 9 cases. (See Figure 22 for signal plots.) The complexity numbers reflect these observations: for all events the LASA complexity number is greater than the NORSAR number, indicating more energy in the coda after the main phase. Blandford and Clark (1975) state that the more complex Kamchatka events seem to emanate from the area of the Kamchatka Cape; the two events in this study from that particular area, Events 20 and 23, do exhibit high complexity at both NORSAR and LASA.

We have also entered in Table VI the LASA complexity of MILROW and LONG SHOT (identical in value) as reported by von Seggern and Lambert (1972); it is lower than that for any of the nine Kamchatka earthquakes recorded at LASA. This discriminant is of course very vulnerable to evasion by a shot array.

Spectral Ratios

Spectral ratios have been calculated at LASA and NORSAR according to (Lacoss, (1969).

$$R = \int_{1.55}^{1.95} A(f)df \Big/ \int_{.45}^{.85} A(f)df$$

Lambert, D. G., D. H. von Seggern, S. S. Alexander, and G. A. Galat, 1969. The Long Shot Experiment, Volume II: Comprehensive analysis, SDL Report Number 234, Teledyne Geotech, Alexandria, Virginia.

von Seggern, D. H., and D. G. Lambert, 1972. Analysis of teleseismic data for the nuclear explosion Milrow, SDL Report Number 258. Teledyne Geotech, Alexandria, Virginia.

Lacoss, R. T., 1969. A large-populations LASA discrimination experiment, Technical Note 1969-24, Lincoln Laboratory, Lexington, Massachusetts.

TABLE VI

Complexities for Kamchatka P-Waves

	Complexity Parameter	
Event	LASA	NORSAR
8	5.56	1.70
12	4.67	1.94
16	4.50	1.24
18	2.18	1.65
20	6.48	3.45
22	4.99	4.63
23	9.80	4.69
24	6.78	5.77
25	2.75	1.46
MILROW/LONG SHOT	2.10	—

where sums of the equivalent terms of the discrete Fourier transform have replaced the integrals. These ratios are plotted versus m_b for the nine earthearthquakes and also for the explosion Milrow in Figure 36. The fact that Milrow registers the highest spectral ratio at LASA is compatible with Lacoss' observations and those of many others for explosions and earthquakes but deserves no great emphasis due to the possibility of propagation effects being different between our Kamchatka source region and the Amchitka source region, thus biasing the spectral ratios.

Radiation Pattern

For body-waves, the lack of rarefactional first motion at teleseismic distances from Kamchatka earthquakes with mechanisms similar to those studied here would not aid discrimination. This could be remedied by placement of ocean-bottom seismometers near Kamchatka, as suggested by Evernden (1976). In regard to surface-waves, we conclude that although the radiation pattern observed by teleseismic stations is compatible with the theoretical patterns for the observed events in some cases, the scatter is too great to infer the source type; i.e., double-couple of earthquake vs. uniform dilation of explosion. Furthermore, the rapidly varying phase-velocity structure near the source introduces large propagation effects, as illustrated by Figures 27 to 29, on 20-second LR waves which vary significantly over small changes in source location; and this phenomena precludes determining source radiation pattern by a master event technique unless there is a small separation between epicenters.

Short-Period S/P Excitation

From the short-period recordings of the WWSSN stations which were analyzed for the nine earthquakes, ratios of S/P ground displacement were compiled. The logarithms of the small sample of 24 ratios nave been plotted in Figures 37 and 38, for SV and SH respectively. The spread is over two orders of magnitude, reflecting the variation in S/P ratios predicted by radiation patterns for double-couple models of an earthquake; and it is comparable to

Evernden, J. F., 1976. Study of seismological evasion, Part III: Evaluation of evasion possibilities using codas of large earthquakes, Bull. Seism. Soc. Am., v. 66, p. 549-592.

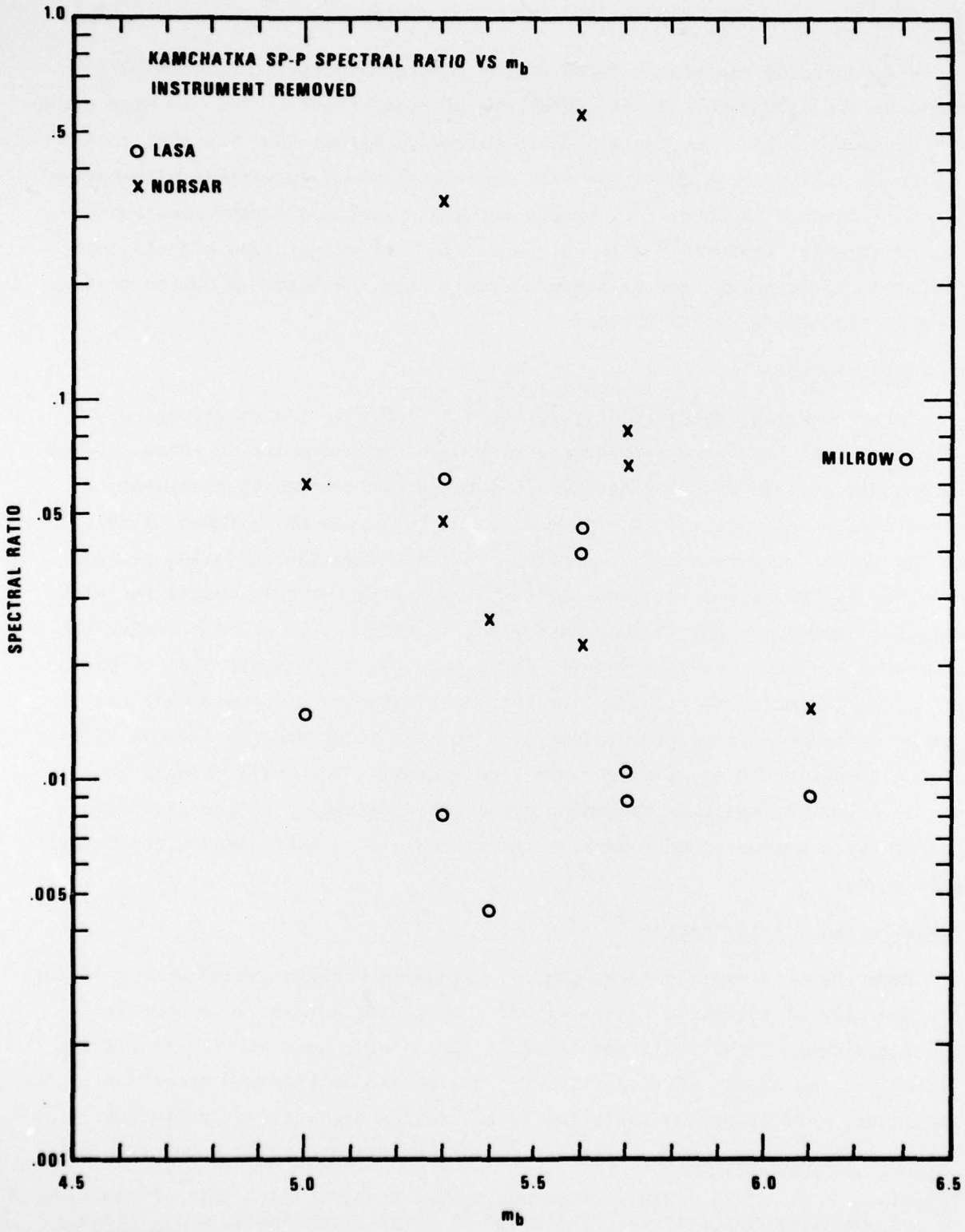

Figure 36 Short-period P spectral ratio vs. m_b for Kamchatka earthquakes recorded at NORSAR and LASA.

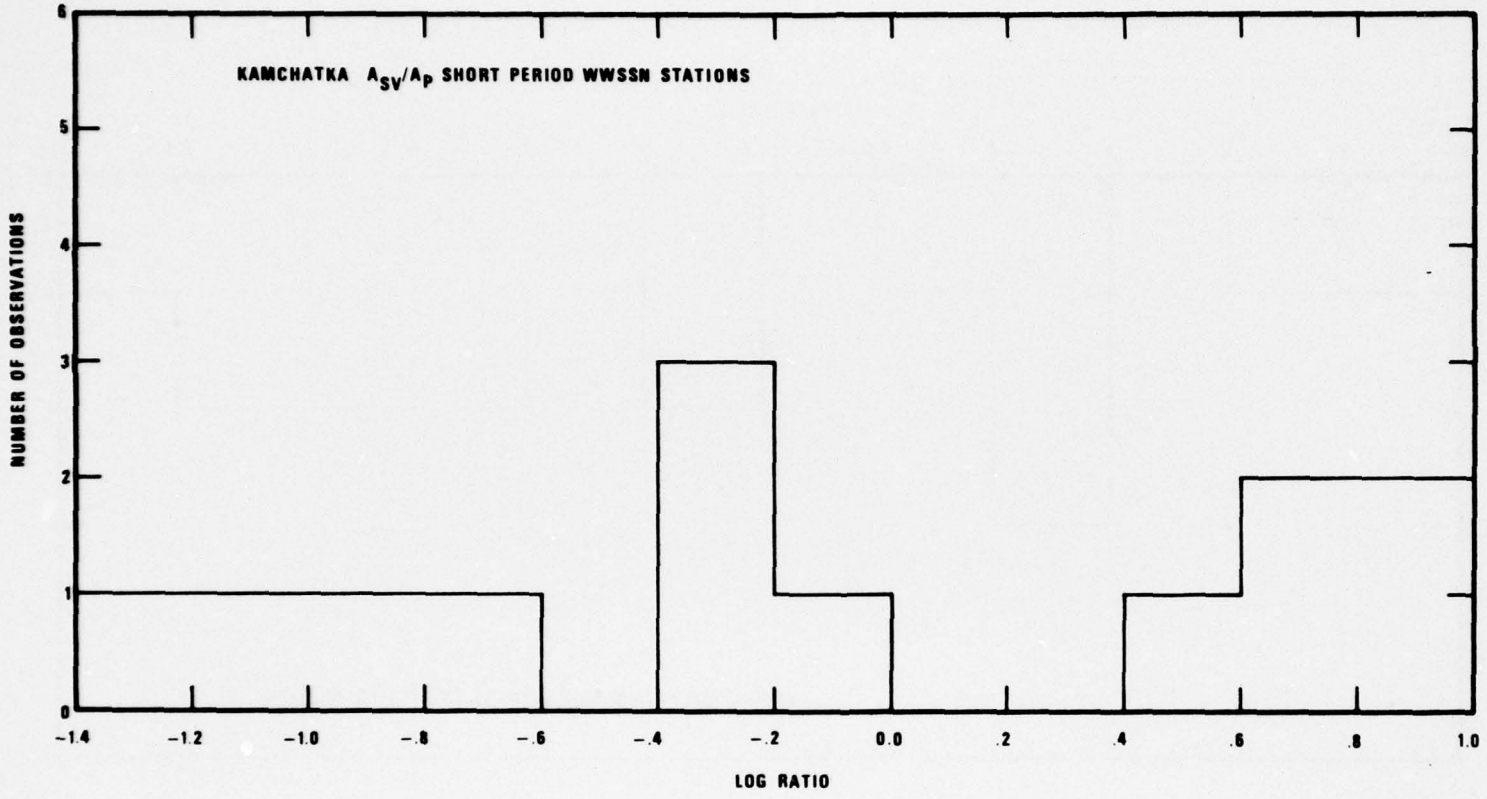

Figure 37 Distribution of ratio (SV/P) for ground displacement from short-period recordings of Kamchatka earthquakes.

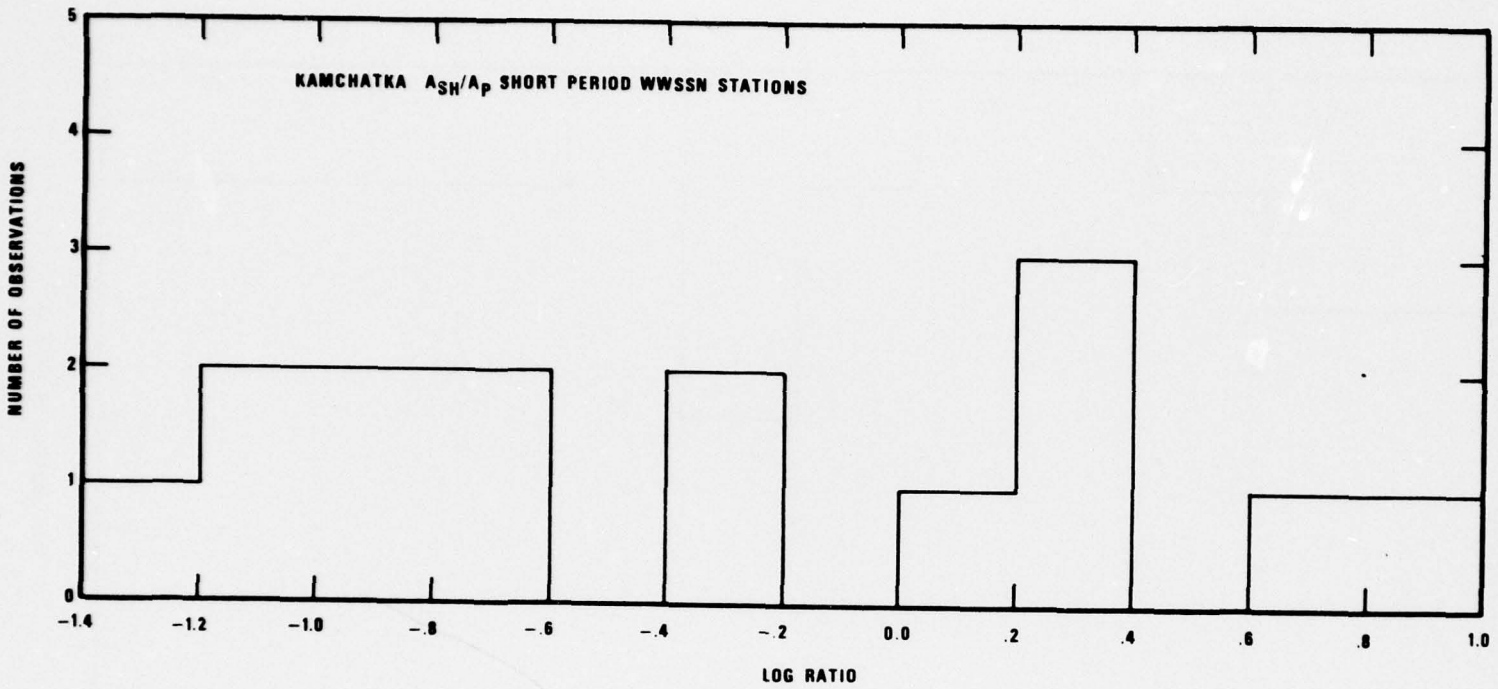

Figure 38 Distribution of ratio (SH/P) for ground displacement from short-period recordings of Kamchatka earthquakes.

that shown by von Seggern (1972) for a much larger sample of global earthquakes recorded by the LRSM network, although the median here is displaced considerably to the left of that larger sample. Von Seggern also plotted a small sample of log (S/P) for Nevada explosions; with a median at roughly -1.0 they overlapped only 10% of the global earthquake sample but would overlap appreciably more with our small Kamchatka sample. The important fact is that all but one of our nine earthquakes had at least one observed S/P ratio, either SV or SH, which exceeded 1.0, or 0.0 on the log scale, a value not nearly reached by any of the few explosion ratios compiled by von Seggern. This, coupled with the scarcity of observations for explosions, suggests that, with magnitudes computed according to Ringdal's (1976) method, this discriminant would show excellent separation.

---

von Seggern, D. H., 1972. Seismic shear waves as a discriminant between earthquakes and underground nuclear explosions, SDL Report Number 295, Teledyne Geotech, Alexandria, Virginia.

SUMMARY

The underthrusting of the Pacific plate below Kamchatka causes a high rate of seismic activity, much of which lies at shallow enough depths that location estimates, with their corresponding uncertainty intervals, could not alone identify as such many earthquakes occuring there in a discrimination context. We have, therefore, studied the behavior of a number of common discrimination parameters calculated for a selected group of typical shallow Kamchatka earthquakes. Several of this group were picked on the basis of preliminary estimates which indicated that they were anomalously low in M_s relative to m_b is close to the discrimination line $M_s = m_b - 1.5$ and, therefore, a priori difficult to discriminant from explosions hypothetically.

Our analysis of these events treated the effects of source and travel path on signal character at many teleseismic stations so that discrimination parameters could be given a physical basis. Salient source effects were found to be as follows:

1) The thrust-fault mechanisms result in compressive first motions at teleseismic stations.
2) Such mechanisms, however, result in distinct pP phases at LASA and other stations.
3) The M_s of such a thrust mechanism is predicted to be roughly one-half that of an explosion of equal moment and equal depth while m_b is predicted to be nearly equal for the two (provided source spectra have the same shape).
4) The effect of moving the earthquake focal depth down from the uppermost layer to the layers in which our events occurred (approximately 30-40 km) is to decrease m_b as much as 1.0 if moment is held constant.
5) Moments and corner frequencies of these selected Kamchatka earthquakes indicate they are of medium stress drop (tens of bars).
6) The corner frequency of these earthquakes is distinctly lower than that of explosions (extrapolation of Amchitka shots) at a given magnitude.
7) The predicted long-period Rayleigh-wave radiation pattern for 20-second amplitude fits the observed data rather well.

Salient path effects were found to be as follows:

1) Ray-tracing of 20-second Rayleigh-waves indicates that the effect of focusing and defocusing on the M_s at certain stations could vary considerably (.3 M_s or more) as the epicenter is moved along the Kamchatka coast over a distance of only 2° or 3°.
2) A t* (travel-time divided by Q) of .25 was inferred for the path Kamchatka-LASA and a t* of .31 for the path to NORSAR.

A major omission of this study was the failure to analyze the effects of the dipping plate on teleseismic P amplitudes. However, published work on the effects of the dipping plate in the similarly configured Aleutian Arc indicate that the amplitude variations in the P-wave are predictable and could be accounted for if locations were reasonably accurate.

Overall, the source and path effects mentioned above are certainly not weighted against correct event discrimination and are unlikely to hinder earthquake identification in a multi-discriminant approach for the Kamchatka source region. A review of common discriminants applied to our selected Kamchatka earthquakes provided the following information:

1) The LR excitation of these events was found to be nearly an order of magnitude more at a given m_b when compared with Amchitka explosion data. We emphasize that several of these events were selected as having low M_s and, therefore, probably represent those Kamchatka events hardest to discriminate by M_s-m_b. Although a thrust fault with moment equivalent to that of an explosion would generate less LR, by up to a factor of two, the success of M_s-m_b is due to lower corner frequencies (meaning larger source time and space dimensions) and to focal depth resulting in lower m_b than would be obtained from equivalent-moment earthquakes near the surface where explosions are detonated.
2) Long-period P and S excitation relative to LR is greater than typical explosions and is in the range of previous observations for global earthquakes on the LRSM network. The S-wave information would help in discriminating against shot arrays which should not generate these waves any better relatively than single explosives.
3) P-wave complexity values at LASA and NORSAR were consistently higher for the Kamchatka earthquakes than for Amchitka tests.

4) P-wave spectral ratios for the Kamchatka earthquakes appear to separate from explosions.

5) Short-period S-wave excitation relative to that of the P-wave was definitely characteristic of earthquakes on the basis of comparison with previous explosion-earthquake results. Again, this type of S-wave data is helpful in rejecting the shot array hypothesis for a suspicious event.

The conclusion is that the few Kamchatka events studied here have characteristics, which when taken together, leave little doubt as to their identity in a discrimination context; and since they represent the lowest M_s events we could find in this source region, we can probably generalize this to include all earthquakes located near or off the coast of Kamchatka, at least those above m_b = 5.0 which is the magnitude of the smallest event in out limited sample.

Regarding possible evasion by the detonation of shot arrays, several of the above points need to be modified. The M_s-m_b discriminant could be impaired by perhaps 0.6 magnitude unit through such a scheme, and this would leave perhaps only 0.0 separation between these composite events and Kamchatka earthquakes with low M_s. Long-period and short-period S waves would still be an effective discriminant since they cannot be created by shot arrays. More work needs to be done on use of these phases for discrimination, especially concerning the effects of t* on their amplitudes. Because of the small separation afforded by complexity and spectral ratio, it is expected that they would become useless to identify shot arrays whose effect is to push there parameters toward the earthquake population. If a shot array were arranged such as to create the illusion of a pP, then this phase would be detected at <u>all</u> stations; but we have seen that the typical thrust mechanism in Kamchatka generates pP preferentially to only <u>some</u> stations.

ACKNOWLEDGEMENTS

Much of the task of data collection and reduction for this study was performed by E. I. Sweetser and D. W. Rivers. A program to compute synthetic body-wave seismograms was made available by Z. Der and T. McElfresh, who also made several helpful suggestions related to its use. Comments on drafts of this report by R. R. Blandford and R. A. Hartenberger are much appreciated.

REFERENCES

Blandford, R. R., T. J. Cohen, and H. L. Husted, 1971. Opportunities for foreign nations to hide an underground nuclear test in an earthquake(U), SDL Report Number 283, Teledyne Geotech, Alexandria, Virginia. Classified

Blandford, R. R., and H. L. Husted, 1973. Extension of Hide-In-Earthquakes (HID) technique to include probability of detection (U), SDL Report Number 303, Teledyne Geotech, Alexandria, Virginia. Classified

Blandford, R. R., and D. M. Clark, 1974. Detection of long-period S from earthquakes and explosions at LASA and LRSM stations with application to positive and negative discrimination of earthquakes and underground explosions, SDAC Report Number SDAC-TR-74-15, Teledyne Geotech, Alexandria, Virginia.

Blandford, R. R., 1975. A source theory for complex earthquakes, Bull. Seism. Soc. Am., v. 65, p. 1385-1406.

Blandford, R. R., and D. M. Clark, 1975. Variability of seismic waveforms at LASA from small subregions of Kamchatka, SDAC Report Number SDAC-TR-75-10, Teledyne Geotech, Alexandria, Virginia.

Der, Z. A., and T. W. McElfresh, 1976. PSV--a program to compute synthetic seismograms, unpublished manuscripts, Teledyne Geotech, Alexandria, Virginia.

Douglas, A., J. A. Hudson, and V. K. Kembhavi, 1971. The relative excitation of seismic surface and body-waves by point sources, Geophys. J., v. 23 p. 451, 460.

Engdahl, E. R., 1972. Seismic effect of the Milrow and Cannikin nuclear explosions, Bull. Seism. Soc. Am., v. 62, p. 1411-1424.

Ericsson, V. A., 1970. Event identification for test ban control, Bull. Seism. Soc. Am., v. 60, p. 1521-1546.

Evernden, J., 1969. Identification of earthquakes and explosions by use of teleseismic data, J. Geophys. Res., v. 74, 3828-3856.

Evernden, J. R., W. J. Best, P. W. Pomeroy, T. v. McEvilly, J. M. Savino, and L. R. Sykes, 1971. Discrimination between small magnitude earthquakes and explosions, J. Geophys. Res., v. 76, p. 8042-8055.

Evernden, J. F., 1975. Further studies on seismic discrimination, Bull. Seism. Soc. Am., v. 65, p. 359-392.

Evernden, J. F., 1976. Study of seismological evasion, Part III: Evaluation of evasion possibilities using codas of large earthquakes, Bull. Seism. Soc. Am., v. 66, p. 549-592.

Fedotov, S. A. 1968. On the Deep structure, properties of the upper mantle, and volcanism of hte Kurile-Kamchatka Island Arc according to seismic data, in The Crust and Upper Mantle of the Pacific Area, AGU Mono. 12, American Geophysical Union, Washington, D.C.

REFERENCES (Continued)

Goryatchev, A. V. 1962. On the relationship between geotectonic and geophysical phenomena of the Kuril-Kamchatka folding zone at the junction zone of the Asiatic continent with the Pacific Ocean, in The Earth Beneath the Continents, AGU Monograph 10, American Geophysical Union, Washington D.C.

Hanks, T. C. and W. Thatcher, 1972. A graphical representation of seismic source parameters, J. Geophys. Res., v. 77, p. 4393-4406.

Herrin, E. and J. N. Taggart, 1968. Source bias in epicenter determination, Bull. Seism. Soc. Am., v. 58, p. 1791-1796.

Hudson, J. A. and A. Douglas, 1975. On the amplitudes of seismic waves, Geophys. J., v. 42, p. 1039-1044.

Lacos, R. T., 1969. A large-populations LASA discrimination experiment, Technical Note 1969-24, Lincoln Laboratory, Lexington, Mass.

Lambert, D. G., D. H. von Seggern, S. S. Alexander, and G. A. Galot, 1969. The Long Shot Experiment, Volume II: Comprehensive analysis SDL Report Number 234, Teledyne Geotech, Alexandria, Virginia.

Lee, T. and T. Teng, 1973. Polar radiation patterns of P and SV-waves in a multi-layered medium, Bull. Seism. Soc. Am., v. 63, p. 547.

Leibermann, R. C. and P. W. Pomeroy, 1969. Relative Excitation of surface waves by earthquakes and underground explosions, J. Geophys. Res., v. 74, p. 1575-1590.

Noponen, I., 1975. Compressional wave power spectrum from seismic sources, Report to the Advanced Research Project Agency, ARPA Order No. AO 2131-1, 64 p.

Ringdal, F., 1976. Maximum-likelihood estimate of event magnitude, Bull. Seism. Soc. Am., v. 66, p. 789-802.

Stauder, W., and L. Mualchin, 1976. Fault motion in the larger earthquakes of the Kurile-Kamchatka Arc and of the Kurile-Hokkaido Corner, J. Geophys. Res., v. 81, p. 297-308.

Tokarov, P., 1970. On the focal layer, seismicity, and volcanicity of the Kurile-Kamchatka Zone, Izvestia, Physics of the Solid Earth, Number 3, p. 152-160.

Veith, K., 1974. The relationship of island arc seismicity to plate tectonics, Ph.D. Thesis, Southern Methodist University, Dallas, Texas.

von Seggern, D. H., 1972. Seismic shear waves as a discriminant between earthquakes and underground nuclear explosions, SDL Report Number 295, Teledyne Geotech, Alexandria, Virginia.

von Seggern, D. H., and D. G. Lambert, 1972. Analysis of teleseismic data for the nuclear explosion Milrow, SDL Report Number 258.

von Seggern, D. H., and P. A. Sobel, 1975. Experiments in refining M_s estimates for seismic events, SDAC Report Number SDAC-TR-75-17, Teledyne Geotech, Alexandria, Virginia.

von Seggern, D. H., 1976. (U) Final report on the analysis of the VLPE network, SDAC Report Number SDAC-TR-76-1, Teledyne Geotech, Alexandria, Virginia. Classified

Weizman, P., 1966. On the deep structure in the Kurile-Kamchatka region, in Continental Margina and Island Arcs, ed. W. Poole, Special Paper 66-15, Geological Survey of Canada, p. 244-251.

Wiechert, D. H., and P. W. Basham, 1973. Deterrance and false alarms in seismic discrimination, Bull. Seism. Soc. Am., v. 63, p. 1119-1132.

Wyss, M., T. C. Hanks, and R. C. Liebermann, 1971. Comparison of P-wave spectra of nuclear explosions and earthquakes, J. Geophys. Res., v. 76, p. 2716-2729.